DESIGN PROPERTIES OF HIGH-STRENGTH STEELS IN THE PRESENCE OF STRESS CONCENTRATIONS AND HYDROGEN EMBRITTLEMENT

PART 3. THE RESPONSE OF HIGH-STRENGTH STEELS IN THE RANGE OF 180,000-300,000 PSI TO HYDROGEN EMBRITTLEMENT FROM CADMIUM ELECTROPLATING

E. P. KLIER

B. B. MUVDI

G. SACHS

SYRACUSE UNIVERSITY

MARCH 1957

WRIGHT AIR DEVELOPMENT CENTER
AIR RESEARCH AND DEVELOPMENT COMMAND
UNITED STATES AIR FORCE
WRIGHT-PATTERSON AIR FORCE BASE, OHIO

FOREWORD

This report was prepared by Syracuse University under USAF Contract No. AF 33(616)-2362, S/A 4(56-445). The contract was initiated under Project No. 7360, "Materials Analysis and Evaluation Techniques," Task No. 73605, "Design and Evaluation Data for Structural Metals." It was administered under the direction of the Materials Laboratory, Directorate of Research, Wright Air Development Center, with Mr. A. W. Brisbane as project engineer. This work was performed in the period between September 1, 1955 and August 31, 1956.

WADC TR 56-395 Pt 3

ABSTRACT

The embrittlement of high strength steels due to the action of hydrogen introduced by Cd-electroplating has been studied in sustained-load, rotating beam fatigue, and bending tests. Strength levels from 180,000 to 300,000 psi as suitable for the various steels were examined for a variety of initial conditions of stress concentration.

All steels were found to be embrittled in some measure after Cd-plating and this embrittlement could not be fully eliminated, as determined in the bend test, through the baking treatment used. The improvement in properties which did result from baking was promoted by a redistribution and not an elimination of hydrogen from the steel.
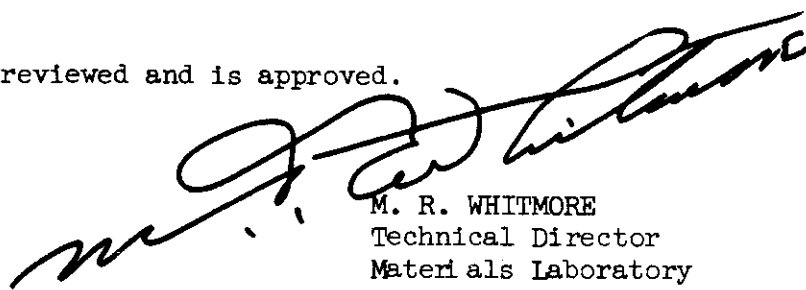
Failure promoted by Cd-plating is affected by the experimental conditions and has been discussed at length in the report. In the hydrogen bearing zone a crack is initiated and then depending on the experimental conditions may propagate to failure of the cross section through overloading. Crack development is apparently dependent, in part, on the composition and is minimized by reduction in carbon content or by an increase in silicon content.

Both the sustained-load and bend tests are suitable tests for evaluation of hydrogen embrittlement in ultra-high strength steels. The rotating beam fatigue test is a relatively insensitive test of hydrogen embrittlement, but can be used to provide an excellent measure of the "static" notch strength of the steel.

PUBLICATION REVIEW
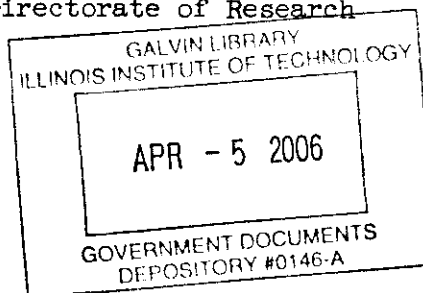
This report has been reviewed and is approved.

FOR THE COMMANDER:

M. R. WHITMORE
Technical Director
Materials Laboratory
Directorate of Research

WADC TR 56-395 Pt 3   iii

TABLE OF CONTENTS

LIST OF TABLES

LIST OF ILLUSTRATIONS

INTRODUCTION*

The failure of high strength steels through the action of electro-deposited hydrogen in the presence of a suitable stress system has been intensively investigated during the past five years. Thus, while hydrogen embrittlement is a very generally encountered phenomenon, it is now possible to describe characteristics of this effect which are perhaps best restricted to the consideration of high strength steels. One of the most characteristic features of hydrogen induced failure in high strength steels is the delay time effect for failure to take place under the action of statically applied loads. The first plausible explanation of this behavior was advanced by Petch and Stables (1) who proposed a suitably modified form of the Griffith-Orowan (2) theory of static fatigue in glass. This theory requires the development of a suitable crack which through reduction in the cross-section leads to eventual overloading of the uncracked cross-section and thus to failure.

The crack formation proposed by Petch and Stables was experimentally verified by Raring and Rinebolt (3), Klier, Muvdi, and Sachs (4) and Barnett and Troiano (5).

Barnett and Troiano have investigated at length the development of the crack for specimens containing electrodeposited hydrogen and propose that failure takes place in three stages, viz.:

1) CRACK INITIATION: The crack develops at the base of the notch and passes rapidly through the hydrogen-rich surface layers.

2) CRACK PROPAGATION: If the applied load is sufficiently low that fracture does not result during stage 1, further crack development is suppressed until hydrogen can diffuse to the crack front. Second stage crack growth is, therefore, controlled by the hydrogen diffusion rate.

3) FRACTURE: If the crack is allowed to propagate indefinitely, the cross-section will be eventually reduced to the point where the fracture strength of the notch section is exceeded and fracturing in the normal way then takes place.

This description of the failure process while stated in greater detail establishes the role of hydrogen in leading to failure in the same terms

---

*Manuscript released by authors August 31, 1956 for publication as a WADC Technical Report.

WADC TR 56-395 Pt 3   1

as proposed by Petch and Stables and Raring and Rinebolt. However, Klier, Muvdi and Sachs, while in agreement that hydrogen induced failure may take place in the manner described above, propose that the fracture process is not fully general as described by Barnett and Troiano. In addition, the concept that the instantaneous notch strength, in general, is not altered by the action of hydrogen (through a change in geometry) as proposed by Barnett and Troiano (5) is incorrect. Thus for a suitably sharp notch there is general agreement (1) (3) (4) (5) as to the manner of crack development. Differences in behavior, however, do follow from the several discussions and these are best emphasized by consideration of Figure 1. Here the instantaneous notch strength, i.e., the notch strength of the metal under the crack at fracture, is plotted in two possible ways. The curve designated II has been measured by Klier, Muvdi and Sachs (4). The implications of these curves are best appraised through consideration of the projected change in properties as the specimen size is changed as presented in Figure 2.

The notch strength for this steel after tempering in the range to promote high strength conditions is dependent on the specimen size (6) (7) (8). With increase in the specimen size, the notch strength is lowered. The notch strength still is much higher than that measured under sustained loads for hydrogen embrittled steel, however. As the specimen size continues to increase, it is probable that the notch strength asymptotically approaches a limiting value, and this corresponds to a limiting notch strength which has the characteristics of a material constant. From the experimental data which have been so far obtained, it is proposed that the limiting notch strength lies above the notch strength observed in the small (0.3 in. dia.) sustained load specimens.

Thus, since the effect of hydrogen in the sustained load tests is effectively to reduce the section and in this way to promote failure, if a larger specimen is employed, the surface to volume ratio will be reduced, the average hydrogen content of the specimen will be reduced, and the crack will penetrate a relatively shorter distance through the specimen. As a consequence, the notch strength of larger specimens electroplated should be relatively raised. In the limit, the notch strength for unembrittled and electroplated specimens should be equal, as is indicated in Figure 2. Thus, if the phenomenon of size effect may be set aside for the moment, embrittlement due to the action of electrodeposited hydrogen should rapidly be minimized according to the representation for Curve I. According to Klier, Muvdi and Sachs, (4) embrittlement in large sections may also be seriously promoted by the action of hydrogen.

Important as is the establishment of the physical characteristics of the failure of high strength steels through the action of hydrogen, a perhaps more pressing need is the elimination in these materials of the phenomenon as a source of structural failures. This, in principle, is possible

either by suitable processing to counteract the effects of hydrogen embrittlement, or by the use of materials which are impervious to fractures arising from the action of electrodeposited hydrogen. A usual processing treatment for the elimination of hydrogen embrittlement is a low temperature baking operation. This treatment is not, however, generally adequate. Practical difficulties arise in the retention of the required properties in the steels and in the electrodeposit, if complete elimination of harmful hydrogen is achieved. Principal emphasis in the present investigation has as a consequence been directed at the evaluation of available materials for susceptibility to hydrogen embrittlement. This has been done by the use of several types of tests, which are categorized as sustained load, fatigue and bend tests. The fracture surfaces obtained for the several types of specimens have been regularly examined and the characteristic types are discussed.

EXPERIMENTAL PROCEDURE

1. Materials:

The compositions and finished form of the steels studied are given in Table I.

2. Heat Treatment:

Specimens were austenitized in a suitable salt bath, oil quenched and tempered for four hours in a forced draft muffle furnace. The austenitizing and tempering treatments employed for the respective steels are given in Table II.

3. Test Specimens:

All specimens were rough machined to +0.015 inch on each surface prior to heat treatment. After heat treatment specimens were machined to the dimensions given in Figure 3.

Smooth specimens were polished by the application of emery cloth under a suitable coolant. The direction of movement of the polishing cloth was along the axis of the specimen.

Notches were obtained by the use of suitably ground cutting tools. The dimensions of the notches as calculated by Peterson (9) from Neuber's theory are given in Table III.

4. Plating Conditions:

In an earlier work the embrittlement action of electrodeposited hydrogen arising from potential cleaning operations was discussed (4). In the present work hydrogen embrittlement due to hydrogen introduced into the steel during cadmium electroplating is studied. The composition of the cadmium plating bath was as follows:

Cadmium Plating Solution

Cadmium Oxide = 4 oz. per gallon
Sodium Cyanide = 16 oz. per gallon

TABLE I

CHEMICAL COMPOSITION OF STEELS USED IN HYDROGEN EMBRITTLEMENT PHASE OF PROGRAM

Alloy	Size and Shape	Percent of Alloying Elements									
		C	Mn	P	S	Si	Ni	Cr	Mo	V	Cu
4340	4-1/4 in. rd.	0.41	0.79	0.013	0.016	0.31	1.83	0.77	0.23	--	--
V-Mod. 4330	3-1/2 in. rd.	0.32	0.82	0.010	0.021	0.28	1.82	0.89	0.41	0.07	--
98B40	4-1/2 in. rd.	0.46	0.80	0.019	0.022	0.41	0.88	0.79	0.20	--	--
Tricent (Inco)	4-1/4 in. sq.	0.39	0.74	0.014	0.014	1.54	1.83	0.83	0.38	0.07	--
Crucible UHS 260	4 in. sq.	0.35	1.20	0.023	0.017	1.62	--	1.26	0.32	0.20	--
Hy-Tuf	4-1/2 in. rd.	0.25	1.30	0.022	0.018	1.47	1.75	0.38	0.38	--	--
Super TM-2	3 in. rd.	0.41	0.72	0.012	0.014	0.61	2.08	1.15	0.44	--	0.14

TABLE II

HEAT TREATMENTS FOR VARIOUS STEELS EXAMINED

Alloy	Austeni-tizing Temp.-°F	Tempering Temp. - °F, and Strength Level- 1000 Psi				
4340	1525	400 (275,000)	500 (270,000)	700 (235,000)	800 (215,000)	1000 (165,000)
V-Mod. 4330	1600	250 (265,000)	500 (235,000)	750 (210,000)	1000 (180,000)	
98B40	1550	400 (300,000)	575 (270,000)	700 (230,000)	800 (205,000)	900 (195,000)
Tricent (Inco)	1600	400 (295,000)	550 (275,000)	700 (270,000)		
Cru. U HS260	1700	550 (270,000)	800 (250,000)			
Hy-Tuf	1575	700 (230,000)				
Super TM-2	1600	500 (275,000)				

TABLE III

STRESS CONCENTRATION FACTORS AND CORRESPONDING NOTCH RADII FOR
STRESS-RUPTURE AND ROTATING-BEAM FATIGUE SPECIMENS

Type	D	d	K	r
Stress-Rupture Specimens	0.300	0.212	3	0.011
			5	0.0035
			10	0.0008
Rotating-Beam Fatigue Specimens	0.265	0.188	3	0.007
			5	0.002
			8	0.0007

D = Unnotched Diameter (inches)

d = Notch Diameter (inches)

r = Notch Root Radius (inches)

The bath was operated at room temperature at a current density of 200 milliamp. per sq. in. The plate thickness obtained was from 0.00025 to 0.0005 inches for smooth specimens. For the notched specimens metallographic examination revealed that plating was satisfactorily continuous along the root of the notch for all but the most sharply notched specimens. For specimens with a notch root radius of 0.001 inch or less a cadmium plate was not obtained to the base of the notch.

5. Sustained Load Tests:

Button-head specimens, Figures 3(a) and 3(b), were loaded on stress-rupture machines to determine the response to sustained load applications of the respective steels. Suitable aligning fixtures were employed to ensure concentricity of load application.

A limited number of 0.9 in. dia. specimens (stress concentration $K = 5$), Figure 3(c), were also tested. These specimens were tested in a suitable aligning fixture in a 300,000 pound capacity testing machine. The load was maintained by manual adjustment of the machine, while tests were limited to a maximum duration of one day.

6. Rotating Beam Fatigue Tests:

All fatigue tests were of the rotating beam type performed at room temperature on an R. R. Moore fatigue machine operated by means of a geared-down motor at approximately 250 rpm. All tests were limited to cycles ranging between approximately 10 and 10,000. The notched and smooth specimens used are presented in Figures 3(d) and 3(e) respectively.

7. Bend Tests:

The suitability of a small size constant strain rate bend test for the evaluation of hydrogen embrittlement in high strength steels has been discussed elsewhere (10). An adaptation of this test* with the use of a large capacity multi-strain rate multi-specimen testing machine (11) has been employed in the execution of bend tests on the present program. A photograph of the testing machine is presented in Figure 4.

The specimens, Figures 3(f), were loaded by the application of a bend-

---

*The test set-up described in (10) and (12) led to a nearly constant strain rate through the test. The present test set-up does not ensure constancy of strain rate, but the deviations are not considered as important to the test results.

ing moment at each end. The rates of twisting which are entered in the
figures were 2.87, 0.359 and 0.006 rpm approximately.

8. Hydrogen Analyses:

Suitable sections of electroplated specimens were submitted to the
National Research Corporation, Cambridge, Massachusetts, for hydrogen de-
termination. The hydrogen-bearing specimens, immediately after electro-
plating, were cooled in dry ice and were shipped by air freight. Specimens
were kept at the reduced temperature until analyzed. The treatment employed
is one which has been used to prevent diffusion of the hydrogen (10) into
the specimen, and that it is probably effective may be gathered from the
fracture results reported by Troiano et al (14).

9. Metallography:

All fractures were regularly examined visually and at low magnifi-
cations. Specimens which remained unbroken after testing were, in selected
instances, sectioned longitudinally and examined for fracture development
at the base of the notch.

10. Representation of the Test Data:

In the development of the text of the report reference is made to
characteristic curves and summary plots of the data. Additional data are
presented by means of photographs.

Full graphical presentation of the data is made in the Appendixes.

All figures are numbered consecutively through the report. This leads
to occasional duplication and where such duplication obtains the number of
the figure for its first appearance is entered parenthetically after the
current figure number.

EXPERIMENTAL RESULTS

1. Hydrogen Analyses of the Steels Studied:

A relatively complete study of the notch properties of 4340 steel containing controlled amounts of gases in essentially uniform distribution has recently been reported by Rinebolt and Raring (15). In the aggregate, hydrogen present in measurable amounts was found to promote delayed failures for sharply-notched specimens subjected to sustained loads. Among other things, the hydrogen content of 4340 steel after different charging conditions and after different room temperature aging times was reported. These data are presented in Figures 5 and 6.

The relationship between the hydrogen pick-up of the steel and the charging time is of interest, but the data are reported here only to provide an index of the uncertainty in the hydrogen measurement at 0 hrs. in Figure 6. It would appear from this comparison that 4340 steel cathodically charged may be expected to contain an average of from 2. to 3. ppm. hydrogen. However, since the hydrogen is now known to be largely concentrated at the surface of the specimen and since the full dimensions of the specimens are not given the numerical values reported in Figures 5 and 6 are not subject to quantitative interpretation. These relationships, qualitatively, are informative. First it is indicated that the average hydrogen level in the steel after the cathodic deposition of hydrogen is relatively low, and secondly that this hydrogen level is rapidly reduced with time of holding at room temperature. However, the hydrogen content is not reduced to 0, but to about 0.5 ppm, the value that was observed for the as-melted, i.e., unembrittled, stock. This would indicate that cathodically introduced hydrogen should prove relatively simple to reduce to a low level. This relationship between hydrogen content and holding time, however, does not exist for plated specimens. Numerical values for the hydrogen analyses completed in this investigation are presented in Table IV.

In all, 74 hydrogen analyses were completed on bend specimens taken from the aggregate of steel compositions. The average hydrogen content for the as-plated specimens was 5.2 ppm. The average hydrogen content for the baked specimens was 5.0 ppm. It is evident from these values that baking has not promoted the outward diffusion and thus elimination of hydrogen from the steel. On the contrary, the Cd-plate has been a total barrier to the outward diffusion of the electrodeposited hydrogen.

The program of hydrogen analyses which was completed is presented in Table IV(a). The data are grouped according to steel and specimen type in Tables IV(b) to IV(o). Despite the large scatter of the values reported in these tables the important additional observations are made as follows:

1. The average hydrogen content for the bend and sustained load specimens differs significantly, with that for the bend specimens being higher.

2. Within the scatter of the data steel composition has no effect on the amount of hydrogen contained in the specimen after Cd-electroplating.

2. Sustained Load Tests:

According to the Griffith-Orowan theory of sustained load failures as developed by Petch and Stables, the notch in a sharply notched specimen constitutes the Griffith crack. As was pointed out earlier, this crack has been observed experimentally to develop and grow. However, as the notch root radius is increased, it may be expected that the notch eventually will no longer function as a Griffith crack. For such experimental conditions the fracture process due to the action of hydrogen may be expected to be different from that described for the very sharp notch. In addition to this, relatively mild notch conditions characterize service applications. Sustained load tests, therefore, are needed to establish the effect of notch sharpness on hydrogen induced crack development.

In all, seven steels have been studied. However, it is necessary to discuss in detail the results obtained for only one steel, as the variables introduced affect the different steels in much the same way. 4340 steel has been selected for detailed examination.

4340 Steel:

Under the most severe notching conditions, 4340 steel was found to be subject to sustained load failures at all strength levels examined, Figure 7. After tempering at 400, 500 and 700°F nearly the same load vs. "time to rupture" curves were obtained and, in general, failure occurred after a loading time of less than 10 hours, at a nominal stress of from 50,000 to 75,000 psi.

Tempering at 800 and 1000°F led to a displacement of the stress vs. "time to failure" curves to the right and to higher stresses. The indicated improvement in properties, therefore, increased progressively as the tempering temperature was raised from 700°F.

For the stress concentration of 10, sustained load failures due to the action of hydrogen introduced on Cd-electroplating are very serious for 4340 steel tempered at from 400 to 700°F inclusively. Reduced properties can be expected from this source after tempering at 800°F. Even after tempering at 1000°F, failures arising from the action of electrodeposited hydrogen may be expected.

For specimens containing a notch leading to a theoretical stress concentration of 5 only slightly modified results are obtained, Figure 8. But as the stress concentration is reduced to 3, Figure 9, rather marked changes in the series of curves take place.

Perhaps the most significant of these changes is that associated with the minimum fracture stress which is plotted in Figure 12. After tempering at from 400 to 700°F a nearly constant minimum stress to produce failure is measured for stress concentrations of 10 and 5. At higher tempering temperatures, the minimum stress is raised. At a stress concentration of 3 a minimum is indicated in the "minimum strength" vs. tempering temperature curve, Figure 12. This occurs at a tempering temperature of about 600°F. At this stress concentration ($K = 3$) increased resistance to hydrogen embrittlement is obtained by tempering at 400°F or at 700°F and above. There is then evidence of the 500°-embrittlement phenomenon for the mildly notched specimens.

The trend of the data for a stress concentration of 3 is established with greater emphasis at a stress concentration of 2, Figures 10 and 12. The data reported in this last set of curves were obtained for a different heat of 4340 steel, (cf. WADC TR 55-18 Part 1) but, none the less, are properly ordered in the present comparisons. Finally, for smooth specimens, i.e., $K = 1$, while sustained load failures occur, Figure 11, such failures take place with little drop in stress. The breaking stress (100 hours) (S_{100}) vs. tempering temperature curve, Figure 12, thus differs little from that measured for unembrittled smooth specimens. Additional detail of interest and presented in Figure 12 is best considered by taking sections of this figure at constant tempering temperature, as has been done in Figure 13.

In Figure 13 the breaking stress at 100 hours is plotted against stress concentration with tempering temperature as parameter. Included in the figure are the strength values for non-plated specimens. It is immediately evident that Cd-plating has introduced major changes in the notch properties of the steel studied for all tempering conditions and for all conditions of notching. In this plot the strength of smooth specimens is indicated as unaffected by the presence of hydrogen.

After tempering at 400, 500 and 700°F the minimum strength (S_{100}) of plated specimens with increasing stress concentration drops abruptly from the values measured for the smooth specimens. This is in contrast to the indicated behavior of the non-plated specimens. Further, little numerical difference is noted for the three tempered conditions.

For specimens tempered at 800 and 1000°F, on the other hand, the minimum strength of plated notched specimens, in keeping with the trends measured for the non-plated specimens, first increases with increase in the stress concentration and then at high values of stress concentration is reduced. In conformance with the concept that the action of hydrogen in the steel is to effectively reduce the cross-section, the trend of these data is that expected.

In brief summary, the above sustained load data show that a profound difference in fracture behavior may be expected from plating 4340 steel which has been tempered at from 400 to 700°F. For this steel tempered at 800 and 1000°F the sustained load data, at first inspection, are understandable in terms of a section reduction arising from the action of hydrogen in the steel. Thus for the notched specimens, the qualitative trends of the data are similar to that for the non-plated specimens. The quantitative differences would then be due to the reduction of the load-bearing section of the specimen through hydrogen induced crack development. The questions of crack development in smooth specimens and the fracture behavior of specimens tempered at and below 700°F are discussed in a later section.

98B40 Steel:

The notch strength (S_{100}) of plated specimens as a function of the tempering temperature is presented in Figure 14 with the stress concentration as parameter. These data with certain variations are in agreement with the results obtained for 4340 steel. Of principal interest are the facts that the 98B40 steel studied is more sensitive to the action of hydrogen in leading to embrittlement for a tempering temperature of 400°F, and that in contrast to 4340 steel the tempering temperature range characterizing greatest sensitivity to hydrogen extends to 800°F and possibly higher. These trends are best shown in Figure 15. Thus at tempering temperatures of 800°F and below, the notch strength of plated specimens drops rapidly with increasing stress concentration from the strength measured for the smooth specimens. Tempering at 900°F promotes an initial increase in the notch strength with increase in stress concentration followed by the expected notch strength reduction at the highest stress concentrations.

4330 V-Mod. Steel:

The notch strength (S_{100}) of plated specimens as a function of the tempering temperature is presented in Figure 16 with the stress concentration as parameter. The notch strength (S_{100}) as a function of stress concentration with the tempering temperature as parameter is presented in Figure 17. These data clearly are related to the data obtained for both the 4340 and 98B40 steels. Thus by the discussion earlier developed in considering the data for 4340 steel, the 4330 V-Mod. steel becomes susceptible to

hydrogen embrittlement at a tempering temperature of 750°F and becomes increasingly embrittled as the tempering temperature is reduced. While the tendency to develop the embrittled condition exists at all but the highest tempering temperatures, the degree of embrittlement for this steel is less than that observed for both the 4340 and 98B40 steels.

The behavior in the sustained load test of the three steels 4340, 98B40 and 4330 V-Mod. suggests that for a series of steels of related composition and tempered to a comparable tensile strength, the order of increasing susceptibility to hydrogen embrittlement is the order of increasing carbon content.

Hy-Tuf Steel:

The three steels 4330 V-Mod., 4340 and 98B40 are low-silicon bearing steels forming a characteristic group. The three steels next to be examined are alloyed with about 1.5% silicon and form a group with characteristic properties which are qualitatively different from those measured for the first three steels. Thus the 1.5% silicon materials are characteristically relatively insensitive to pronounced embrittlement through the action of electrodeposited hydrogen, as is emphasized in the stress-rupture data for Hy-Tuf steel presented in Figures 18 and 19. This steel at a strength level of 230,000 psi, while subject to sustained load failures, suffers such failures only when the applied loads are high and sustained for a long period of time. This steel, therefore, is only slightly embrittled through Cd-electroplating.

Crucible UHS-260 Steel:

The 1.5% silicon steels as a group develop tensile properties which are modified only slightly for relatively wide changes in tempering temperature. The Crucible UHS-260 steel available for the present study was heat treatable to strength levels of 250,000 psi and 270,000 psi. This steel heat treated to these strength levels provides much needed data to bridge the large gap between the tensile strengths measured for Hy-Tuf and Tricent steels. The notch strength (S_{100}) vs. tempering temperature and the notch strength vs. stress concentration data are presented in Figures 20 and 21.

These data indicate that Crucible UHS-260 like Hy-Tuf is relatively insensitive to the embrittling action of electrodeposited hydrogen. It is interesting to observe that for this steel susceptibility to embrittlement increases as the tempering temperature is raised from 550 to 800°F.

Tricent Steel:

The notch strength (S_{100}) of plated specimens as a function of the

tempering temperature is presented in Figure 22 with the stress concentration as parameter. The response of this steel to the action of hydrogen is complex and at the present time no reasons for this behavior can be advanced. Thus for mild notch conditions (K = 3), maximum resistance to hydrogen induced failures obtains after tempering at 400°F. For the intermediate notch severity (K = 5) optimum properties are obtained after tempering at 550°F. For the sharpest notch, properties at all tempering temperatures are equal.

The steel is relatively notch sensitive despite the high notch strength (S_{100}) as may be gathered from Figure 23. The notch strength rapidly drops from the stress measured for the smooth specimen as the notch severity is increased.

Super TM-2 Steel:

This steel was studied at a strength level of 275,000 psi obtained by tempering at 500°F. The stress rupture and notch strength (S_{100}) data are presented in Figures 24 and 25.

3. Sustained Load Strength vs. Tensile Strength:

For the steels studied three are regularly heat treatable to a tensile strength of 290,000 psi, but of the materials studied in this work only 98B40 and Tricent clearly attain this specified strength level. At this strength level superior properties are obtained with Tricent as is clearly indicated in Figure 26. The 98B40 steel at a tensile strength of 290,000 psi is evaluated as highly sensitive to the action of hydrogen.

Similar comparisons of the data for tensile strength levels of 270,000; 250,000; 230,000; 210,000 and 180,000 psi are presented in Figures 27 to 31. The trends of these data may be profitably appraised also when plotted against tensile strength while the stress concentration factor is held constant as in Figures 32 to 34. These data have an immediate application in the evaluation of the properties of small sections of the steels heat treated to the pertinent strength levels.

4. Sustained Load Strength vs. Specimen Size:

In Figure 2 it was pointed out that the effects of hydrogen, introduced into the metal as a consequence of electroplating, in leading to sustained load failures should be minimized as the specimen size increases. To examine this prediction a series of sustained-load tests were completed on Cd-plated 0.9 in. dia. specimens. The limited test results obtained are presented in Figure 35. Of particular interest is the fact that specimens tempered

WADC TR 56-395 Pt 3   15

at 400°F are much more susceptible to the action of electrodeposited hydrogen than are the specimens tempered at 600°F These results are compared in Figure 36 with data obtained for the plated 0.3 in. dia. specimens and with data obtained for variously sized non-plated specimens.

In this figure the pronounced roles of size for the non-plated specimens and hydrogen induced brittleness for the plated specimens are clearly set forth. Since the notch strength values plotted are nominal, the data in this figure are singularly significant.

Thus, for the unplated specimens a monotonically decreasing notch strength is measured as the specimen size increases. For the plated specimens a monotonically increasing notch strength is measured. These two quantities must eventually bound a notch strength which is a limiting quantity for the steel and heat treatment. A transition from a high to a low numerical value is indicated for this quantity but the data available are not sufficient to allow a complete discussion of this transition at this time.

The sustained load tests which have been discussed for the small specimens are directly applicable to the evaluation of properties to be expected in service applications of the steels studied when the service members are small. However, it is evident that as the structural member increases in size the adverse effect of hydrogen embrittlement will be minimized. This does not mean, however, that properties of small size unembrittled specimens will be realized because with increase in section size an adverse section size effect may be introduced. Since the changes in section size affect the notch properties differently for the different steels, it is not possible to propose without reservation the properties to be expected in large electroplated sections. Maximum notch strengths, however, can be estimated from the data obtained in the section size study and reported in WADC TR 56-395 Part 1. Selected data are presented in Figure 37. These data are offered as probably qualitatively indicating the trends of the notch properties in high strength electroplated steels. These predicted trends, however, should be checked by suitable tests.

5. Fracture Development Under the Joint Action of Hydrogen and Sustained Load:

Crack development resulting from the joint action of hydrogen and stress as it has been described previously (3) (4) (5) is essentially from the base of the notch into the core of the specimen. The machined notch, therefore, functions as a Griffith crack and the experimental conditions, i.e., hydrogen induced crack growth, lead to the extension of this crack with eventual failure of the section. The conditions here described are not obtained for a smooth or mildly notched specimen and the failure of these latter type specimens is a point of interest. Two examples of the fractures obtained for smooth plated specimens are presented in Figures 38 and 39.

While these fractures resulted from the action of hydrogen, at least in point of initiation, it is striking that the preliminary stage of crack development has led to the extension of internal cracks. For Figure 38 the crack is clearly nucleated at or near the surface, but for Figure 39, there is no obvious connection between the internal crack and the surface until after the fracture is completed. Thus for both specimens fracture has taken place due to the separation of zones in the specimen which are expected to be relatively hydrogen free (5). Further while the broken sections are modified cup-cone fractures, in contrast to what would be expected, the reduction of area (Figure 38) is either nil or very small. This signifies that the indicated shear failures were generated in the hydrogen rich zones with greater ease than could be the failure associated with the maximum normal stress.

The fracture sequence is then describable in stages as follows:

1. Figure 38:

    a. A fracture nucleus obtains at or very near the specimen surface,
    b. Due to the action of hydrogen this nucleus is activated and grows,
    c. The crack surface that develops functions as an effective stress raiser and strengthens the critical section in which it is developed. This strengthening effect is sufficient to arrest further crack development in the absence of hydrogen,
    d. Due to the presence of hydrogen, however, the crack continues to develop until it leaves the hydrogen containing zone, due to mechanical overloading,
    e. Further crack development takes place until mechanical equilibrium is established. The crack then stops, and at this stage the internal crack has developed to the degree indicated by the granular fracture surface in Figure 38,
    f. Final failure takes place when the hydrogen has diffused through the remaining intact metal to a sufficient degree to allow precipitation along the indicated shear planes of failure. This hydrogen precipitation is proposed to allow the shear failure to progress without requiring general plastic deformation.

2. Figure 39:

    a. For this specimen no surface nucleation of fracture is observed, while the fracture is a cup-cone fracture,
    b. Fracturing has taken place after significant plastic strain, as measured by reduction of area,
    c. The fracture is considered as differing but little from a normal tension fracture,
    d. It is proposed that fracture for this specimen resulted from an overloading of the specimen due to the weakening of the outer fibers of the specimen through the presence of hydrogen.

When specimens containing a mild notch are tested after electroplating, behavior similar to that described for Figure 38 may be observed, Figure 40. For this specimen a crack was nucleated under but close to the surface-- the crack then developed by internal extension with eventual fracture resulting from the consequent eccentricity of loading with the development of a nearly continuous shear lip about the base of the notch.

That the fracture nucleus may develop under the surface of the notch is emphasized by consideration of Figure 41. The small independent fracture nuclei here present, clearly do not extend to the surface, but, in the aggregate, have eventually promoted failure.

From the above discussion it may be seen that the fractures resulting from crack formation due to the action of hydrogen arise from the interaction of a complex of factors. Among these factors are: a) the notch geometry, b) the hydrogen distribution, and c) the role of normal and shear stresses in leading to crack formation.

It is evident from the discussion of Figures 40 and 41 that mild notches do not function as suitable Griffith cracks. The fracture nuclei which originate at the surface in smooth and mildly notched specimens, probably are associated with tool marks or inclusions. Internal fracture nuclei may be associated with inclusions initially and their growth can be likened to the development of "fish eyes" associated with hydrogen induced failures in softer steels. However, still another potentially pertinent factor is the condition of triaxiality of stresses.

If a limiting condition of triaxial stress is required to produce fracture, this condition could be established by a suitable inclusion. It potentially could be established also at the cupic point* for the stress system induced by the notch. For sharp notches this point would lie close to the surface near the root of the notch. For mild notches this point would be increasingly toward the center of the specimen. Considering the depth of hydrogen penetration immediately after plating (5) for sharp notches the condition of maximum triaxiality would obtain in a hydrogen enriched zone, while for mild notches hydrogen diffusion would be required to reach this point. For a very sharp notch it would be difficult to differentiate between a crack arising through extension of the notch base and one which arises discontinuously by separation at the cupic point and subsequent extension to the surface.

Examination of numerous specimens for shear lip development, which may be taken as evidence of subsurface fracture nuclei formation, revealed that a shear lip frequently obtained. Typical results are sketched in Figures 42 to 45. From these data it follows that a hydrogen induced shear failure regularly accompanies crack formation. Such shear failures can be of two types, the first of which has already been described while the second

*In reality a sub-surface ring for the type specimens used in this investigation.

is indicated in Figure 46, which is a vertical section through the notch base of a 0.9 in. dia. specimen which had been loaded after Cd-plating.

The stress concentration of 5 was obtained for this specimen with a notch root radius of 0.005 inch. For this geometry the cupic point lies about 0.005 inch under the notch base while a condition of maximum shear stress exists at the base of the notch and at $\pm 45°$ into the specimen. Hydrogen fractures are well developed both in the vicinity of the cupic point due to the action of maximum normal stresses at the cupic point and along the lines of maximum shear stresses. It is interesting to note that none of the cracks has clearly opened to the surface in Figure 46a. In Figure 46b, on the other hand, the shear stress induced cracks clearly open to the surface, while that due to the action of the maximum normal stress does not.

For a specimen that generates multiple cracks such as are presented in Figure 46, it is probable that the notch strength modification due to the action of hydrogen will be relatively small. However, crack development can take place in a second way which is much more serious. Such crack development is indicated in Figure 47.

For the specimen in Figure 47 fracture growth progressed at a maximum rate in the vicinity of the nucleus which was apparently subsurface. The growth of the crack progressed with the development of the nearly semicircular "mirror surface." A consequence of this was the development of progressive eccentricity of loading with eventual cataclysmic crack development from the top region in the photograph to the bottom. This type of loading pattern, crack development and fracture propagation is probably the most common type leading to structural failures.

6. Fatigue Tests:

The fatigue properties of 4340 steel containing electrodeposited hydrogen introduced through a potential cleaning operation have been discussed in an earlier report (WADC TR 55-18 Sup. 1) (16). In this earlier work it was found that the rotating beam fatigue test as executed was a relatively insensitive test of the degree of hydrogen embrittlement. However, in the low-cycle high-stress range the hydrogen introduced through the impregnating treatment used led to early failure. Very closely related behavior is observed for Cd-plated specimens from a different heat of 4340 steel, Figures 48 to 52.

Where compatible the earlier results are introduced into these figures as the dotted lines. It is evident from these figures that in the fatigue test Cd-electroplating is somewhat less embrittling at low cycles than was the cathodic treatment previously used.

In the fatigue test for 4340 steel nearly uniform S-N behavior was

observed for all notched specimens. For Tricent steel on the other hand the notch acuity played an important role in determining the test results, Figure 53. As the tempering temperature was raised, the influence of the notch acuity became less important, Figures 54 and 55. The trends observed are thus related to the notch strength trends observed in the sustained load tests, Figure 22.

The S-N data for sharply notched specimens for the various steels tempered to the specified strength levels, viz., 290,000; 270,000; 250,000; 230,000; 210,000 and 180,000 psi, are presented in Figures 56 to 61. It is evident from these curves that relatively minor alterations in the fatigue results have been introduced by Cd-electroplating and these variations are so small that the fatigue test as here executed gives slight direct information concerning the phenomenon of hydrogen embrittlement.

7. Fracture Development in the Fatigue Test:

For hydrogen impregnated smooth rotating beam fatigue specimens crack development progresses from numerous nuclei. When the consequent section reduction exceeds an amount that depends on the notch sensitivity of the steel and the applied load, fracture takes place. Typical fractures for smooth specimens are presented in Figure 62.

The fracture development in the smooth specimens depends on chance nucleation of the fatigue crack. The crack as a consequence develops from a highly restricted point and the detailed role of the ultimate crack configuration in leading to failure cannot be determined in quantitative terms. Qualitatively the section reduction depends on the applied load and notch sensitivity of the steel.

For notched specimens, on the other hand, the crack develops within a few cycles after the specimen is loaded and is developed circumferentially at a much higher rate than it is radially. This is true for all notch dimensions which have been used in the present work. Again the crack development is determined by the load on the specimen and by the notch sensitivity of the steel as is indicated in Figure 63.

The fatigue test on notched specimens thus is a test which allows a crack to be initiated and propagated under initially controlled conditions. As the crack is developed, the stress on the uncracked section increases until the fracture strength is exceeded. The fracture strength is a dynamic notch strength for which at the present time absolute numerical values cannot be advanced, but relative measurements can be made. Thus from Figure 63, diameter measurements for a given initial load can be made for the material examined as a function of tempering temperature. Such measure-

ments* for 98B40, 4340 and 4330 V-Mod. steels are presented in Figure 64. For these steels the indicated change in fracture diameter corresponds to a change in the notch strength of about 50%, as determined from Figure 63.

Thus the fracture area changes given in Figure 64 result from notch strength changes as given in Figure 65. These data plotted against tensile strength are given in Figure 66. It is evident that the fracture area data provide an excellent method for determining the notch sensitivity of the steels under investigation. It is pointed out, with reference to the present investigation, however, that the test data here presented characterize the hydrogen free core of the specimen tested and thus are not of necessity an index of the embrittling effect of electrodeposited hydrogen.

8. Bend Tests:

The general behavior in the bend test of a high strength steel containing electrodeposited hydrogen has been discussed in detail elsewhere (4) (10). At high rates of bending, ductility is high; at low rates of bending, ductility is reduced and in some at present unspecified relationship, in proportion to the amount and distribution of the hydrogen deposited. Hydrogen introduced by Cd-electroplating may be expected to produce comparable behavior to that earlier reported for relatively severe cathodic embrittlement. (10)

For the 4340 steel, Figure 67, it is shown that the magnitude of the embrittlement is a function of the strength level for the steel as well as of the strain rate. Specifically, 4340 steel tempered at 800 and 1000°F is not indicated as embrittled by the electroplating. Specimens tempered at 400, 500 and 700°F are embrittled. Baking is relatively effective in removing the embrittlement due to hydrogen, but from the results of the analyses earlier reported it is apparent that the improvement in ductility results from a redistribution of the hydrogen and not from its elimination from the steel.

The results for the 4340 steel are perhaps more revealing when plotted as in Figure 68. Here the pronounced effect of tempering temperature on the susceptibility of the steel to hydrogen embrittlement is emphasized. According to these data, the 4340 steel is highly susceptible after tempering at temperatures below 700°F. The "500°-embrittlement" range is also indicated. Baking has largely restored the original ductility of the steel, but the "500°-embrittlement" range is still observed.

Qualitatively the 98B40 and 4330 V-Mod. steels respond in a manner very similar to that observed for the 4340 steel.

*These measurements in the present work have not been made with high precision, but such measurements can readily be made.

The 4340, 98B40, and 4330 V-Mod. steels as a group are steels which tend to become increasingly susceptible to hydrogen embrittlement, due to the action of electrodeposited hydrogen, as the tempering temperature is reduced or as the tensile strength increases above a value of about 200,000 psi. A second group of steels has been studied in the present investigation for which, in some measure, contrary performance is observed. That is, optimum resistance to hydrogen embrittlement is obtained at low or intermediate tempering temperatures and this embrittlement resistance may be reduced by tempering at either lower or higher temperatures. The best example of this behavior is provided by the proprietary steel Tricent, Figure 69. By the bend test "Tricent" is seen to be nearly unaffected by the presence of hydrogen introduced into the steel during Cd-electroplating, for a tempering temperature of 550°F. As the tempering temperature is lowered or raised from 550°F, embrittlement of the steel is increasingly severe.

Tempering temperature effects were less completely studied for Hy-Tuf, Crucible UHS-260 and Super TM-2. For the single tempering treatment used for Hy-Tuf steel, no embrittlement effect due to Cd-electroplating was observed in the bend test, Figure 70.

Crucible UHS-260 steel responded to the action of hydrogen with change in tempering temperature in a manner closely related to that observed for Tricent. Characteristic bend data vs. testing speed are presented in Figure 70. Here it will be noted that the fracture angle vs. testing speed curves tend to maximize. The low rate at which the bend angle is reduced as the testing speed is reduced is an indication of the resistance of this steel to hydrogen embrittlement. The slight reduction at the high strain rate may be accidental and should be evaluated by properly designed tests.

Super TM-2 steel was also found to possess good resistance to hydrogen embrittlement, Figure 71. Behavior of this steel in the bend test was closely related to that observed for Crucible UHS-260.

The data taken in the bend test depend on the testing speed. It is probable then that the test to be of optimum value should be completed at a specified testing speed. The test data taken for the different steels tempered to specified strength levels are, therefore, compared in Figures 72 to 77.

Two steels only were found to reach the 290,000 psi tensile strength level, namely 98B40 and Tricent, Figure 72. Tricent is evaluated in the bend test throughout as superior to 98B40 over the range of testing speeds studied. Both steels at this strength level, however, are clearly susceptible to embrittlement due to the action of hydrogen.

At the strength level of 270,000 psi the 4340 and 98B40 steels are very sensitive to hydrogen embrittlement. Tricent, Super TM-2 and Crucible UHS-260 are insensitive to this embrittlement, Figure 73.

At the strength level of 250,000 psi the greatest resistance to hydrogen embrittlement is observed for Crucible UHS-260 steel, Figure 74.

As the tensile strength is reduced to 230,000 psi, several steels, in the bend test, are evaluated as relatively insensitive to hydrogen embrittlement from the action of electrodeposited hydrogen through Cd-plating, Figure 75. The most resistant steel, however, is Hy-Tuf. At lower strength levels several steels are evaluated as highly resistant to hydrogen embrittlement arising from Cd-electroplating, Figures 76 and 77.

The bend test results for the lowest testing speed are summarized in Figure 78. As a function of increasing tensile strength, the two groups of steels previously noted are clearly indicated. An appraisal of the several similarities and dissimilarities among these steels suggests the importance of the presence or absence of silicon as an alloying addition in the steels compared. For the silicon dilute steels, embrittlement due to electrodeposited hydrogen becomes increasingly severe as the tensile strength is allowed to increase. For the silicon bearing steels, sensitivity to hydrogen embrittlement may be markedly reduced as indicated in the bend test at a tensile strength as high as 270,000 psi.

The several steels which have been studied clearly possess optimum resistance to hydrogen embrittlement in restricted tensile strength ranges. (It is assumed as probable that this embrittlement resistance is more properly related to a tempering temperature range for each steel and thus indirectly to the tensile strength.) As a consequence, there is no indicated general purpose steel which will possess high hydrogen embrittlement resistance throughout the tensile strength range of 180,000 to 300,000 psi. The steels possessing the superior properties in the normally specified tensile strength intervals above 180,000 psi are given in Figure 79, as determined in the bend test.

On the basis of this figure it is indicated that minimum resistance to hydrogen embrittlement is obtained at the tensile strength levels 250,000 and 290,000 psi. As indicated in the bend test, materials resistant to hydrogen embrittlement can be obtained for the other strength levels examined by a proper selection of steels.

9. Fracture Development in Bend Specimens:

The development of the crack leading to failure in the bend specimen took place in much the same way for each steel.

Thus termination of the test took place either with the specimen intact or with the development of a failure which was either complete or partial as given in Figure 80. As is evident in this photograph, the crack has developed in a manner characterizing a shear fracture. The general de-

velopment of this fracture suggests the likely formation of small shear fractures over the surface of the specimen and the eventual failure of the specimen due to the subsurface extension of such a network of cracks and consequent overloading of the section.

A macrograph of the postulated surface crack nuclei developed in a selected specimen is presented in Figure 81.

From this photograph it is evident that the postulated nucleation and crack growth mechanism may obtain. However, the general development of the network of fracture nuclei depends on the strain to fracture. Thus for low fracture strains few fracture nuclei are formed, but such nuclei as do form may grow extensively, Figure 82, in contrast to the behavior when the fracture strain is high. In the latter case the fracture nuclei are numerous and highly localized, as in Figure 81.

At high testing speeds the fracture nuclei are associated with pronounced plastic deformation, while at low testing speeds the fractures tend to be brittle shear type fractures, cf. Figure 38.

The bend data may be interpreted as follows:

1. At high strain rates the outer fibers of the specimen are strained at a rate which minimizes the action of hydrogen in leading to embrittlement. All specimens then fail through mechanical overloading and the results of the test are then essentially uniformly constant.

2. At low strain rates crack development sets in at a relatively low strain as indicated by bend angle. For those materials which are notch sensitive an early transverse crack develops to dimensions such that it can run freely and the specimen breaks at a low bend angle.

   For notch tough materials, on the other hand, the transverse crack can form only in the notch sensitive hydrogen-containing surface layers of the specimen. Failure, if it occurs, then develops through mechanical overloading of the section due to the bending action and not through the notch sensitizing action of the hydrogen induced crack development. The bending angle measured for this condition then tends to be near that measured at the high strain rates.

DISCUSSION AND CONCLUSIONS

Hydrogen induced delayed failures result from the development of suitably propagating cracks. The development and extension of the hydrogen induced cracks are functions of the loading condition, the stress concentration, the notch sensitivity of the steel, and the hydrogen distribution. For the three tests which have been used in this program, the factors, except ostensibly the notch sensitivity, vary in a unique way for each test.

For the sustained load test on notched specimens the crack, once formed, constitutes a severe stress raiser. The load on the section in the presence of this stress raiser is not, in general, sufficient to cause the crack to propagate due to overloading. The crack propagates due to the diffusion of hydrogen to the critical section and the re-establishing of the conditions which initially led to crack development. Crack propagation, therefore, is controlled by the diffusion of hydrogen.

In the rotating beam test, the loading conditions, in their own right, are sufficient to cause crack development. Even in an unembrittled notched specimen, the crack begins to form at the base of the notch shortly after the load is applied so that a crack is driven through the outer fibers of the specimen within a relatively short number of cycles. Thus, except for a test condition which runs for only a few cycles to failure, the fatigue test in the presence of cadmium plating leads to failure by fatigue loading of the metal. The test, further, is a high strain rate test and even when run at the reduced rate employed in this investigation, it is probable that the hydrogen introduced into the specimen plays only a secondary role* in the crack development. It is due to this phenomenon, however, that the notch fatigue test is an excellent test for the appraisal of the notch sensitivity of the steel, as was discussed above.

The bend test like the fatigue test predicates eventual failure. However, unlike the fatigue test the bend test is conveniently run at a strain rate which will allow crack nucleation to be controlled by the hydrogen entrapped in the specimen during electroplating. Once the crack is nucleated it is free to run if the metal under the crack is notch sensitive. If the metal is notch tough, further crack development is possible only if the specimen is sufficiently strained.

---

*In the high stress-low cycle range it is difficult to separate the sustained-load and fatigue effects, but when the test ran for a hundred cycles or more the effect due to hydrogen was slight.

Crack development takes place at a low rate in the sustained load specimens, at an intermediate rate in the bend specimens, and at a high rate in the fatigue specimens. The role of hydrogen in leading to failure in sustained loading clearly is a dominant one. In the bend test the hydrogen promotes the development of suitable surface cracks when the strain rate is low. At high strain rates surface cracks are formed through mechanical overloading. For notch sensitive metal cracks introduced into the surface cause failure at low strains. For notch tough materials the hydrogen induced cracks do not cause failure on their appearance and failure of the section is delayed until the fracture strain of the non-hydrogen bearing core is exceeded. In the fatigue test it cannot clearly be demonstrated from the tests completed that crack development is markedly influenced by the electrodeposited hydrogen.

On considering the manner of crack development in the above tests, it is at first sight surprising that data from each test can be found to correlate in the evaluation of the sensitivity of a steel to hydrogen embrittlement. It should be evident, however, that embrittlement due to electrodeposited hydrogen is in reality largely sensitivity to notches. Since, as it has been shown, at the time of failure in each of the tests, notches, in the form of cracks, exist, correlation of the results from each of the three tests should be possible if compatible indexes of notch sensitivity are employed. A proper index is some measure of notch strength.

In the sustained load tests a notch strength value is measured directly. The real average stress, however, is obtained by correcting for the section loss during crack development. In this way a "static crack" strength (17) is obtained. A compatible "static crack" strength is qualitatively deducible from the central fracture area in the fatigue test.* Here changes in the fracture area provide a measure of the fracture strength with the restriction only that the external load applied to the specimens remains constant.

In the bend tests it is most convenient to measure fracture strains. Fracture strains, however, are an index of the notch strength of high strength steels. The bend angle at fracture then should provide a usable index of hydrogen embrittlement.

Measurements of the minimum sustained load strength,** fracture angle and the reciprocal of the fracture area (fatigue test) for the 4340 steel are plotted in Figure 83. Also included in the figure are sustained load notch strength measurements made on 0.9 in. dia. Cd-plated specimens.

---

* Strain-rate effects are observed in the fatigue test, but they are second order effects and need not be considered here.
**Suitable area measurements were not completed on these specimens to allow static crack strength measurements.

Qualitatively the data compared are in good agreement. However, quantitative discrepancies of significance exist. There can be little question, however, but that the hydrogen embrittlement effect measured for Cd-plated high strength steels is in reality notch sensitivity. It is, therefore, possible to use the pertinent criterion for each of the tests to obtain an index of notch sensitivity and, therefrom, to measure or predict susceptibility to hydrogen embrittlement. However, it must be kept in mind that none of the tests studied is an absolute test and the results for each must be evaluated in a proper frame of reference. Of the three tests studied the sustained load and bend tests are practical tests for the evaluation of hydrogen embrittlement. The fatigue data can be misleading in the evaluation of the susceptibility of a silicon-bearing steel to embrittlement due to Cd-plating.

According to the fatigue test, the 4330 V-Mod. steel should be the most resistant to hydrogen embrittlement. The silicon-bearing steels at comparable strength levels, however, possess superior properties in both the sustained load and bend tests. This possibly indicates a reaction between the silicon and hydrogen leading to a reduced hydrogen embrittling effect in the silicon rich materials. Failures arising from the action of hydrogen in high strength steels are complex phenomena, but it is evident that certain of the materials studied have superior properties in the strength range above 200,000 psi. These materials have been indicated in the course of the presentation of the experimental results. The experimentation has, however, been largely completed on small specimens and it becomes necessary to determine the probable effect of specimen size change on the results measured. The problem of size effect thus arises. Limited data have already been presented by which this phenomenon has been examined directly. Limited data are available which provide an indirect approach to the examination of this question.

Among the various factors which vary when the phenomenon of size effect is considered is that of notch ductility. If notch ductility is high, size effect is not observed (18). If notch ductility is low, size effect is encountered. It follows from this that those factors which modify notch ductility are potentially usable in the development of a better understanding of size effect. Factors which probably influence notch ductility and which to some degree are readily accessible experimentally are, the testing temperature, the testing speed and the notch geometry. Specifically, if the testing temperature is sufficiently lowered; if the testing speed is sufficiently raised; and if the notch acuity is sufficiently increased, it is to be expected that notch ductility may be reduced to a minimum value. The notch strength then measured should correspond to the notch strength for a very large specimen and should constitute a limiting value. A few data are available to allow examination of these predictions.

The strain rate factor may be introduced by the completion of strength measurements in the tension impact test. Low temperature notch tension tests

have previously been reported (13). The notch strength in the presence of an infinitely sharp notch can be derived as has been done in this work. The data suitable for comparison are presented in Figure 84.

The impact tension data are seen to be indifferent for the purposes of the present comparison, but from the results of Clark and Wood (19) this is to be expected because of the relatively low strain rates used in the present work. Further the deformation processes in the strain rate interval, which is potentially characteristic for the present impact tension tests, are complex (20). The low temperature tension tests and the sustained load tension tests, on the other hand, establish trends which are those expected. Thus as the tempering temperature is lowered below about 800°F notch ductility is potentially impaired in the notch tension test. The notch strength which depends on the notch ductility is then reduced. Since the notch strength of a non-ductile material is essentially temperature independent (21), a change in size which may be required to suppress notch ductility at any given testing temperature should affect the fracture strength, to a first approximation, only in so far as it affects the notch ductility. Qualitative agreement between this theory and the available experimental data is indicated in Figure 84. The quantitative differences in these data, however, emphasize the need for additional work both on the 4340 steel for which these data are significant and for other types of steels for which no comparable data exist.

SUMMARY

A series of low alloy steels heat-treated to tensile strengths from about 180,000 to 300,000 psi has been studied for susceptibility to embrittlement due to Cd-electroplating. To determine the susceptibility three tests, namely, sustained load, fatigue and bend tests were used. Selected specimens after Cd-electroplating were analyzed for hydrogen content. The results and conclusions are summarized below.

1. Hydrogen introduced into Cd-electroplated specimens may be as high as that introduced through severe cathodic impregnation. The average amount of hydrogen, which, it is emphasized, varies with specimen dimensions, measured for flat bend and cylindrical stress-rupture Cd-plated specimens was 5.2 ppm and $\sim$ 2.5 ppm respectively.

2. Baking Cd-plated specimens sufficiently to restore ductility in the bend specimens led to no significant change in the average hydrogen content. The change in properties observed is thus assumed to result from a redistribution of the hydrogen through diffusion induced by the baking treatment.

3. By a suitable adjustment of the applied load, all steels for all strength levels examined can be made to fail under sustained loads by Cd-plating.

4. The susceptibility of a steel to sustained load failure after Cd-plating depends on the severity of the notching conditions, and on the metallurgical structure of the steel. The steels studied fall into two groups, one of which is comprised of steels which become increasingly insensitive to the embrittling action of Cd-plating with increasing tempering temperature, while the second is made up of steels which possess maximum insensitivity at intermediate tempering temperatures. The first group of steels is silicon dilute; the second is silicon rich.

5. While all steels studied can be made to fail in sustained-load after Cd-plating, steels possessing high resistance to this embrittlement can be obtained to strength levels as high as 270,000 to 280,000 psi. Structural control at these strength levels, however, must be ensured.

6. It can be predicted that with an increase in specimen size, susceptibility to sustained-load failures should decrease. The limited tests which have been completed support this prediction.

7. Sustained-load failures result principally from the formation of cracks due to the action of electrodeposited hydrogen. Crack formation, however, is a complex phenomenon, and the experimental conditions may be such that crack nucleation may be a surface or subsurface phenomenon, while crack propagation may take place in hydrogen-containing or hydrogen-free metal.

8. The high-load low-cycle fatigue properties of a steel are modified by Cd-plating. However, as an index of susceptibility to embrittlement due to Cd-plating this test is of limited applicability.

9. As a possible means of determining the notch sensitivity of a steel, the high-load low-cycle fatigue test offers much promise. This use of the test has been discussed in the body of the report.

10. Bend tests as completed in the present investigation offer a simple and reasonably adequate means for the evaluation of the susceptibility of a steel to embrittlement through Cd-plating. The order of the steels established in this test corresponds approximately to that established in the sustained-load test with small specimens at a stress concentration (K) of 5, Figure 85.

11. Failure in the bend test results from the nucleation and growth of surface cracks.

12. The manner of crack development in the three tests examined has been discussed at length. The significance of the experimental results as measures of notch sensitivity and in this way as measures of susceptibility to embrittlement through Cd-plating has been examined.

13. It has been proposed that size effect is intimately related to the notch ductility and data which bear on this question have been presented and discussed.

REFERENCES

1. Petch, N. J. and Stables, P., Delayed Fracture of Metals Under Static Load, Nature, Vol. 169, No. 4307 (1952) p. 842.

2. Orowan, E., Fundamentals of Brittle Behavior in Metals, in book "Fatigue and Fracture of Metals," Technology Press of Mass. Inst. of Tech. and J. Wiley and Sons (1952) p. 139.

3. Raring, R. H. and Rinebolt, J. A., Static Fatigue of High-Strength Steel, Trans. Am. Soc. Metals, Vol. 48 (1955) p. 198.

4. Klier, E. P., Muvdi, B. B. and Sachs, G., Hydrogen Embrittlement in an Ultra-High-Strength 4340 Steel, Trans. Am. Inst. Mining Met. Engrs., in press.

5. Barnett, W. J. and Troiano, A. R., Crack Propagation in the Hydrogen-Induced Brittle Fracture of Steel, Trans. Am. Inst. Mining Met. Engrs., in press.

6. Klier, E. P., Weiss, V. and Sachs, G., A Stepped Austenitizing Treatment for 4340 Steel, Tech. Note submitted to Am. Inst. Mining Met. Engrs.

7. Klier, E. P., Muvdi, B. B. and Sachs, G., The Static Properties of Several High-Strength Steels, submitted to Am. Soc. Test. Mat.

8. Muvdi, B. B., Sachs, G. and Klier, E. P., Design Properties of High-Strength Steels in the Presence of Stress Concentrations and Hydrogen Embrittlement, Part 1: Dependence of Tension and Notch-Tension Properties of High-Strength Steels on a Number of Factors, WADC TR 56-395 Pt 1 (1956).

9. Peterson, R. E., "Stress Concentration Design Factors," John Wiley and Sons, Inc., New York (1953).

10. Beck, W., Klier, E. P. and Sachs, G., Constant Strain Rate Bend Tests on Hydrogen Embrittled High Strength Steels, J. Metals, Vol. 8, P. 1263 (1956).

11. Tong, K. N., Plastic Flow and Fracturing of Metals, WAL 893/154-16, Summary Report to Watertown Arsenal (1955).

12. Tong, K. N., Plastic Flow and Fracturing of Metals, WAL 893/154-15, Final Report No. 5 to Watertown Arsenal (1955).

13. Sachs, G., Weiss, V. and Klier, E. P., Effect of a Number of Heat Treating and Testing Variables on the Notch Strength of 4340 Steel, Preprint No. 71, Am. Soc. Test. Mat. (1956).

14. Johnson, R. D. Johnson, H. H., Barnett, W. J. and Troiano, A. R., Hydrogen Embrittlement and Static Fatigue in High-Strength Steel, WADC TR 55-404 (1955).

15. Rinebolt, J. A. and Raring, R. H., The Effect of Gases in Steel, NRL Report No. 4683 (1956).

16. Muvdi, B. B., Sachs, G. and Klier, E. P., Design Properties of High-Strength Steels in the Presence of Stress Concentrations and Hydrogen Embrittlement, Sup. 1: Effects of Hydrogen Embrittlement on High-Strength Steels (Fatigue Properties) WADC TR 55-18 Sup 1 (1956).

17. Gensamer, M., Static Crack Strength of Metals: Its Determination and Significance, Metal Progress, Vol. 38 (1940) July, p. 59.

18. Weiss, V. and Klier, E. P., Factors Responsible for Notch Embrittlement of High-Strength Steels, Final Report No. 2 to Bureau of Aeronautics, Contract No. NOas 55-377-c (1955).

19. Clark, D. S. and Wood, D. S., Final Report, Contract N6-onr-24418, Proj. Desig. NR031-285, Sept. (1955).

20. Klier, E. P., Feola, N., Viggiano, A. and Weiss, V., The Properties of Constructional Metals as a Function of Temperature and Strain Rate in Torsion, WADC 56-216 (1956).

21. Georgieff, M. and Schmid, E., Bi, Z. Physik, Vol. 36 (1926) p. 759.
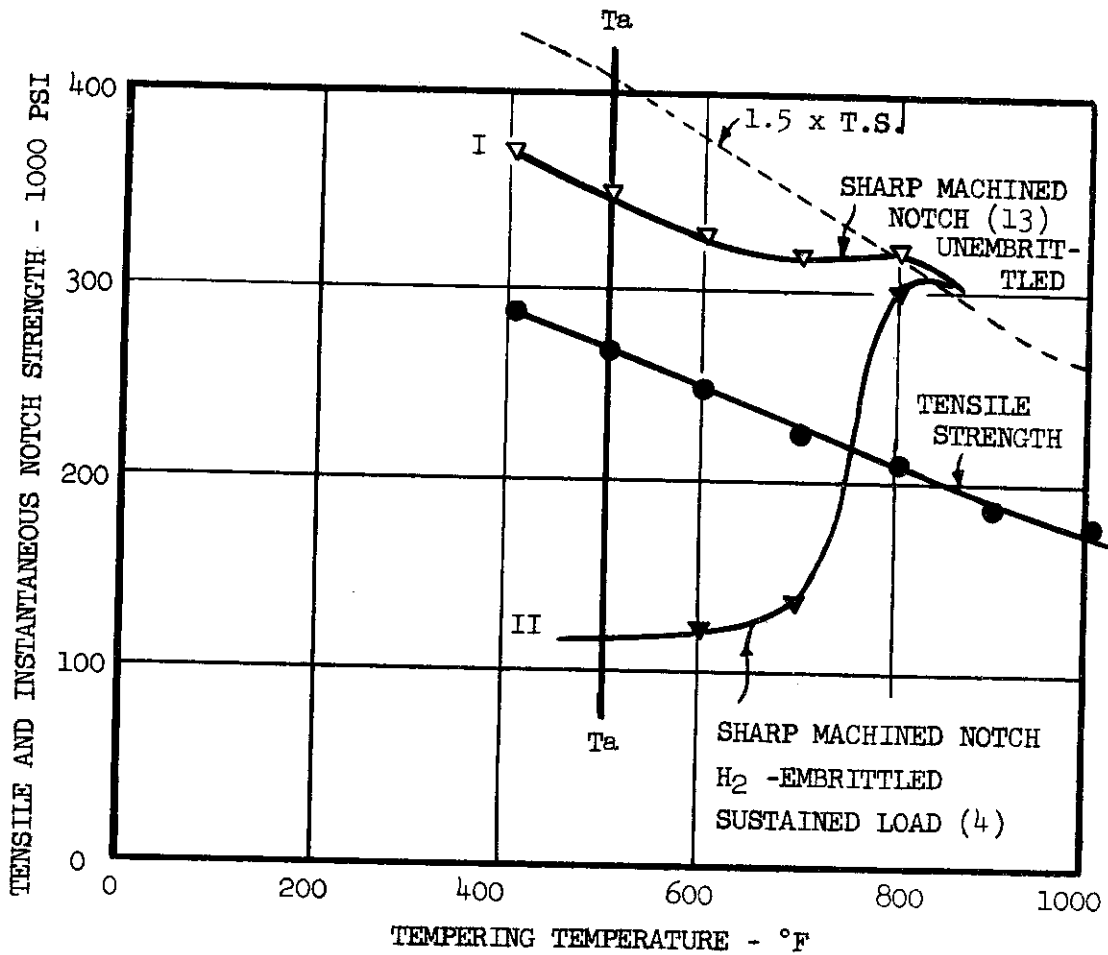
FIG. 1 THE INSTANTANEOUS NOTCH STRENGTH AT FRACTURE VS. TEMP-
ERING TEMPERATURE FOR 0.3 IN. DIA. SHARPLY NOTCHED
SPECIMENS FOR THE INDICATED CONDITIONS.
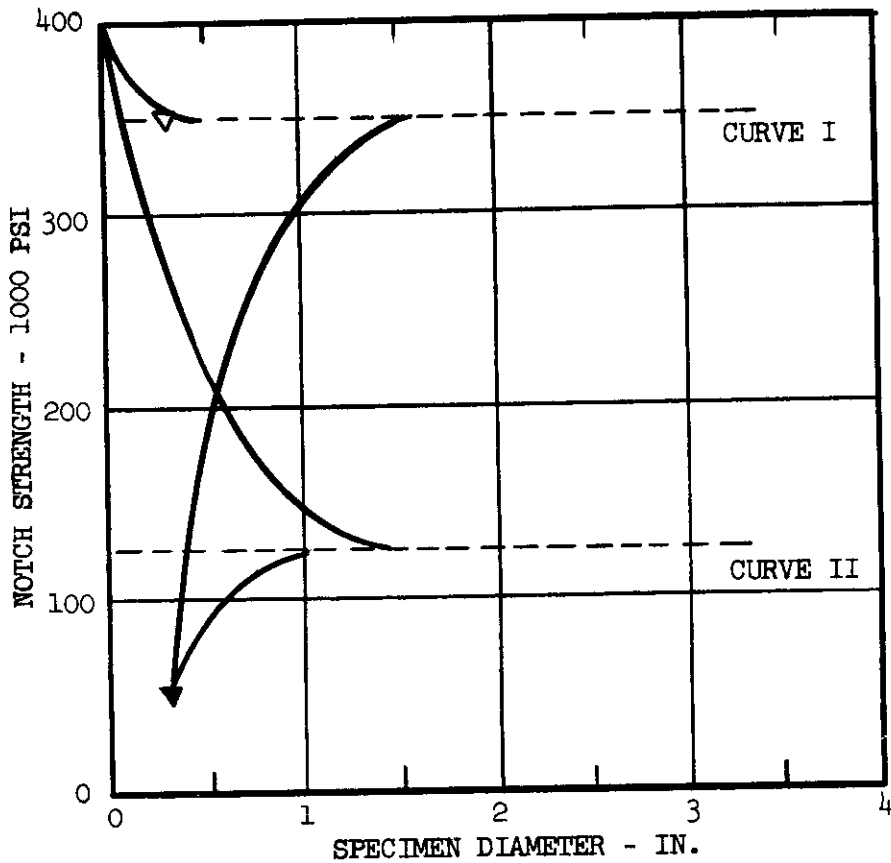
FIG. 2 NOTCH STRENGTH VS. SPECIMEN SIZE AS PREDICTED
BY CURVES IN FIGURE 1. (ABOVE CURVES ARE CON-
STRUCTED FOR TEMPERING TEMPERATURE Ta IN FIG-
URE 1.)
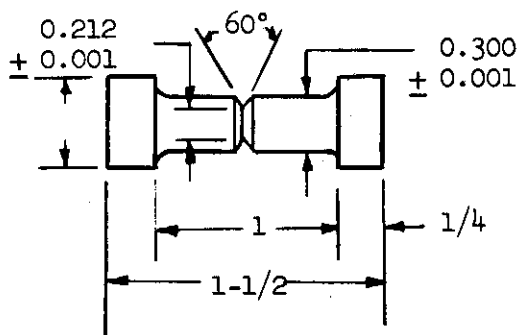
(a) 0.3 IN. DIA. STRESS-RUPTURE NOTCH SPECIMEN.
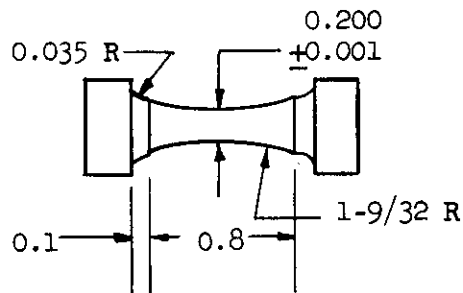
(b) 0.2 IN. DIA. STRESS-RUPTURE SMOOTH SPECIMEN.
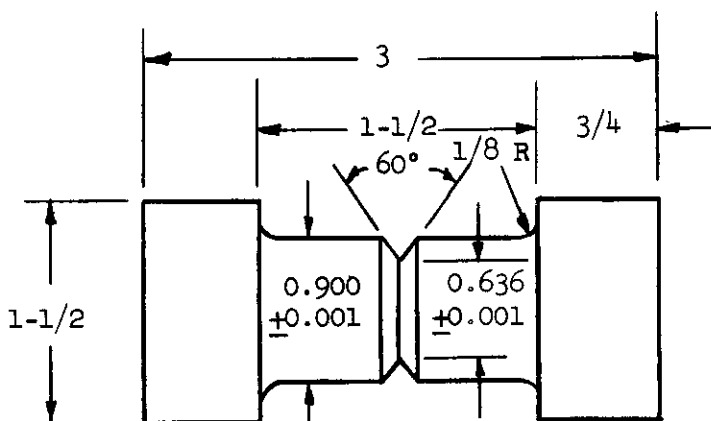
(c) 0.9 IN. DIA. STRESS-RUPTURE NOTCHED SPECIMEN.
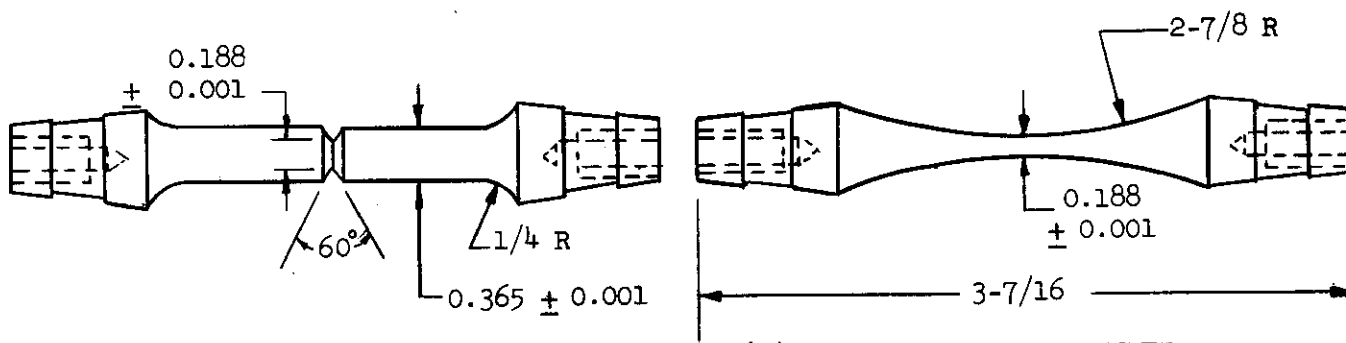
(d) NOTCHED FATIGUE SPECIMEN.

(e) SMOOTH FATIGUE SPECIMEN.
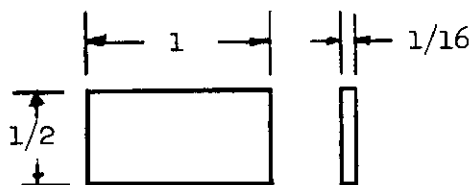
(f) BEND SPECIMEN

FIG. 3 TEST SPECIMENS.
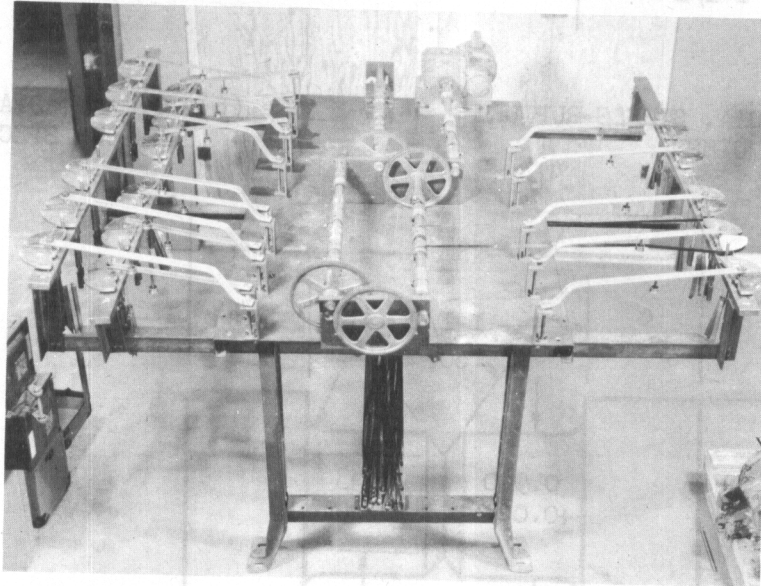
FIG. 4 PHOTOGRAPH OF THE MULTI-STRAIN RATE MULTI-SPECIMEN BEND MACHINE.

0.14 AMPS/SQ.IN.
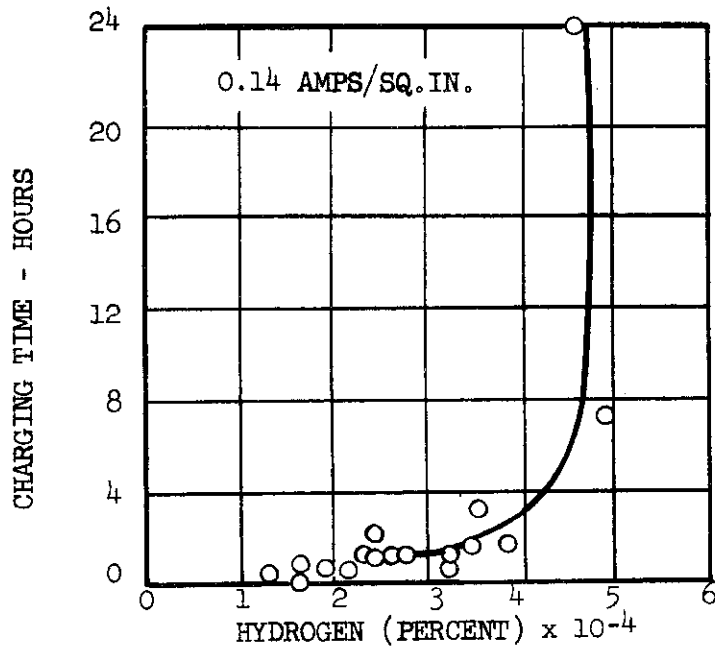
FIG. 5 THE EFFECT OF CHARGING TIME ON THE ABSORPTION
OF HYDROGEN IN AISI 4340 STEEL AT 230,000 PSI
TENSILE STRENGTH. (15)
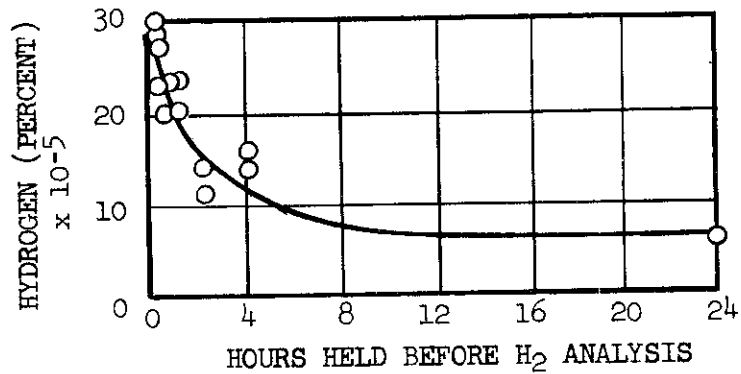
FIG. 6 THE EVOLUTION OF HYDROGEN WITH TIME FROM
CATHODICALLY CHARGED STEEL (15).

37
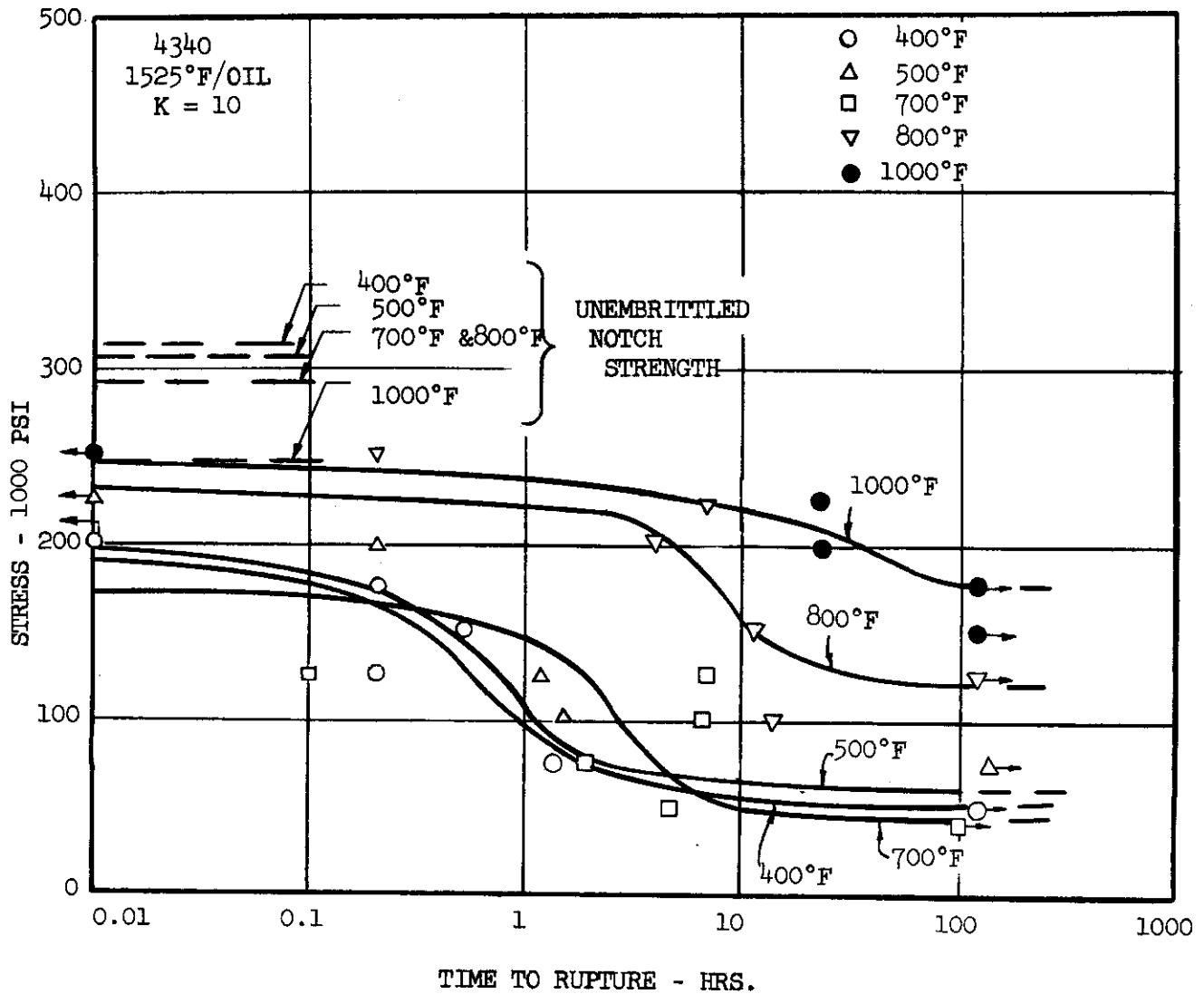
FIG. 7   THE STRESS-TIME TO RUPTURE CURVES FOR Cd-PLATED 4340 STEEL TEMPERED AS
INDICATED.   STRESS CONCENTRATION (K) = 10.
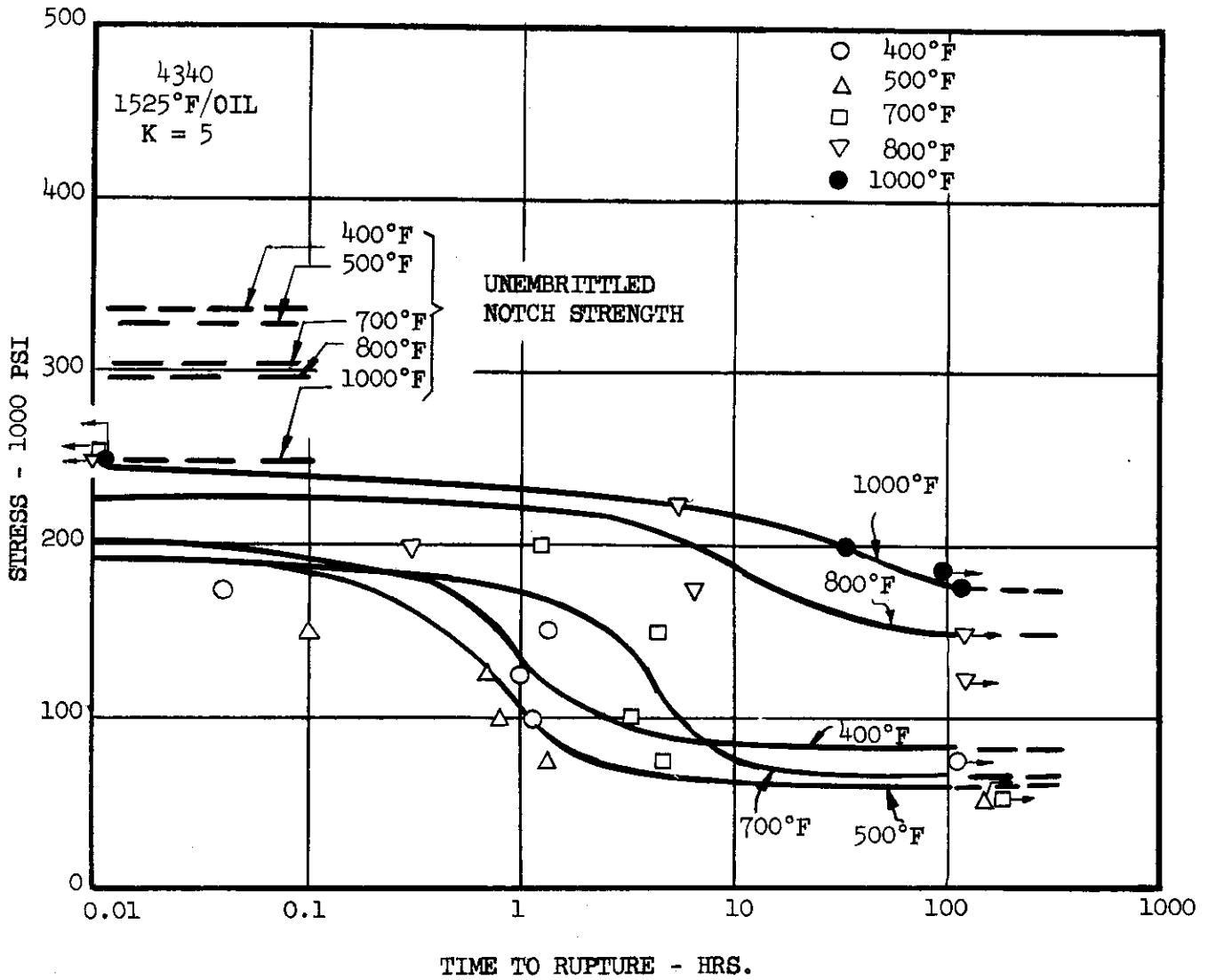
FIG. 8 THE STRESS-TIME TO RUPTURE CURVES FOR Cd-PLATED 4340 STEEL TEMPERED AS INDICATED. STRESS CONCENTRATION (K) = 5.
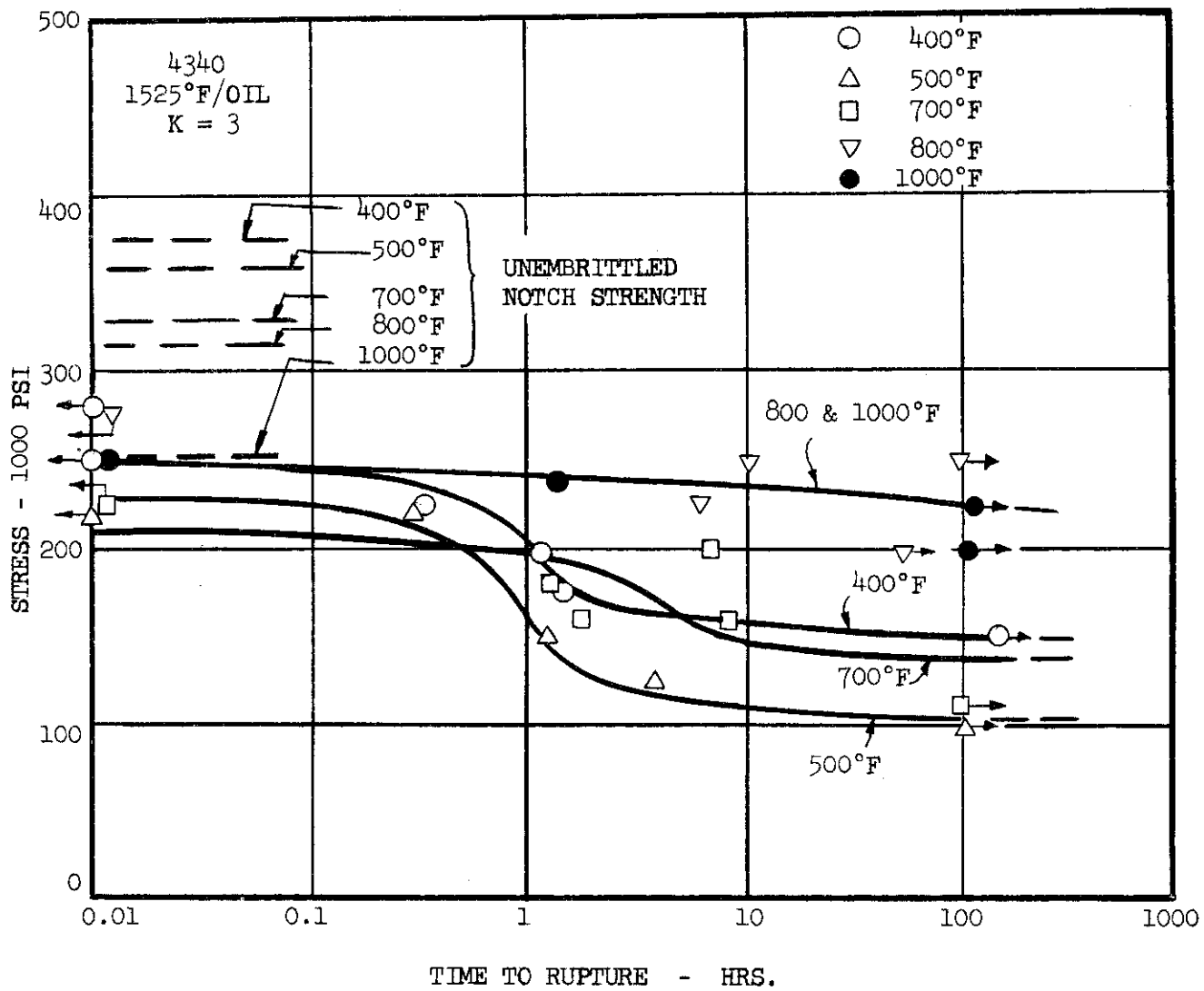
FIG. 9 THE STRESS-TIME TO RUPTURE CURVES FOR Cd-PLATED 4340 STEEL TEMPERED
AS INDICATED. STRESS CONCENTRATION (K) = 3.
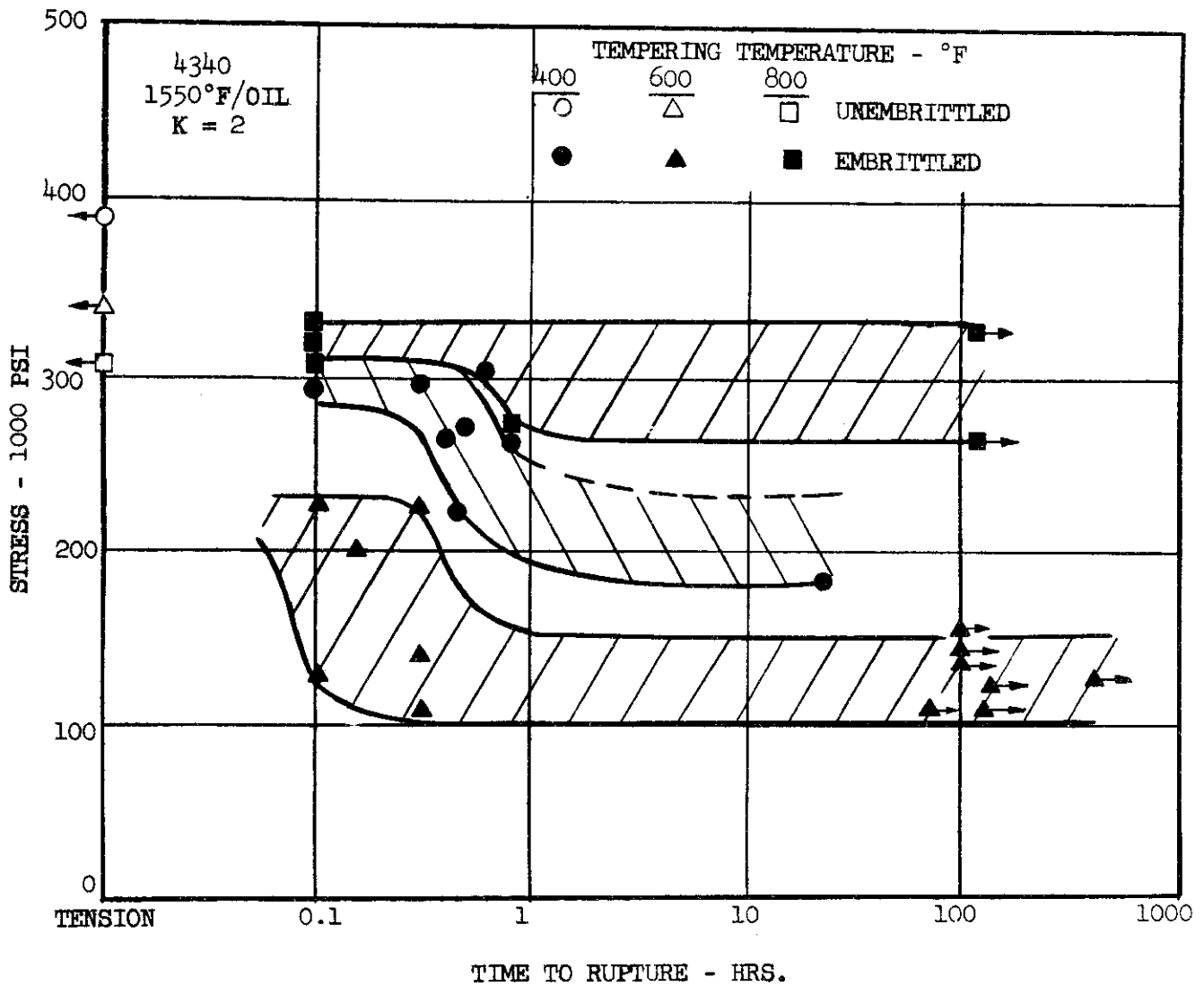
FIG. 10   THE STRESS-TIME TO RUPTURE CURVES FOR Cd-PLATED 4340 STEEL TEMPERED
AS INDICATED.   STRESS CONCENTRATION (K) = 2.

WADC TR 56-395 Pt 3   41
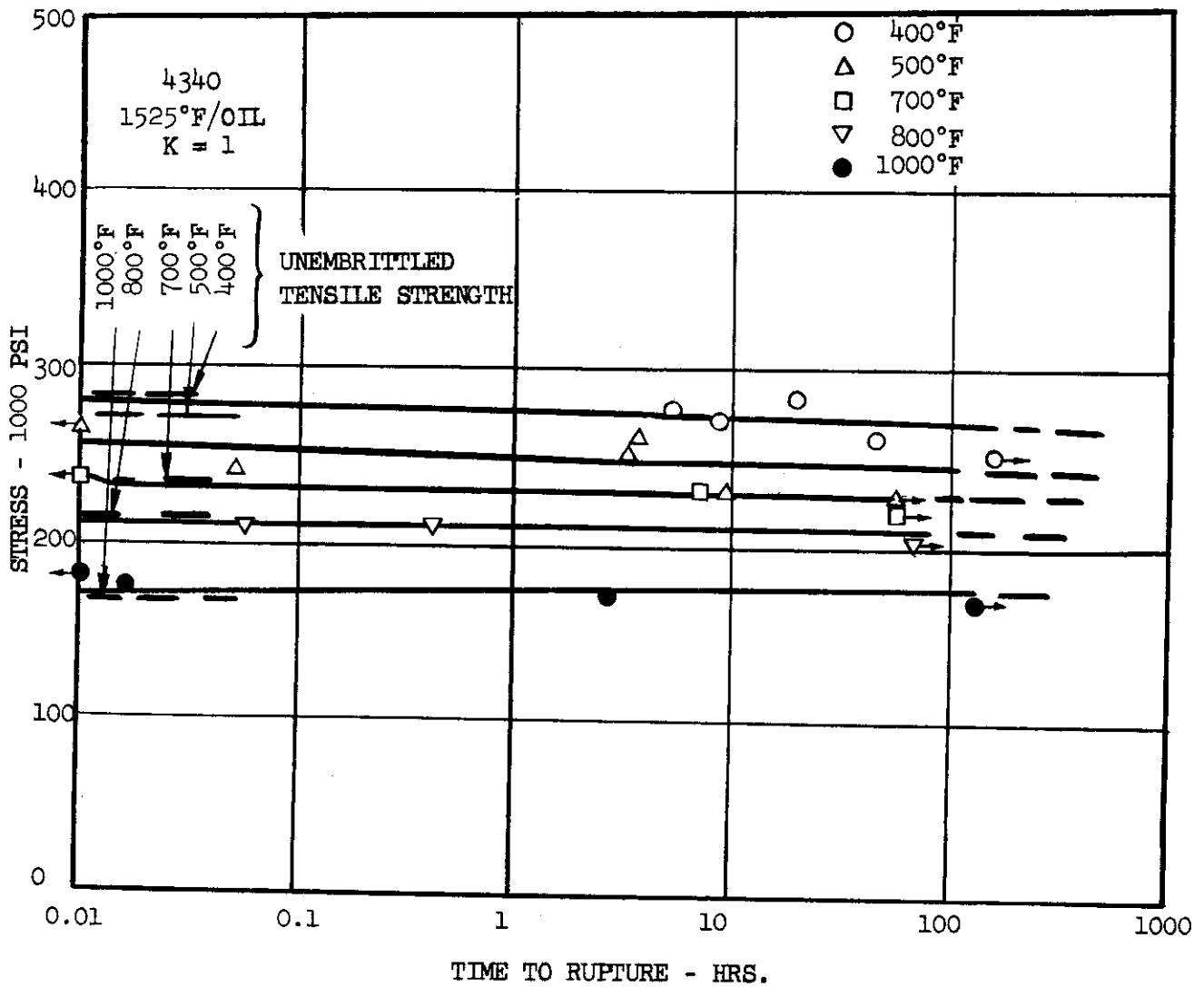
FIG. 11 THE STRESS – TIME TO RUPTURE CURVES FOR Cd–PLATED 4340 STEEL TEMPERED AS INDICATED. STRESS CONCENTRATION (K) = 1.
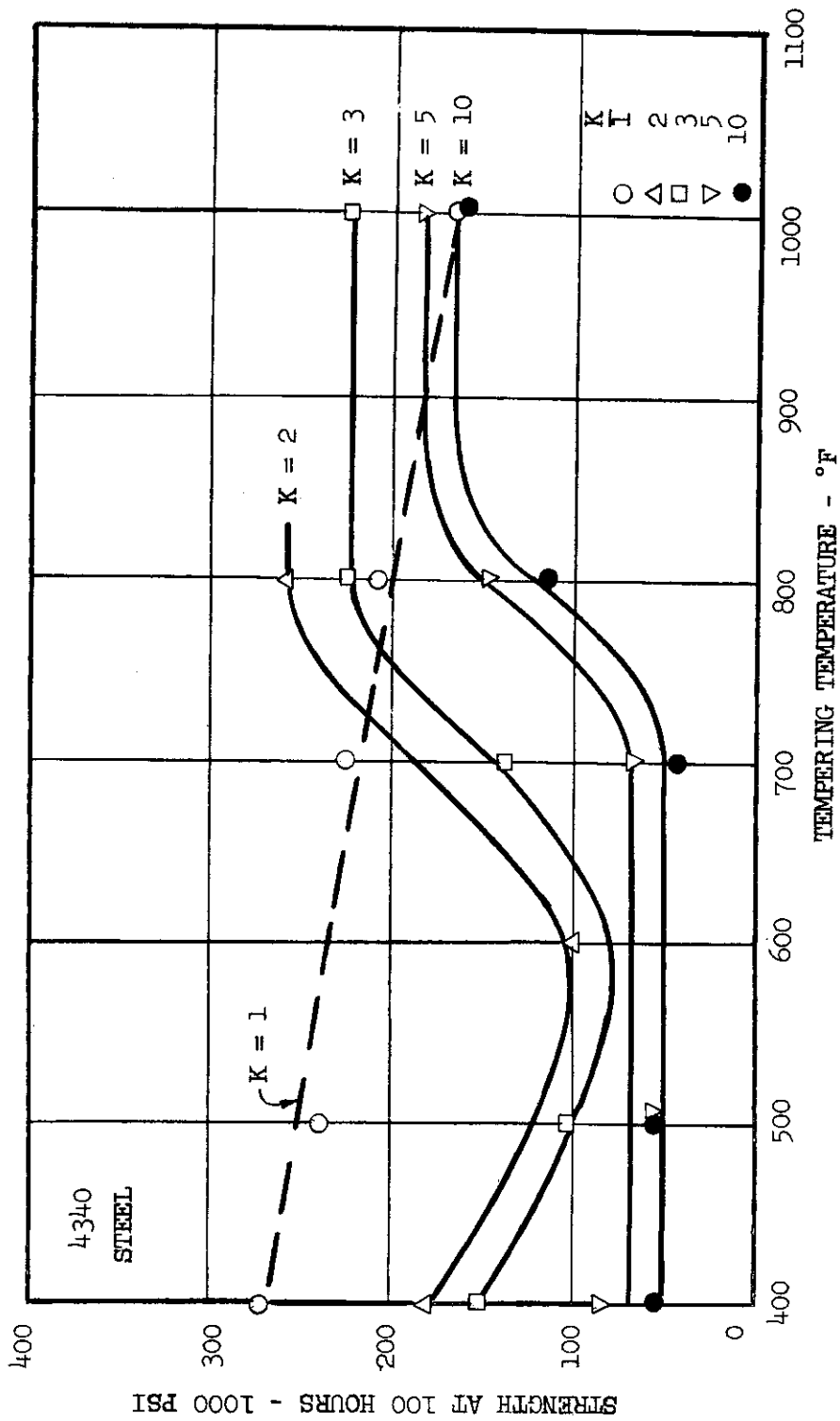
FIG. 12 THE RUPTURE STRENGTH AT 100 HOURS VS. TEMPERING TEMPERATURE WITH STRESS CON-
CENTRATION AS PARAMETER FOR Cd-PLATED 4340 STEEL.
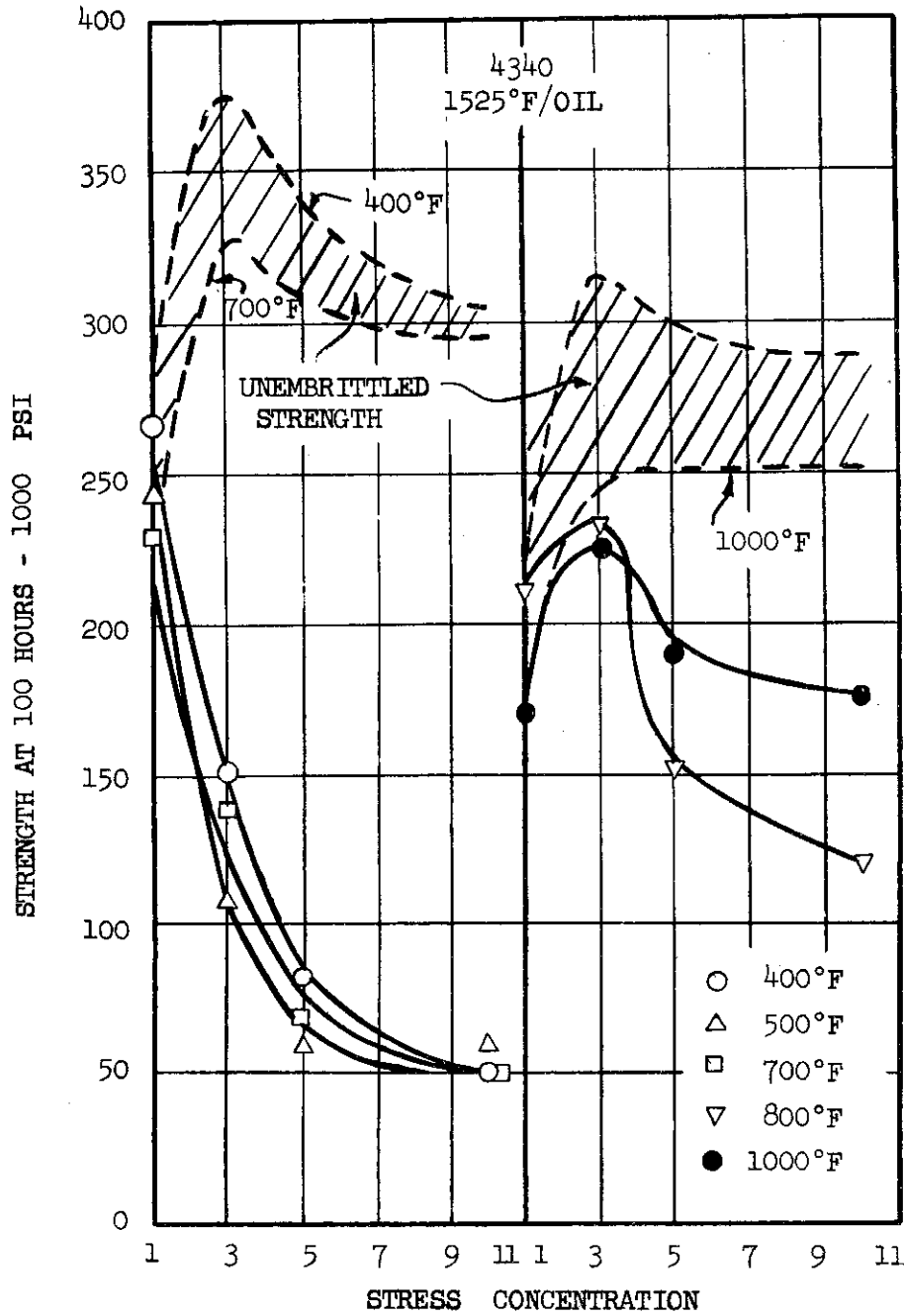
FIG. 13   THE RUPTURE STRENGTH AT 100 HOURS VS. STRESS CONCEN-
TRATION WITH TEMPERING TEMPERATURE AS PARAMETER FOR
Cd-PLATED 4340 STEEL.
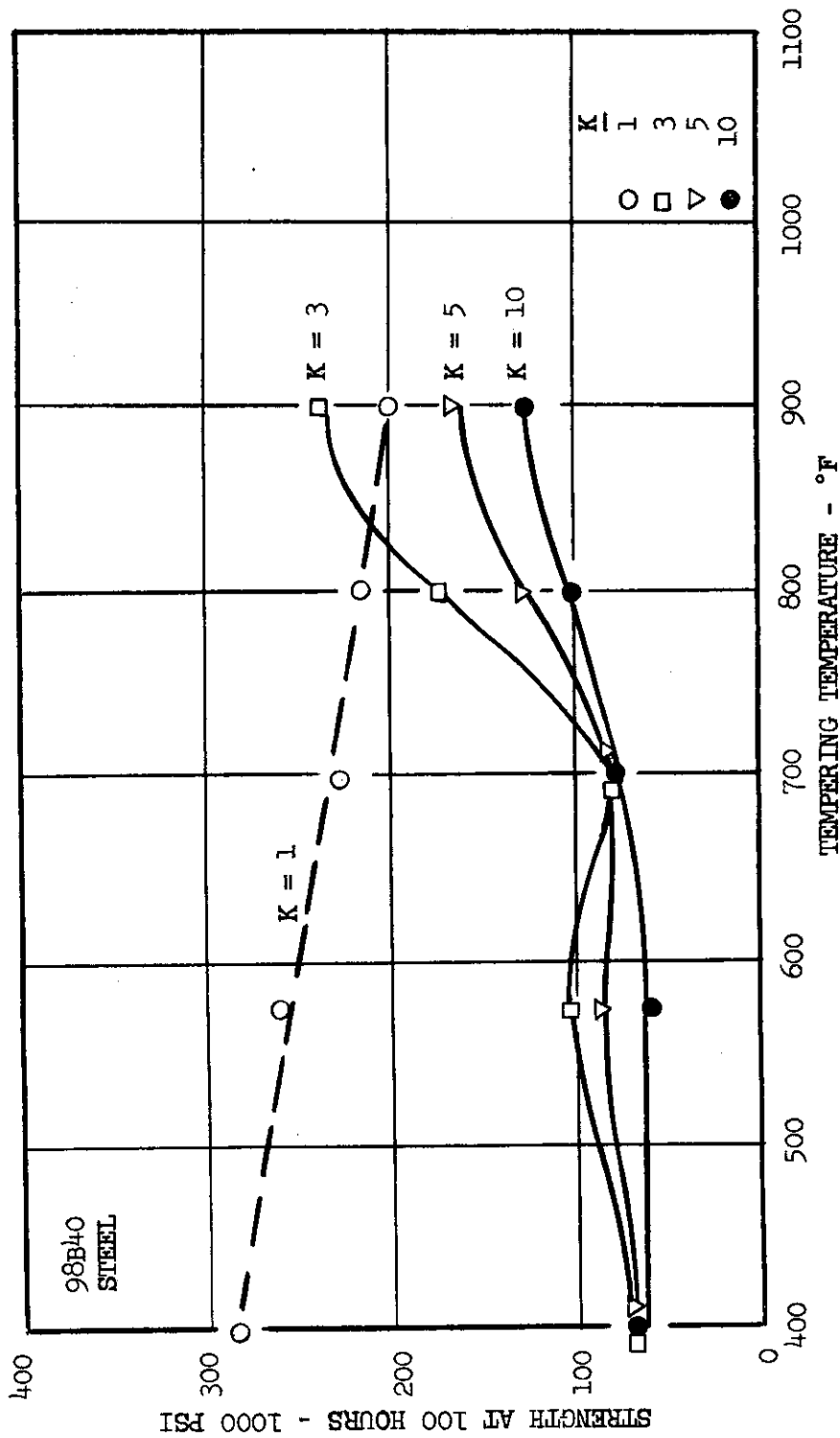
FIG. 14   THE RUPTURE STRENGTH AT 100 HOURS VS. TEMPERING TEMPERATURE WITH STRESS CONCEN-
TRATION AS PARAMETER FOR Cd-PLATED 98B40 STEEL.
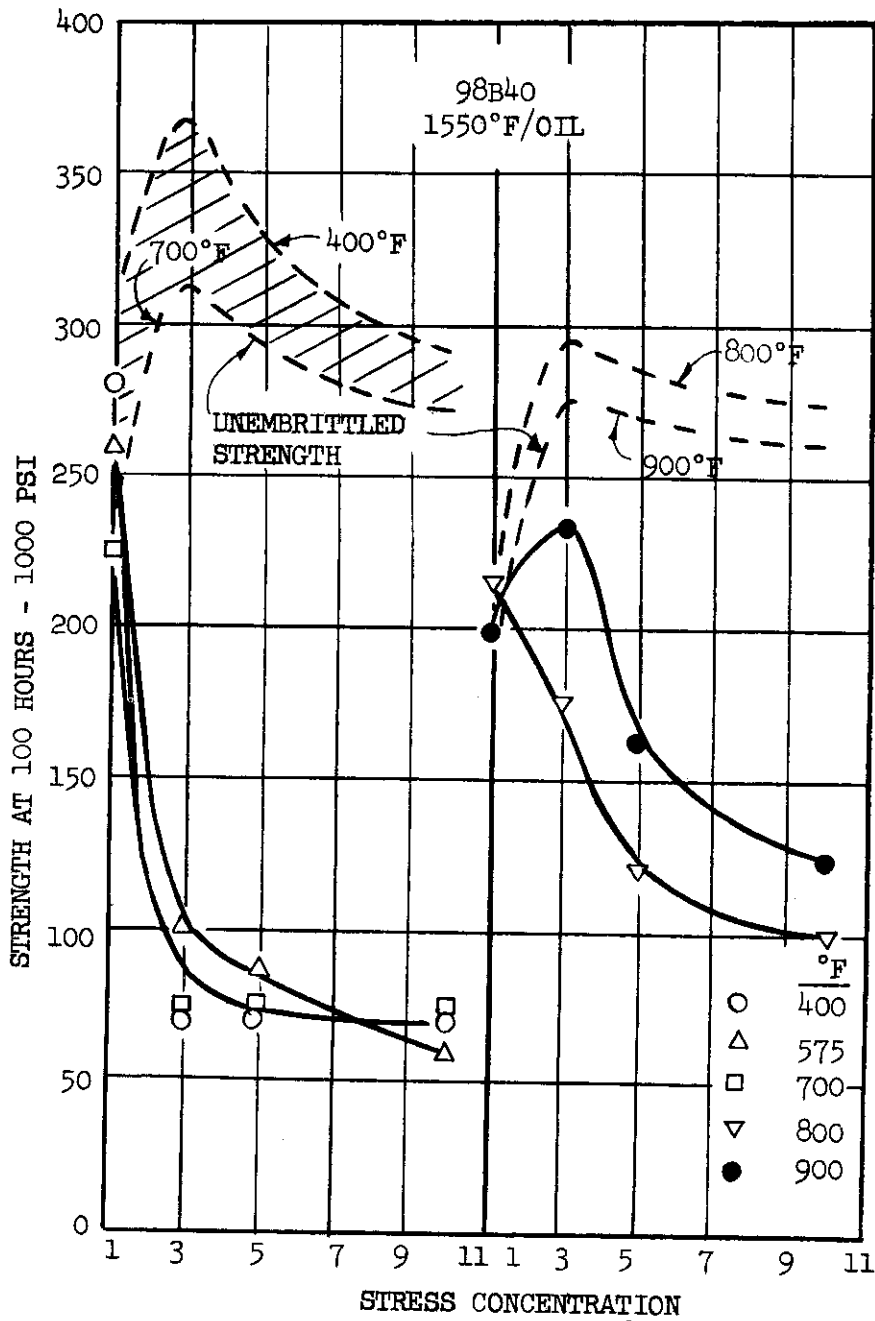
FIG. 15   THE RUPTURE STRENGTH AT 100 HOURS VS. STRESS
CONCENTRATION WITH TEMPERING TEMPERATURE AS
PARAMETER FOR Cd-PLATED 98B40 STEEL.
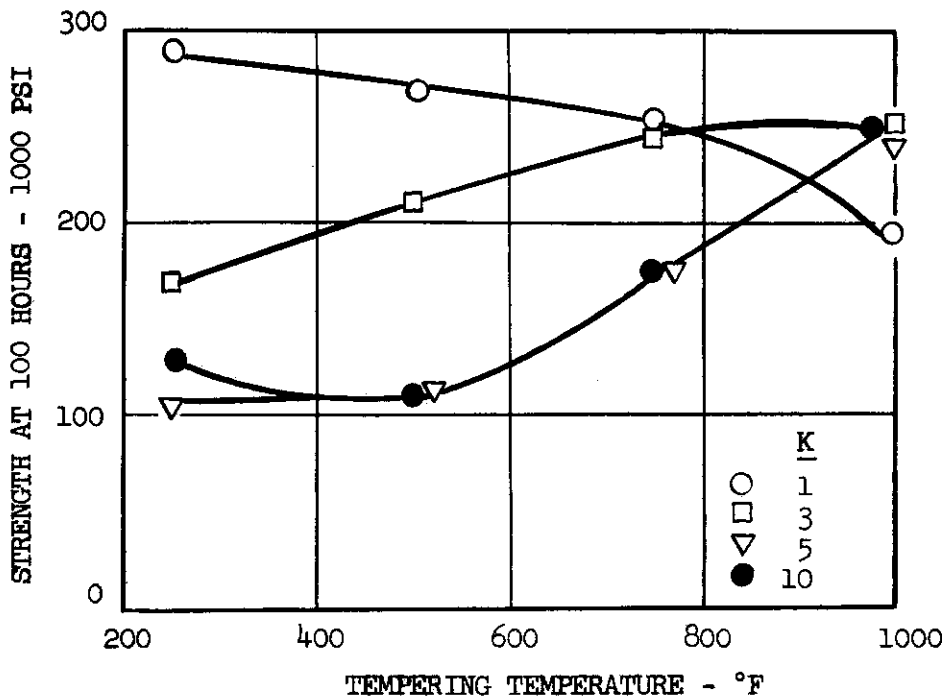
FIG. 16   THE RUPTURE STRENGTH AT 100 HOURS VS. TEMPERING
TEMPERATURE WITH STRESS CONCENTRATION AS PARAMETER
FOR Cd-PLATED 4330 V-MOD. STEEL.
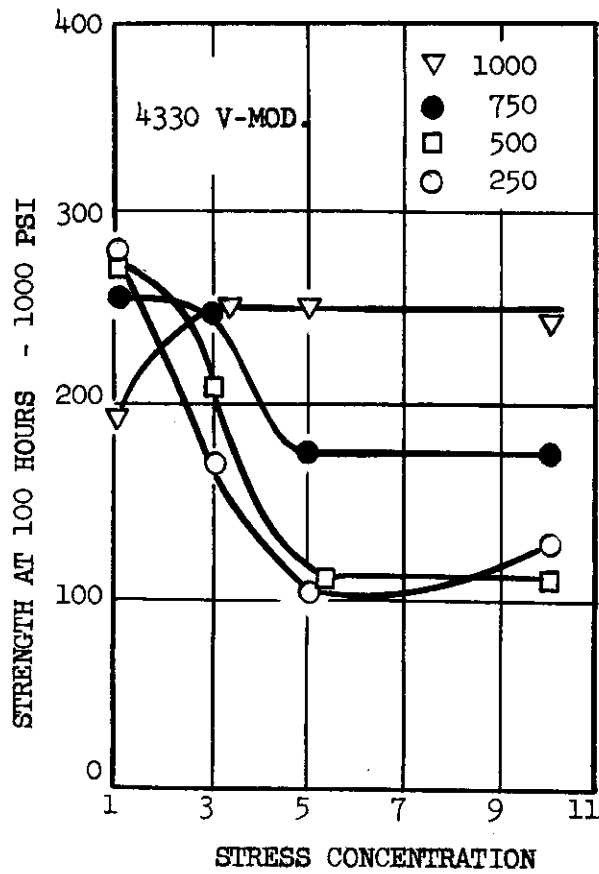
FIG. 17 THE RUPTURE STRENGTH AT 100 HOURS VS.
STRESS CONCENTRATION WITH TEMPERING
TEMPERATURE AS PARAMETER FOR Cd-PLATED
4330 V-MOD. STEEL.
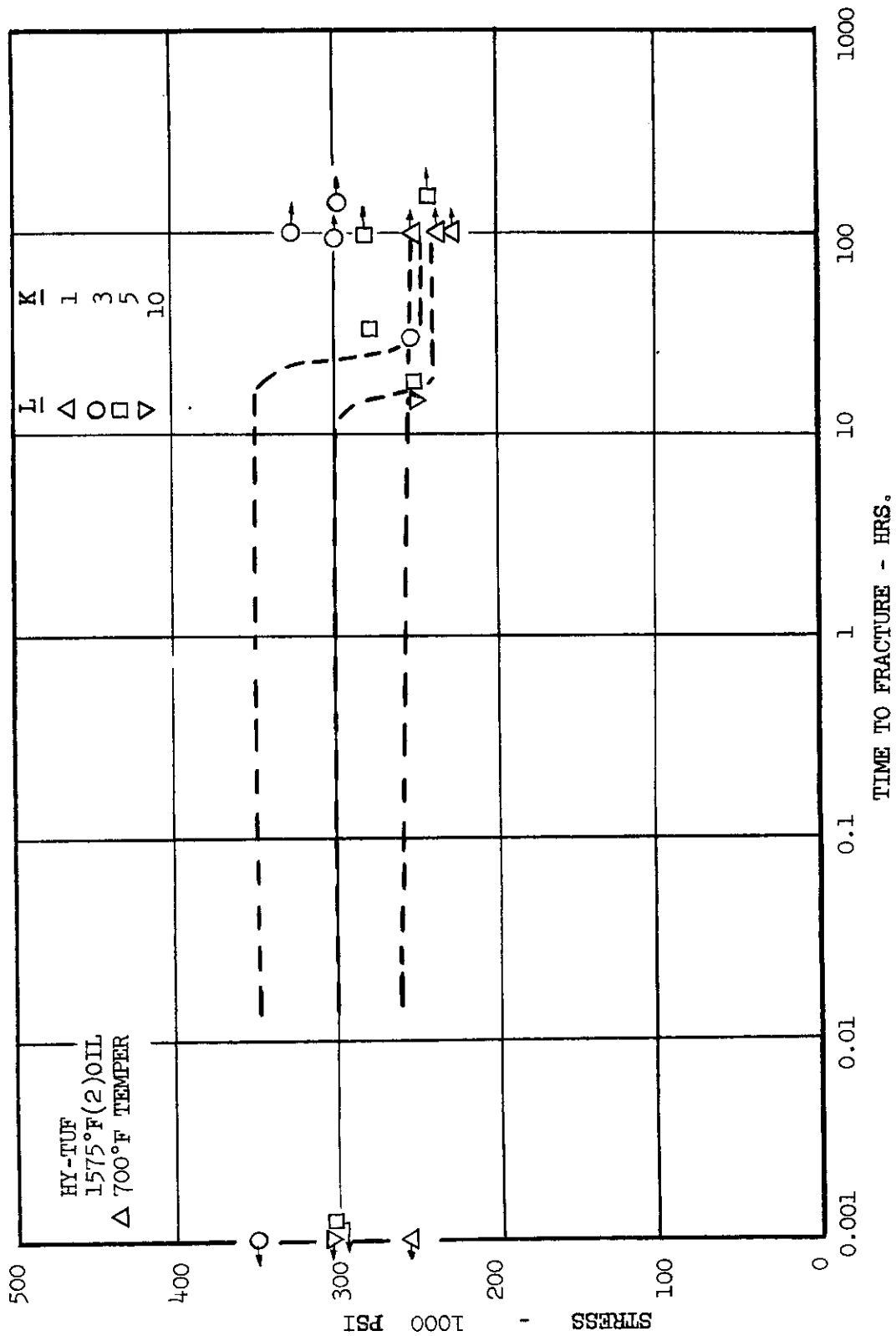
FIG. 18 THE STRESS-TIME TO RUPTURE CURVES AT INDICATED STRESS CONCENTRATION FOR Cd-PLATED HY-TUF STEEL TEMPERED AT 700°F.
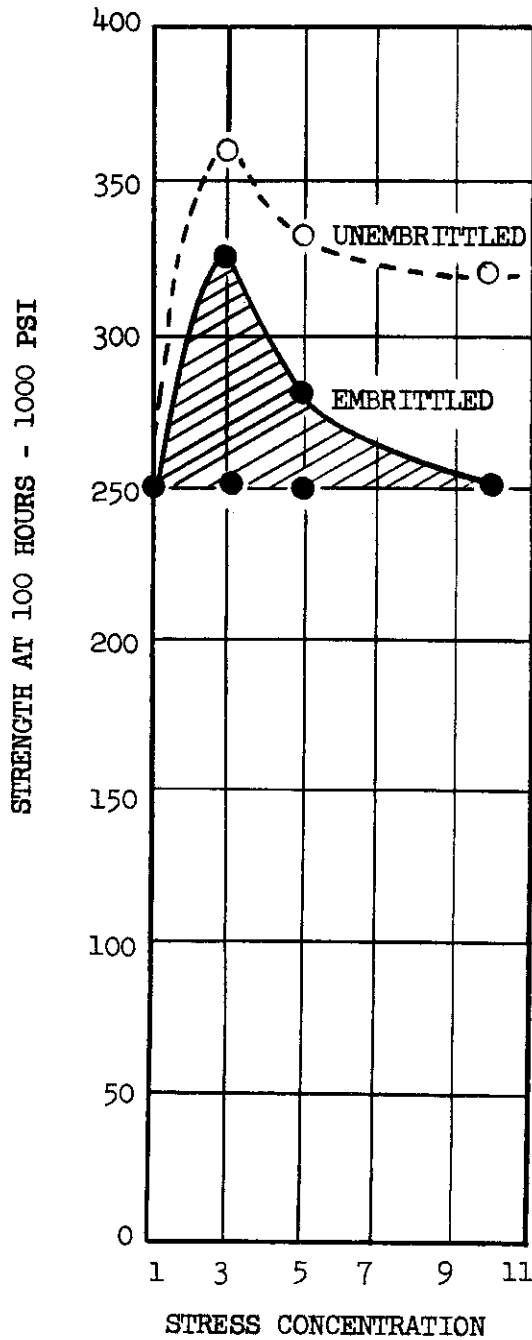
FIG. 19 THE RUPTURE STRENGTH AT 100 HOURS VS.
STRESS CONCENTRATION FOR Cd-PLATED
HY-TUF STEEL TEMPERED AT 700°F.
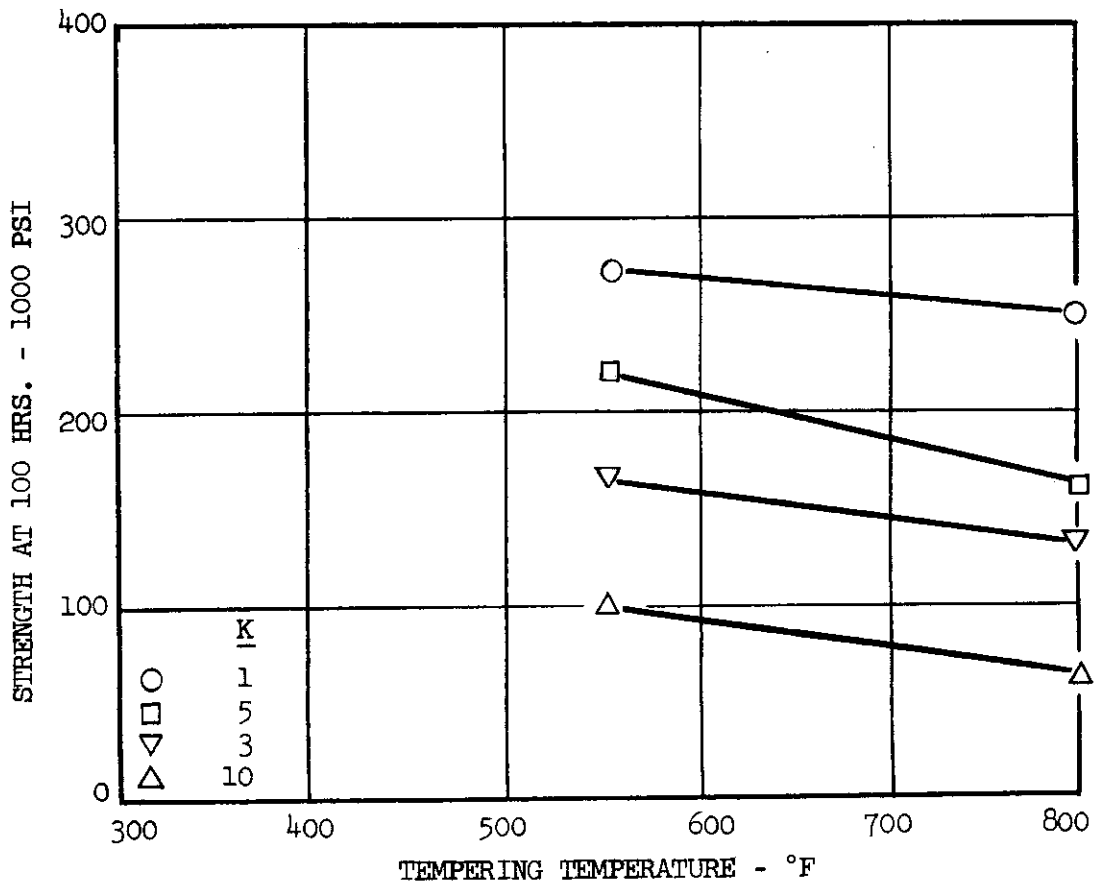
FIG. 20 THE RUPTURE STRENGTH AT 100 HOURS VS. TEMPERING TEMPERATURE
WITH STRESS CONCENTRATION AS PARAMETER FOR Cd-PLATED CRUCIBLE
UHS-260 STEEL.
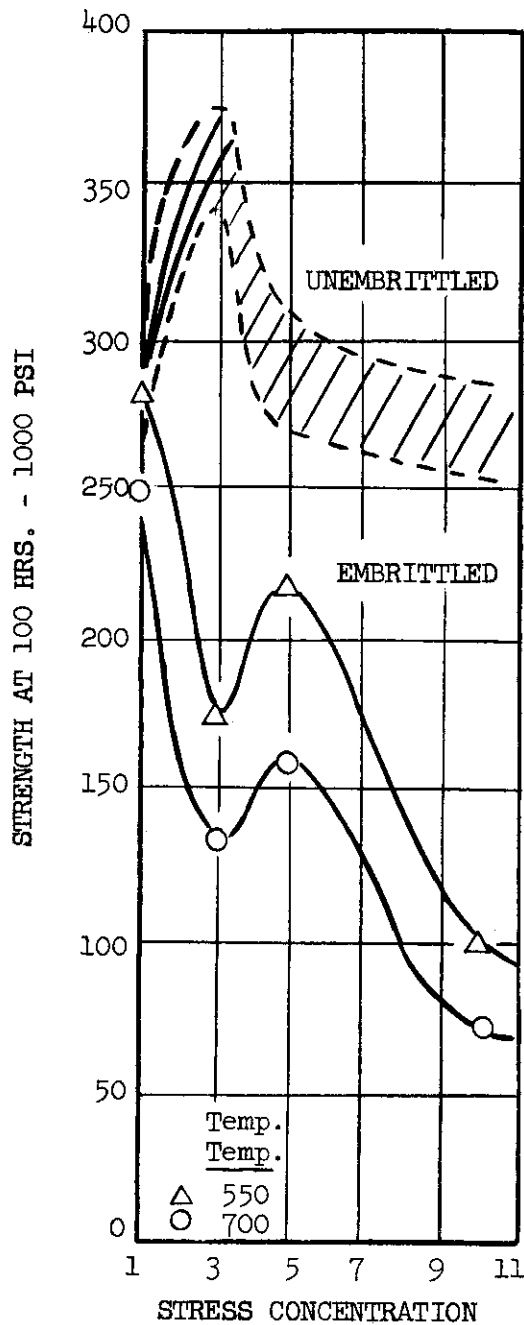
FIG. 21 THE RUPTURE STRENGTH AT 100 HOURS VS.
STRESS CONCENTRATION WITH TEMPERING
TEMPERATURE AS PARAMETER FOR Cd-PLATED
CRUCIBLE UHS-260 STEEL.
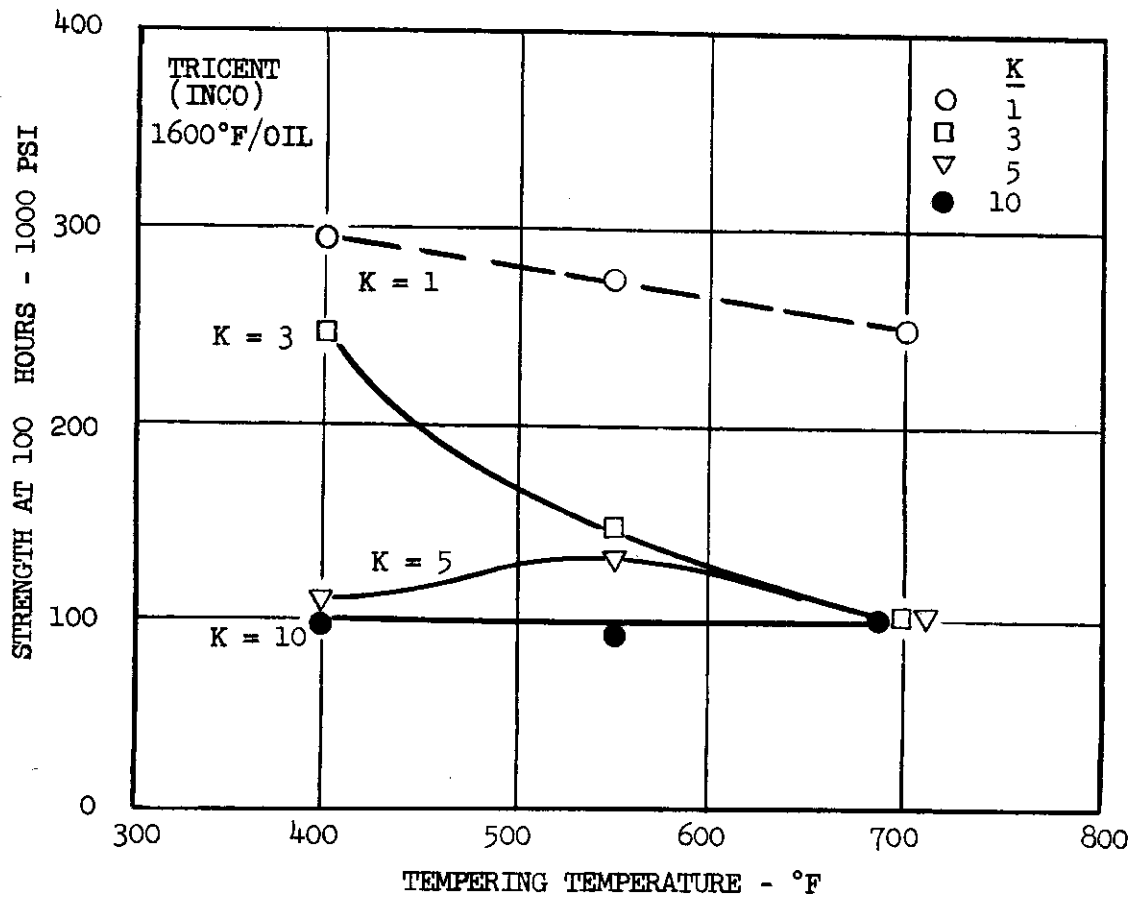
FIG. 22 THE RUPTURE STRENGTH AT 100 HOURS VS. TEMPERING TEMPERATURE
WITH STRESS CONCENTRATION AS PARAMETER FOR Cd-PLATED TRICENT
STEEL.
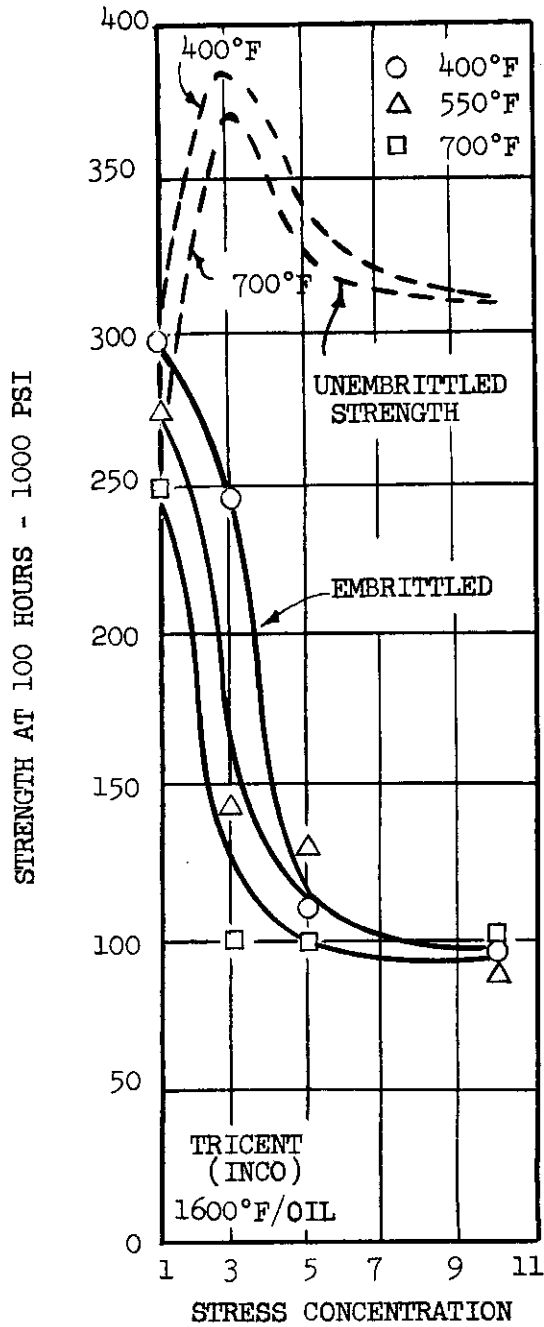
FIG. 23 THE RUPTURE STRENGTH AT 100 HOURS VS. STRESS CONCENTRATION WITH TEMPERING TEMPERATURE AS PARAMETER FOR Cd-PLATED TRICENT STEEL.
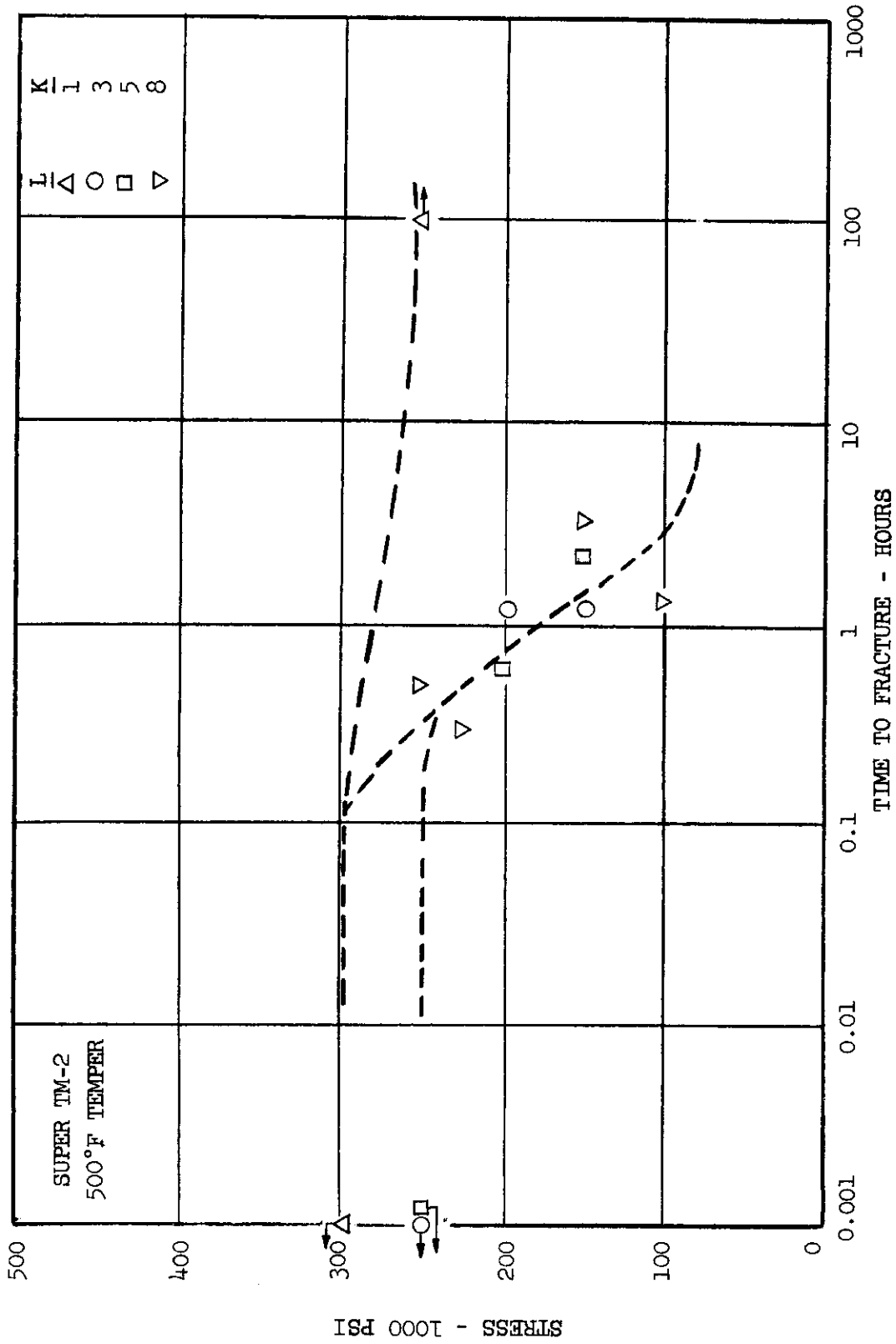
FIG. 24   THE STRESS-TIME TO RUPTURE CURVES AT INDICATED STRESS CONCENTRATIONS FOR Cd-PLATED SUPER TM-2 STEEL TEMPERED AT 500°F.
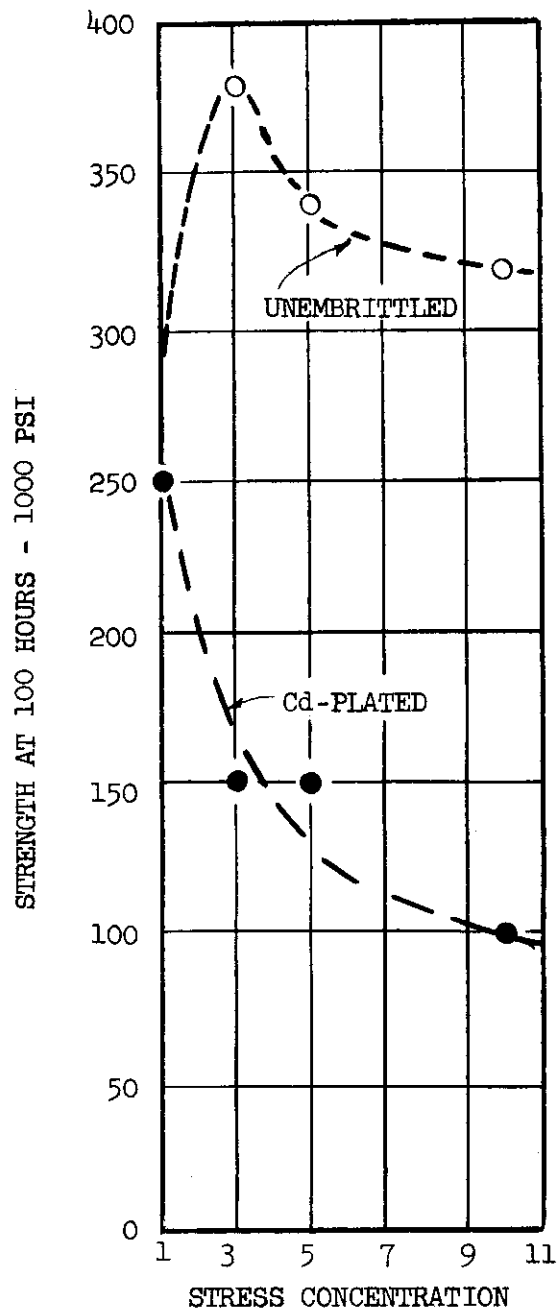
FIG. 25   THE RUPTURE STRENGTH AT 100 HOURS VS.
STRESS CONCENTRATION FOR Cd-PLATED SUPER
TM-2 STEEL TEMPERED AT 500°F.
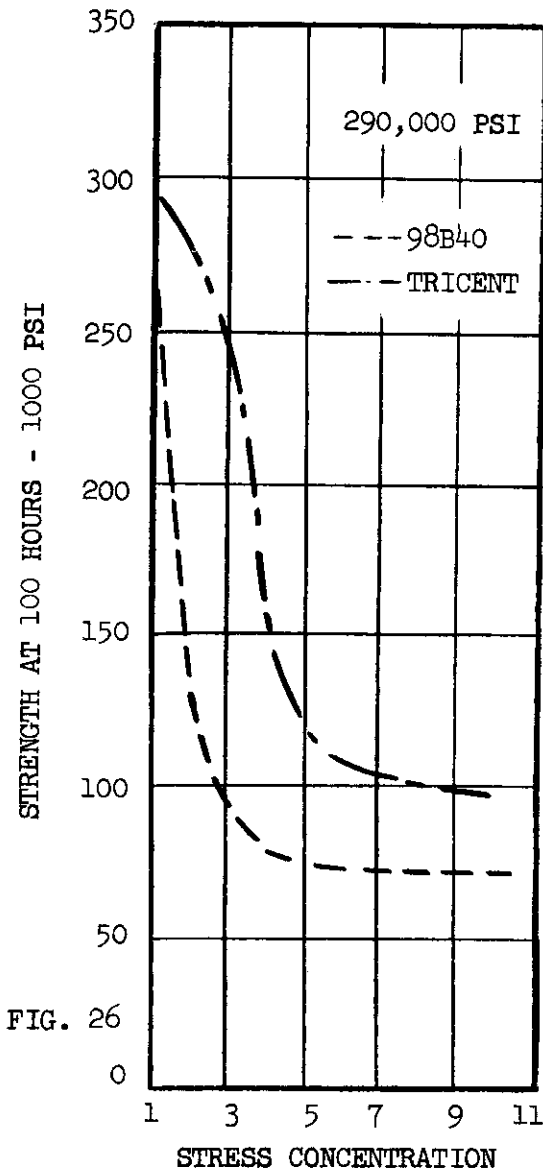
FIG. 26
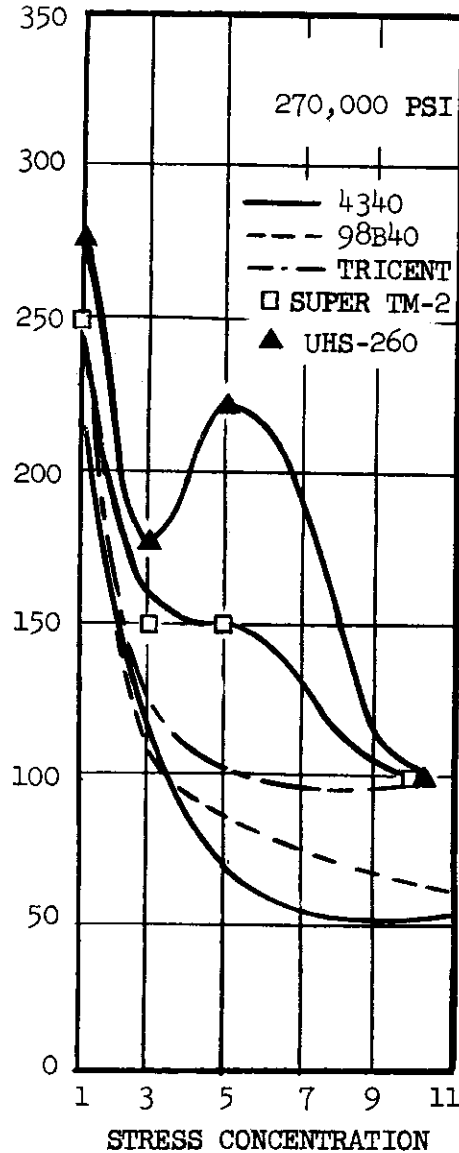
FIG. 27

FIGS. 26 AND 27   THE RUPTURE STRENGTH AT 100 HOURS VS. STRESS
CONCENTRATION FOR THE INDICATED STEELS TEMPERED
TO THE INDICATED TENSILE STRENGTHS.

FIG. 26   290,000 PSI
FIG. 27   270,000 PSI
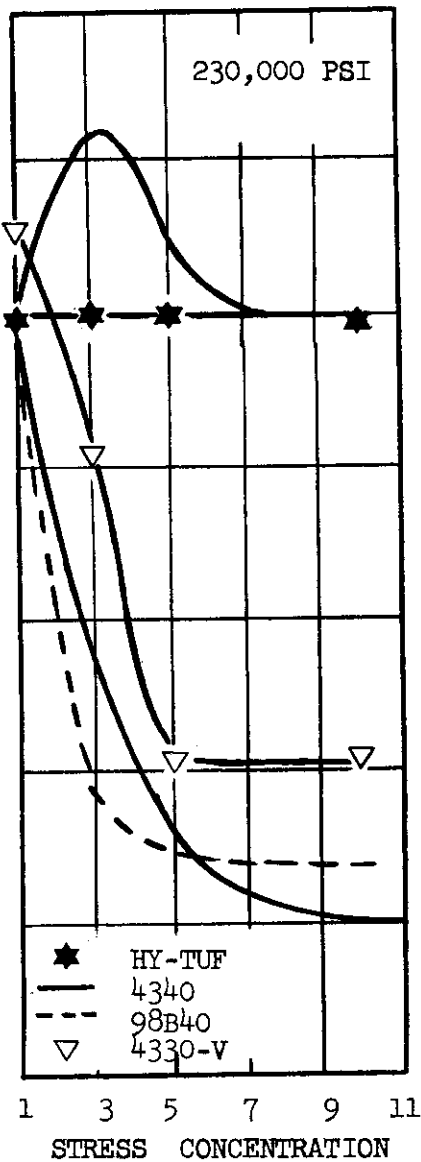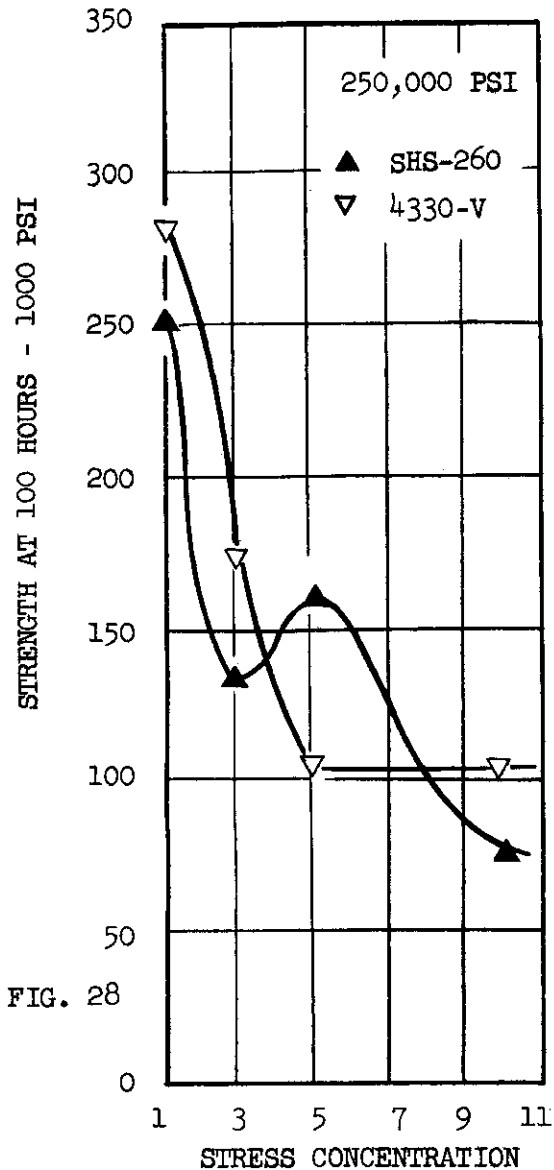
FIGS. 28 AND 29   THE RUPTURE STRENGTH AT 100 HOURS VS. STRESS CON-
CENTRATION FOR THE INDICATED STEELS TEMPERED TO
THE INDICATED TENSILE STRENGTHS.

FIG. 28   250,000 PSI
FIG. 29   230,000 PSI

WADC TR 56-395 Pt 3   58
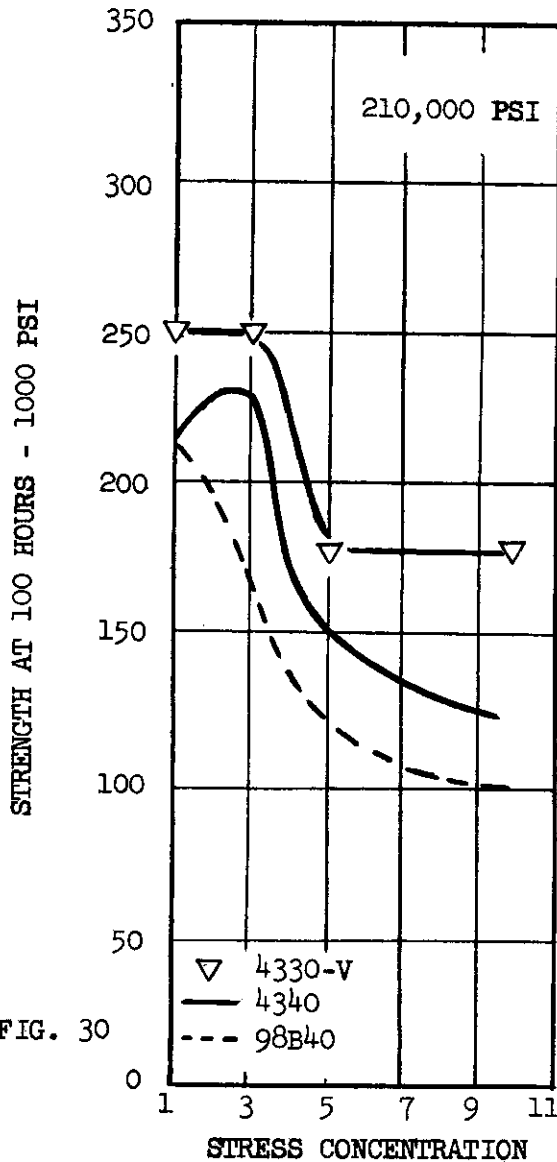
FIGS. 30 AND 31   THE RUPTURE STRENGTH AT 100 HOURS VS. STRESS
CONCENTRATION FOR THE INDICATED STEELS TEMPERED
TO THE INDICATED TENSILE STRENGTHS.

FIG. 30   210,000 PSI
FIG. 31   180,000 PSI

WADC TR 56-395 Pt. 3   59
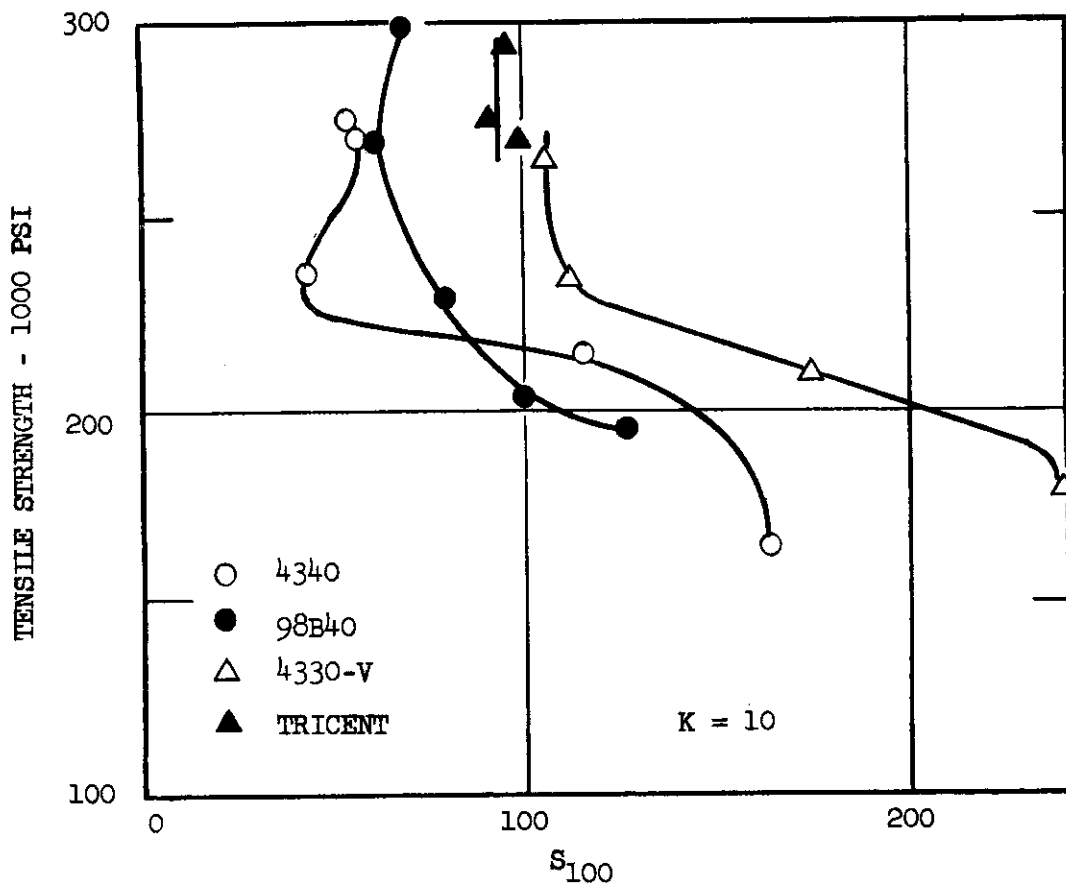
FIG. 32   THE RUPTURE STRENGTH AT 100 HOURS VS. TENSILE STRENGTH
FOR THE INDICATED STEELS WITH STRESS CONCENTRATION (K) = 10.
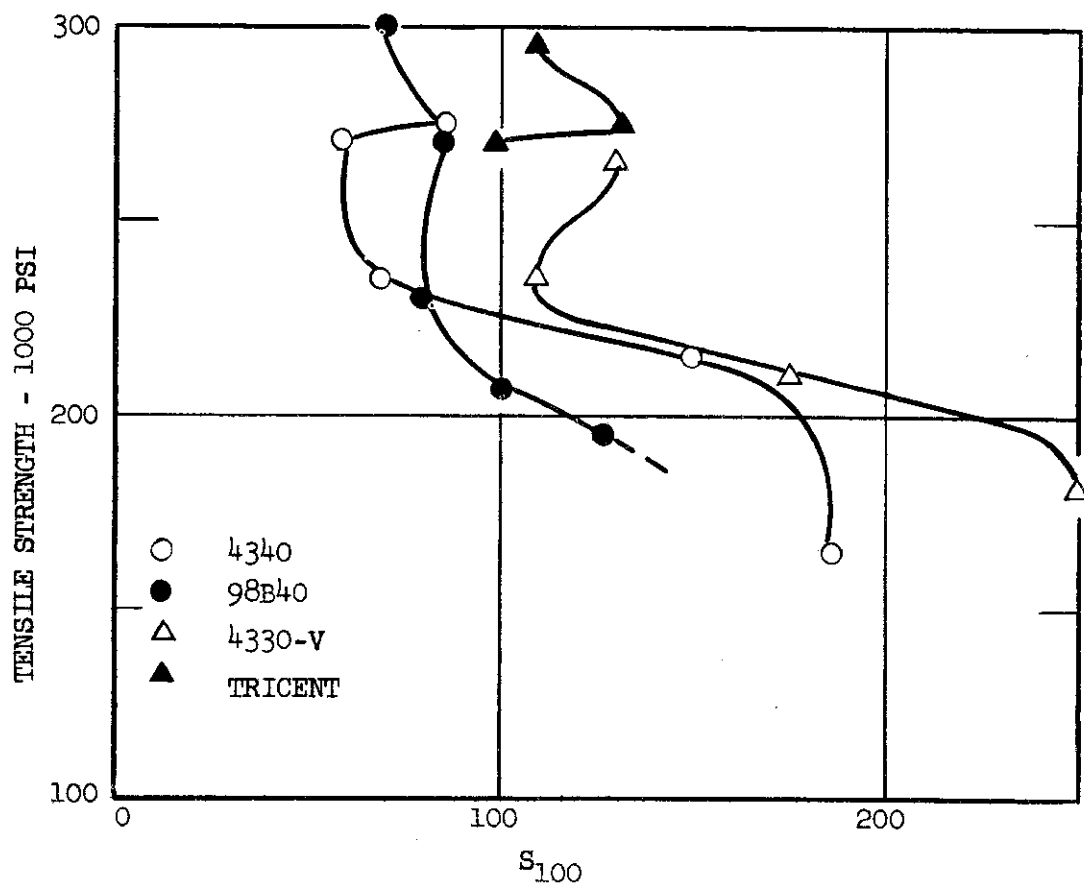
FIG. 33   THE RUPTURE STRENGTH AT 100 HOURS VS. TENSILE STRENGTH
FOR THE INDICATED STEELS WITH STRESS CONCENTRATION (K) = 5.
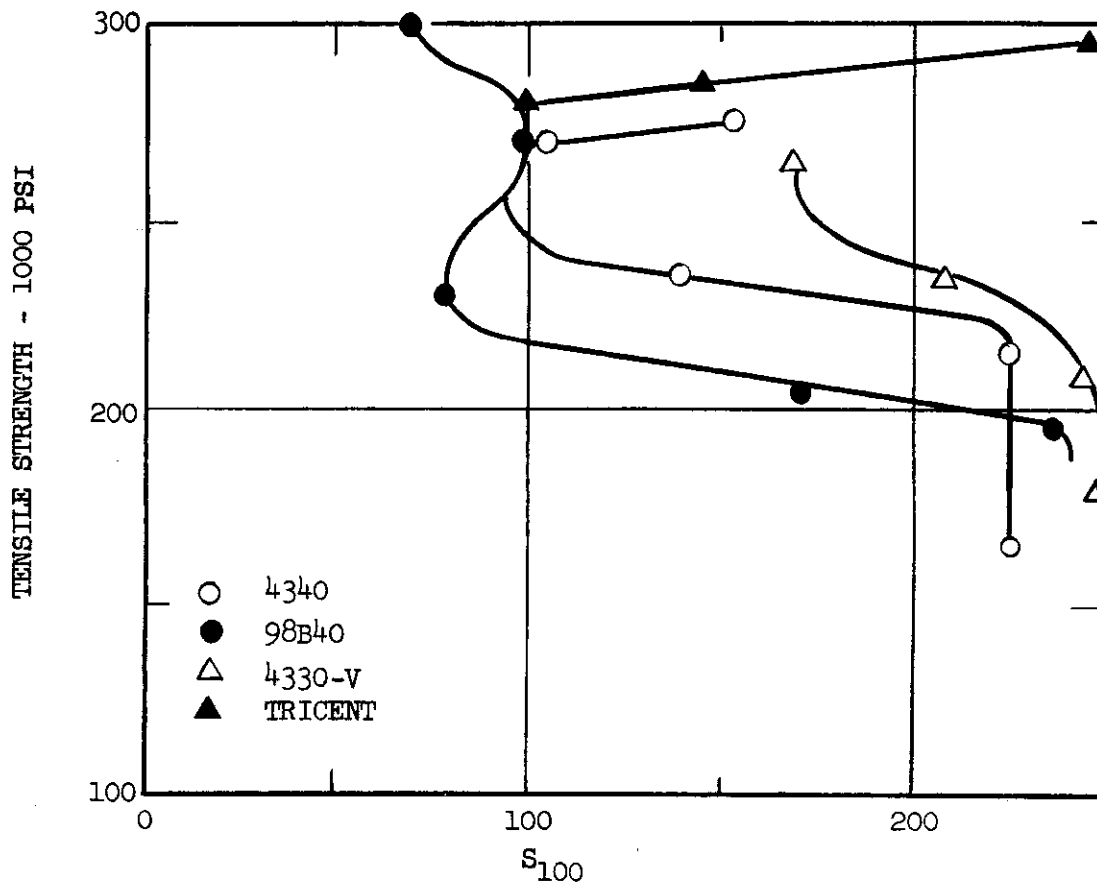
FIG. 34 THE RUPTURE STRENGTH AT 100 HOURS VS. TENSILE STRENGTH
FOR THE INDICATED STEELS WITH STRESS CONCENTRATION (K) = 3.
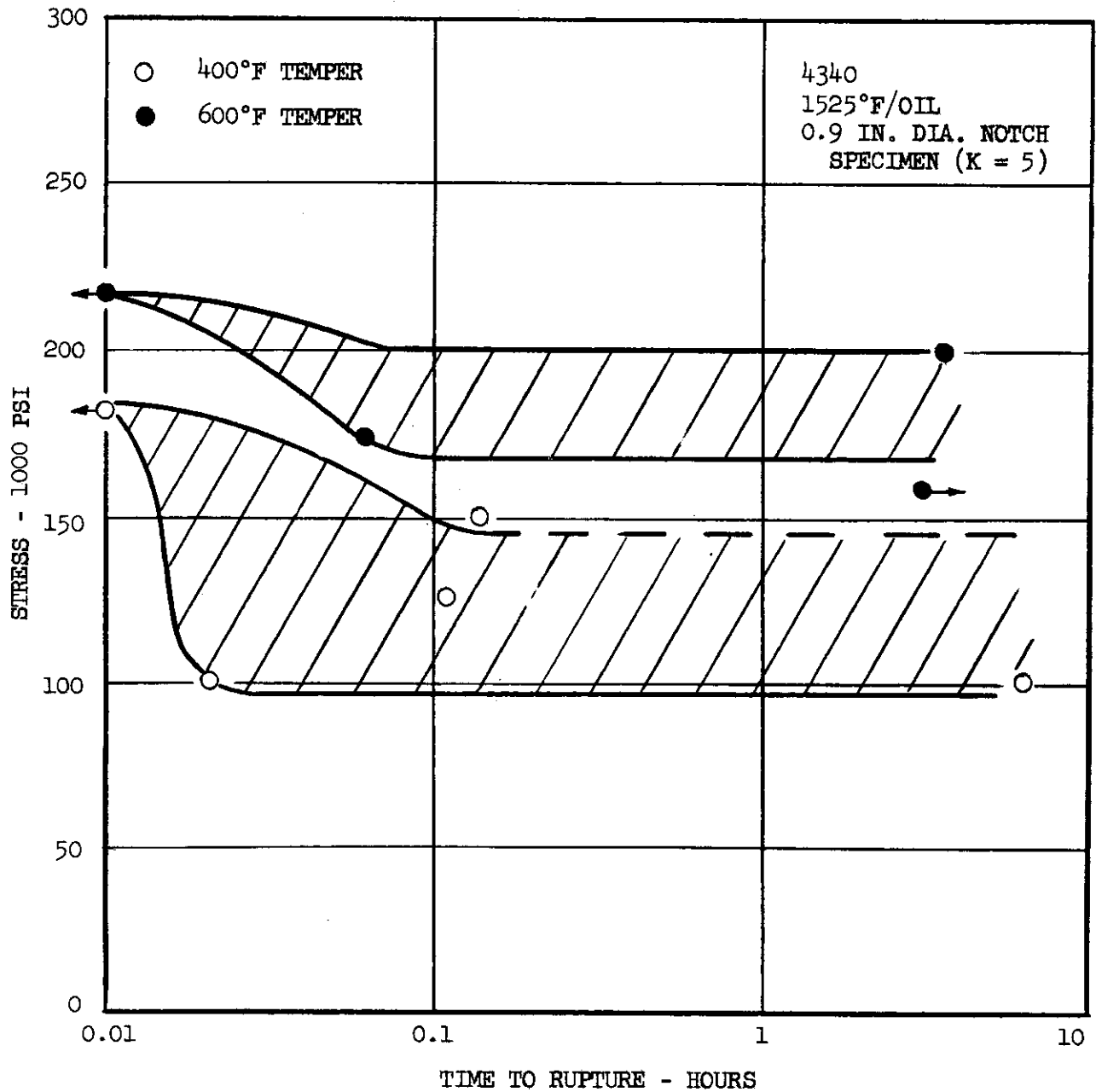
FIG. 35   THE STRESS-TIME TO RUPTURE CURVES FOR 0.9 IN. DIA. SPECIMENS OF
Cd-PLATED 4340 STEEL.   STRESS CONCENTRATION (K) = 5.
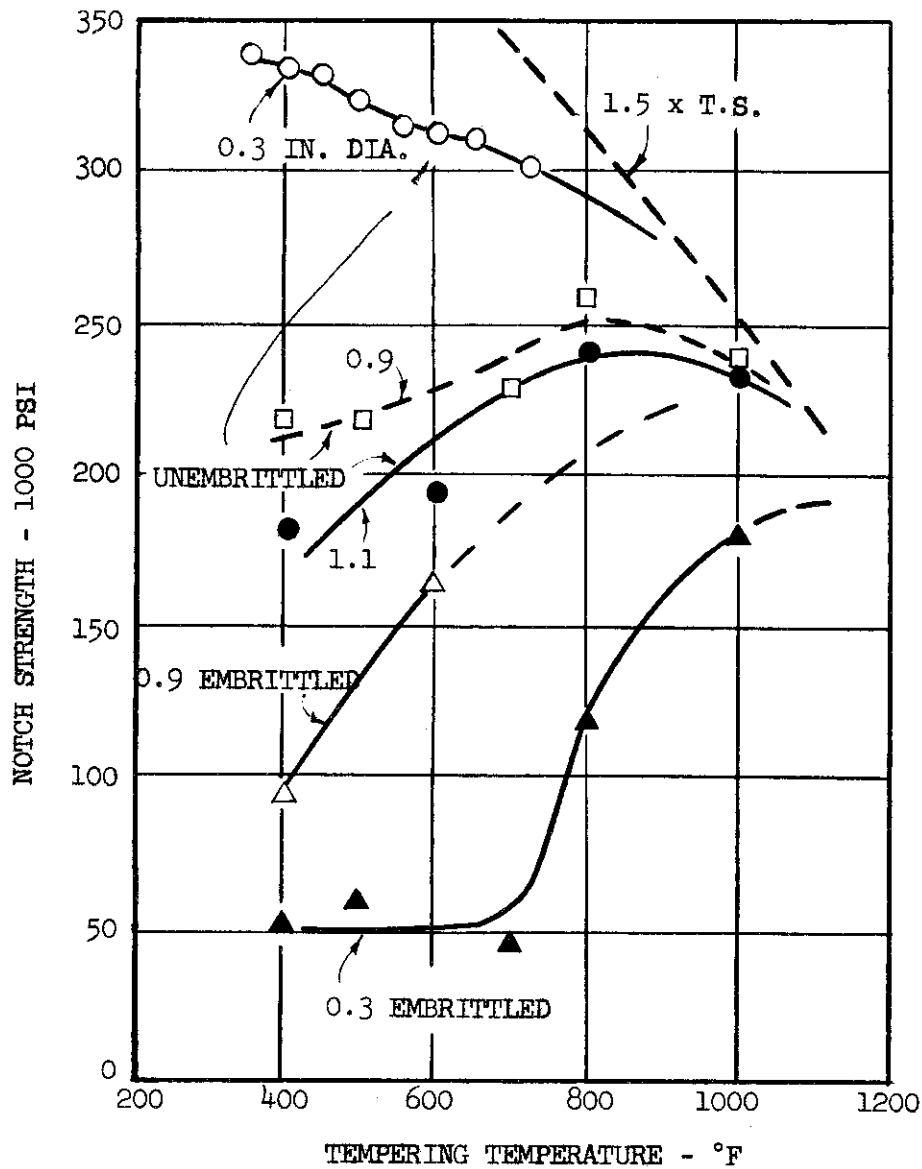
FIG. 36 THE NOTCH STRENGTH MEASURED FOR EMBRITTLED AND
UNEMBRITTLED SPECIMENS OF THE INDICATED SIZES
VS. TEMPERING TEMPERATURE. (THE NOTCH STRENGTH
FOR THE EMBRITTLED SPECIMENS WAS MEASURED UNDER
SUSTAINED LOADING.)
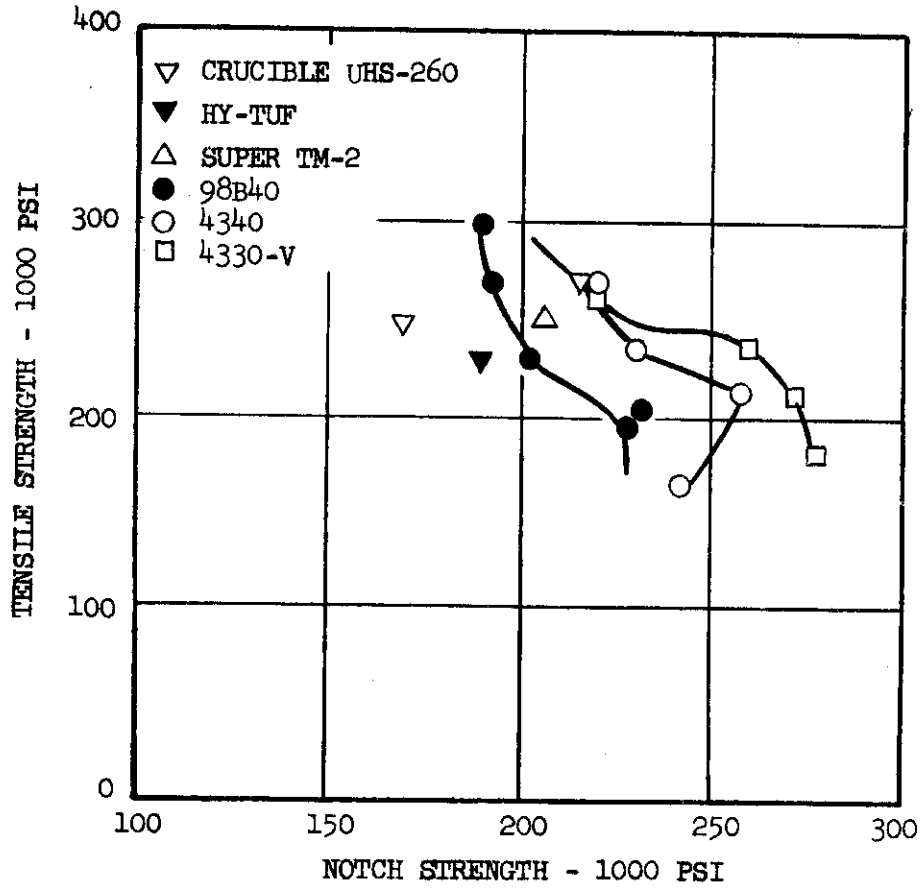
FIG. 37 THE NOTCH STRENGTH FOR 0.9 IN. DIA. SPECIMENS
(K = 10) VS. TENSILE STRENGTH FOR THE INDICATED
STEELS.
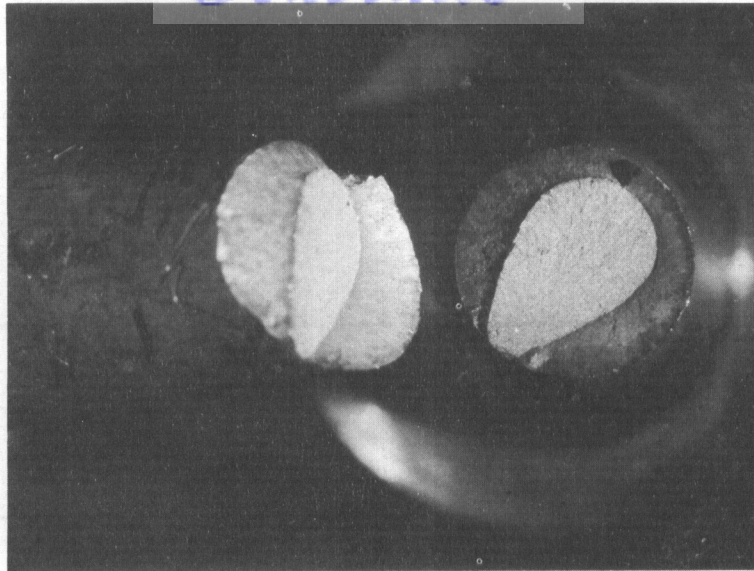
FIG. 38 SUSTAINED LOAD FRACTURE FOR Cd-PLATED SMOOTH
SPECIMEN. 4340 STEEL. NUCLEATION AT OR NEAR SURFACE.
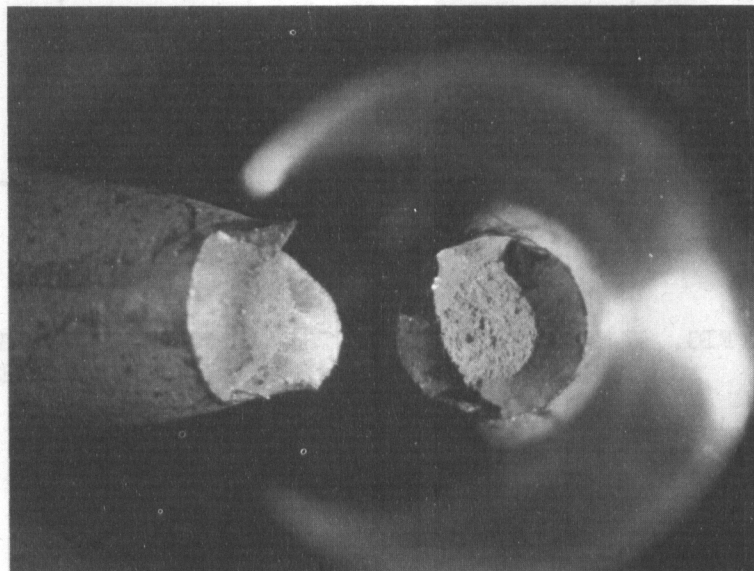
FIG. 39 SUSTAINED LOAD FRACTURE FOR Cd-PLATE SMOOTH
SPECIMEN. 4340 STEEL. NUCLEATION SUBSURFACE.
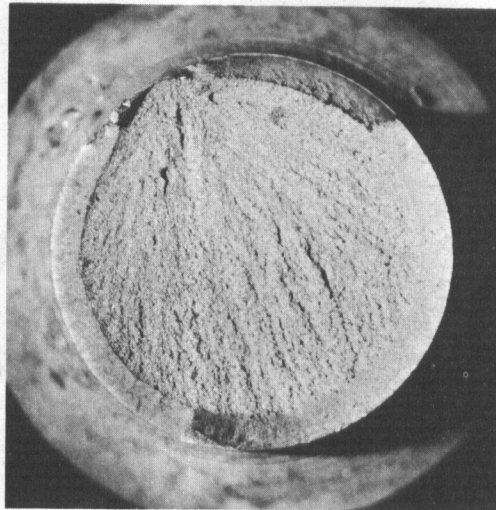
FIG. 40 SUSTAINED-LOAD FRACTURE FOR Cd-PLATED
NOTCHED SPECIMEN. K = 2. NUCLEATION AT
OR NEAR SURFACE. TEMPERED AT 400º F FOR
4 HOURS.
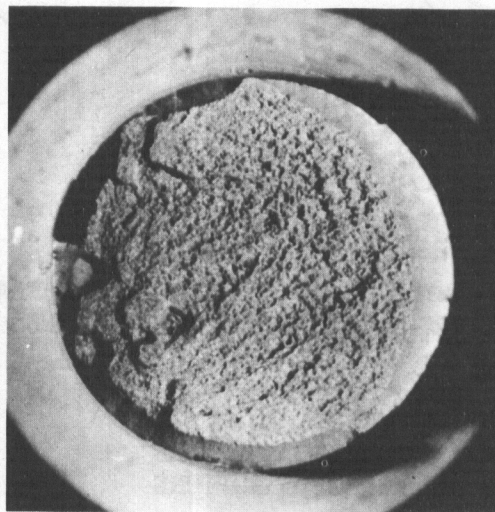
FIG. 41 SUSTAINED-LOAD FRACTURE FOR Cd-PLATED
NOTCHED SPECIMEN. K = 2. NUCLEATION
SUBSURFACE. TEMPERED AT 600º F FOR
4 HOURS
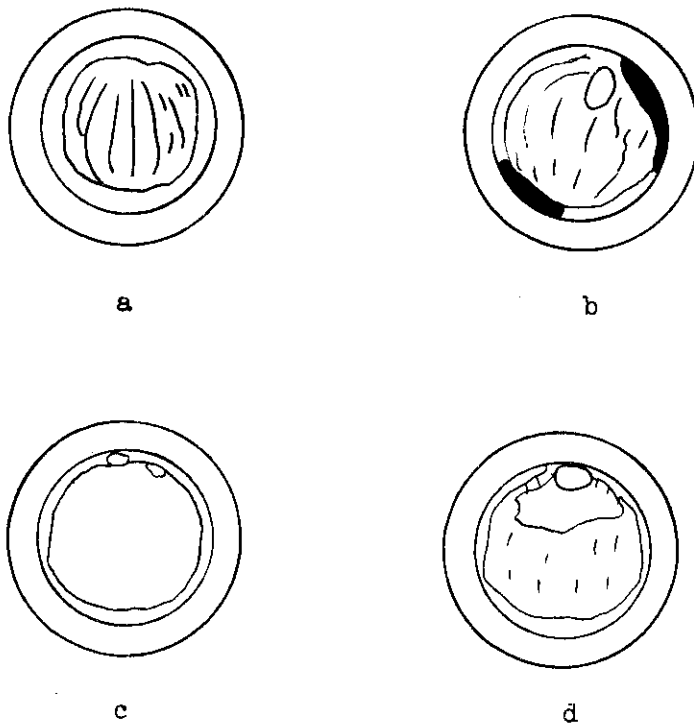
FIG. 42 CHARACTERISTIC SUSTAINED-LOAD FRACTURE DEVELOPMENT
FOR Cd-PLATED NOTCHED SPECIMENS. K = 2.

a. TENSION TEST
b. 30 SECONDS TO RUPTURE
c.   7 HOURS TO RUPTURE
d. 30 HOURS TO RUPTURE
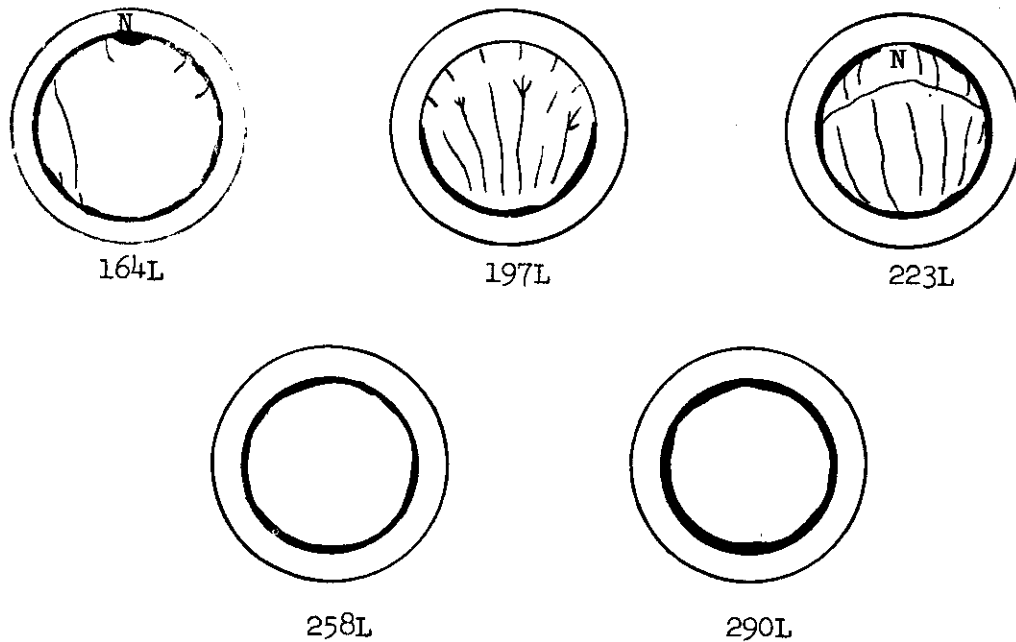
FIG. 43   CHARACTERISTIC SUSTAINED-LOAD FRACTURE DEVELOPMENT
          FOR Cd-PLATED NOTCHED SPECIMENS.   K = 3.

          164L   TEMPERED AT 400°F; FRACTURE TIME: 1.4 HOURS
          197L   TEMPERED AT 500°F; FRACTURE TIME: 3.8 HOURS
          223L   TEMPERED AT 700°F; FRACTURE TIME: 6.8 HOURS
          258L   TEMPERED AT 800°F; FRACTURE TIME: 6.2 HOURS
          290L   TEMPERED AT 1000°F; FRACTURE TIME: 1.3 HOURS
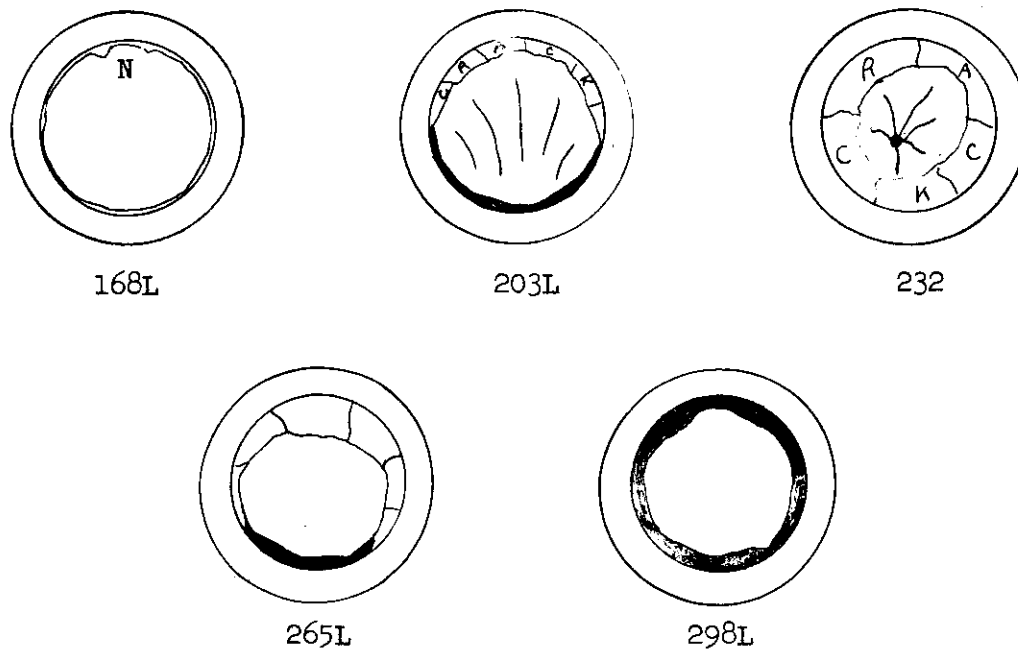
FIG. 44   CHARACTERISTIC SUSTAINED-LOAD FRACTURE DEVELOPMENT FOR
Cd-PLATED NOTCHED SPECIMENS.   K = 5.

168L   TEMPERED AT 400°F; FRACTURE TIME: 1.4 HOURS
203L   TEMPERED AT 500°F; FRACTURE TIME: .8 HOURS
232   TEMPERED AT 700°F; FRACTURE TIME: 4.4 HOURS
265L   TEMPERED AT 800°F; FRACTURE TIME: 6.5 HOURS
298L   TEMPERED AT 1000°F; FRACTURE TIME: 32.6 HOURS

180L　　　　　　209L　　　　　　239L

271L　　　　　　307L
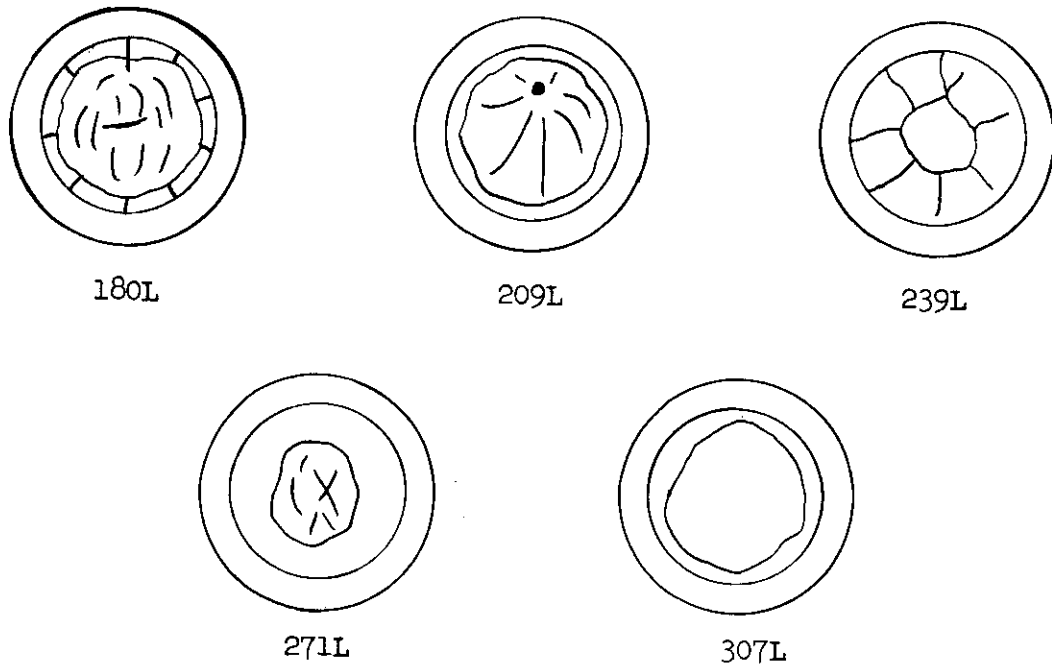
FIG. 45　CHARACTERISTIC SUSTAINED-LOAD FRACTURE DEVELOPMENT FOR
Cd-PLATED NOTCHED SPECIMENS.　K = 10.

180 L　TEMPERED AT 400°F;　FRACTURE TIME 1.2 HOURS
209 L　TEMPERED AT 500°F;　FRACTURE TIME 6.6 HOURS
239 L　TEMPERED AT 700°F;　FRACTURE TIME 6.5 HOURS
271 L　TEMPERED AT 800°F;　FRACTURE TIME 13.8 HOURS
307 L　TEMPERED AT 1000°F; FRACTURE TIME 23.9 HOURS
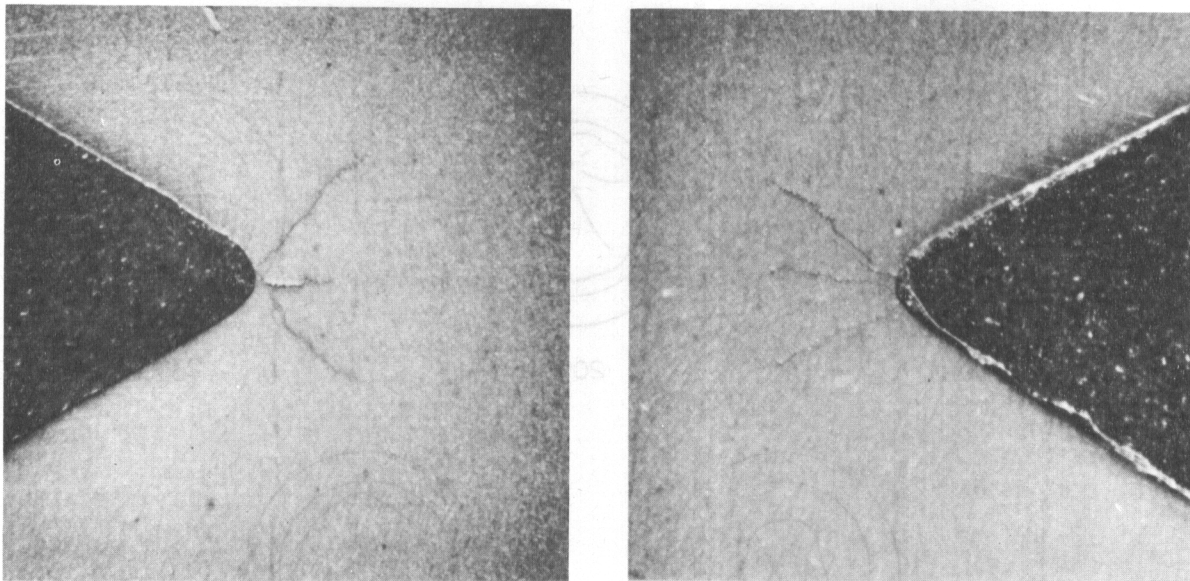
FIG. 46 CRACK DEVELOPMENT IN Cd-PLATED 0.9 IN. DIA.
SPECIMEN. K = 5. 4340 STEEL TEMPERED AT 600º F.
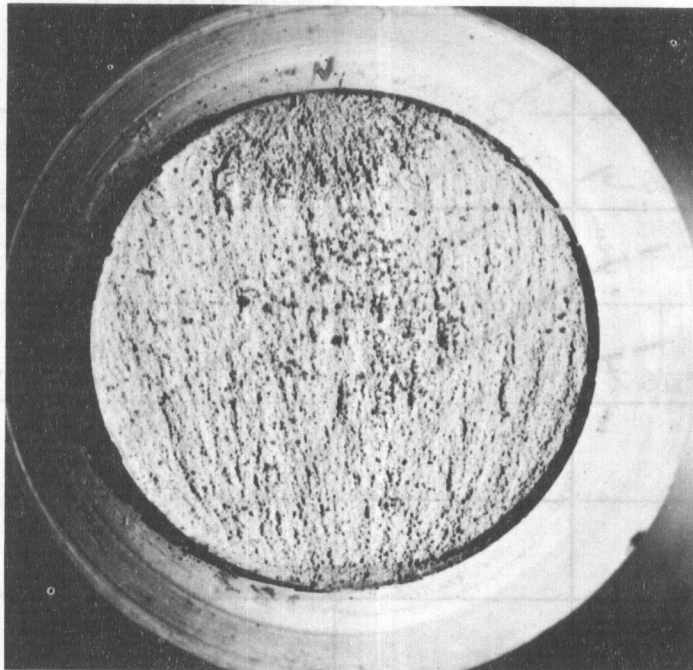
FIG. 47   SUSTAINED-LOAD FRACTURE IN 0.9 IN. DIA.
Cd-PLATED SPECIMEN (NOTE FRACTURE NUCLEUS
AND SHEAR LIP).
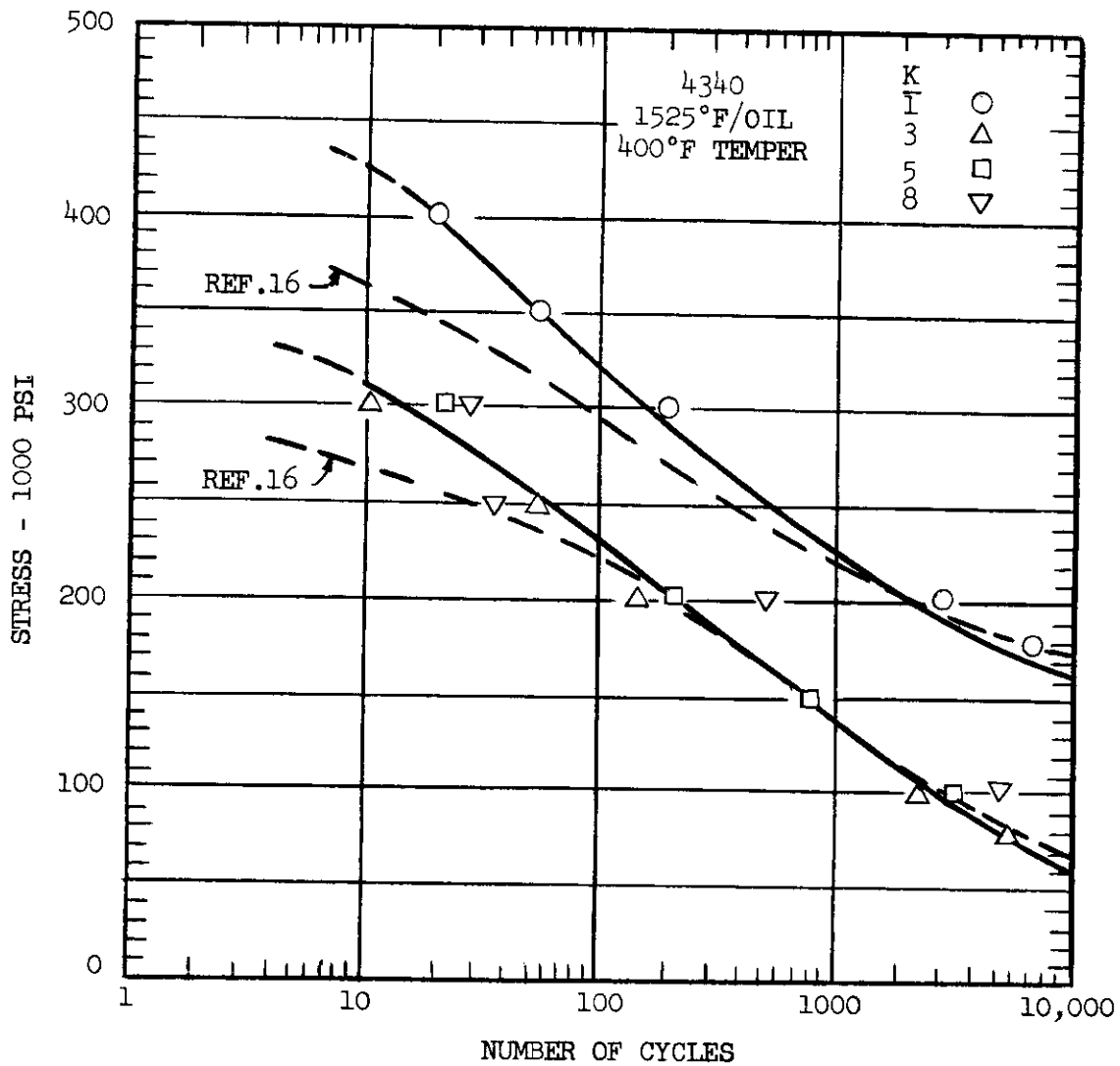
FIG. 48 S-N CURVES FOR EMBRITTLED SMOOTH AND NOTCHED ROTATING
BEAM FATIGUE SPECIMENS FROM TWO HEATS OF 4340 STEEL
TEMPERED AT 400°F.
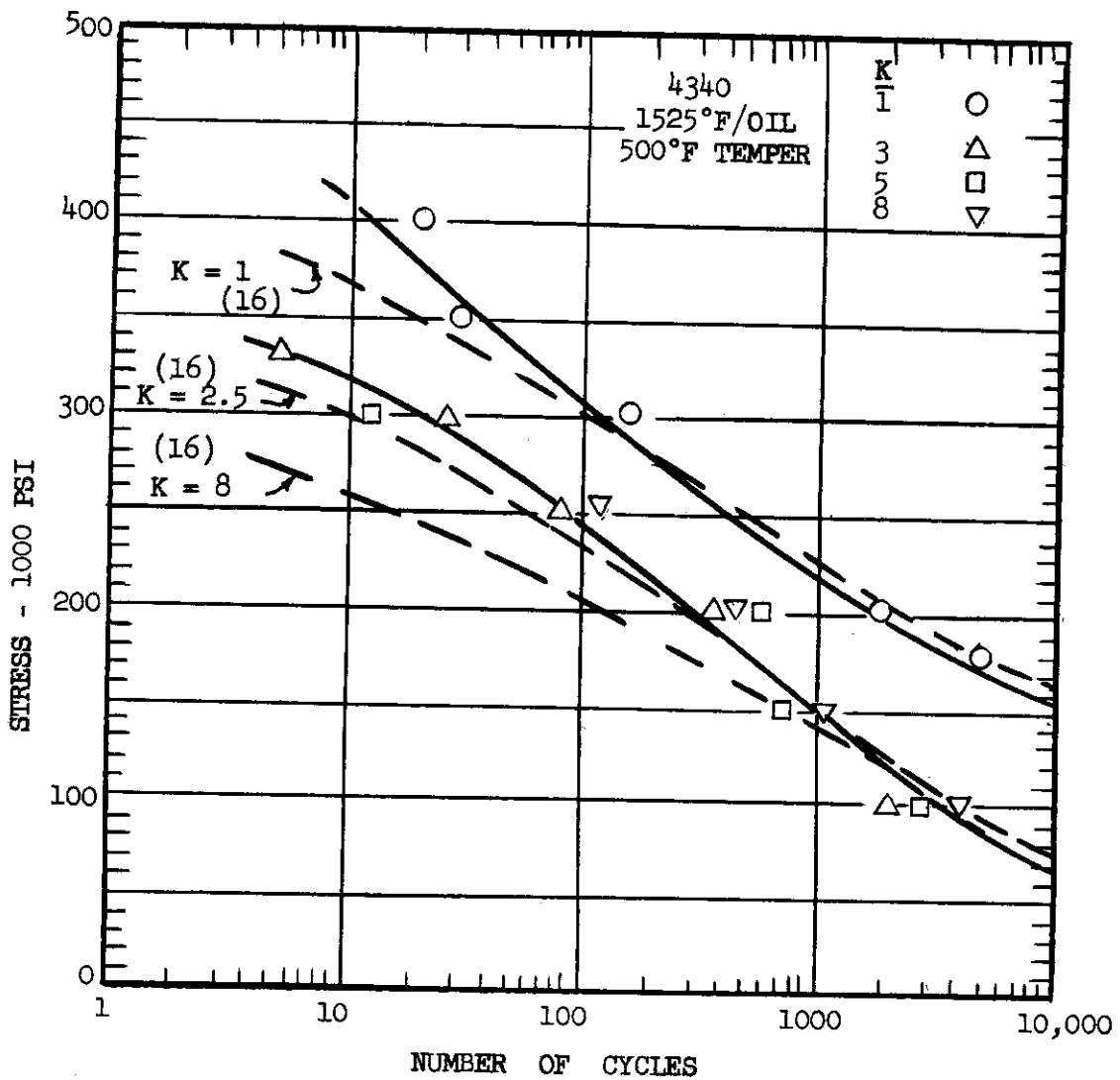
FIG. 49 S-N CURVES FOR EMBRITTLED SMOOTH AND NOTCHED ROTATING
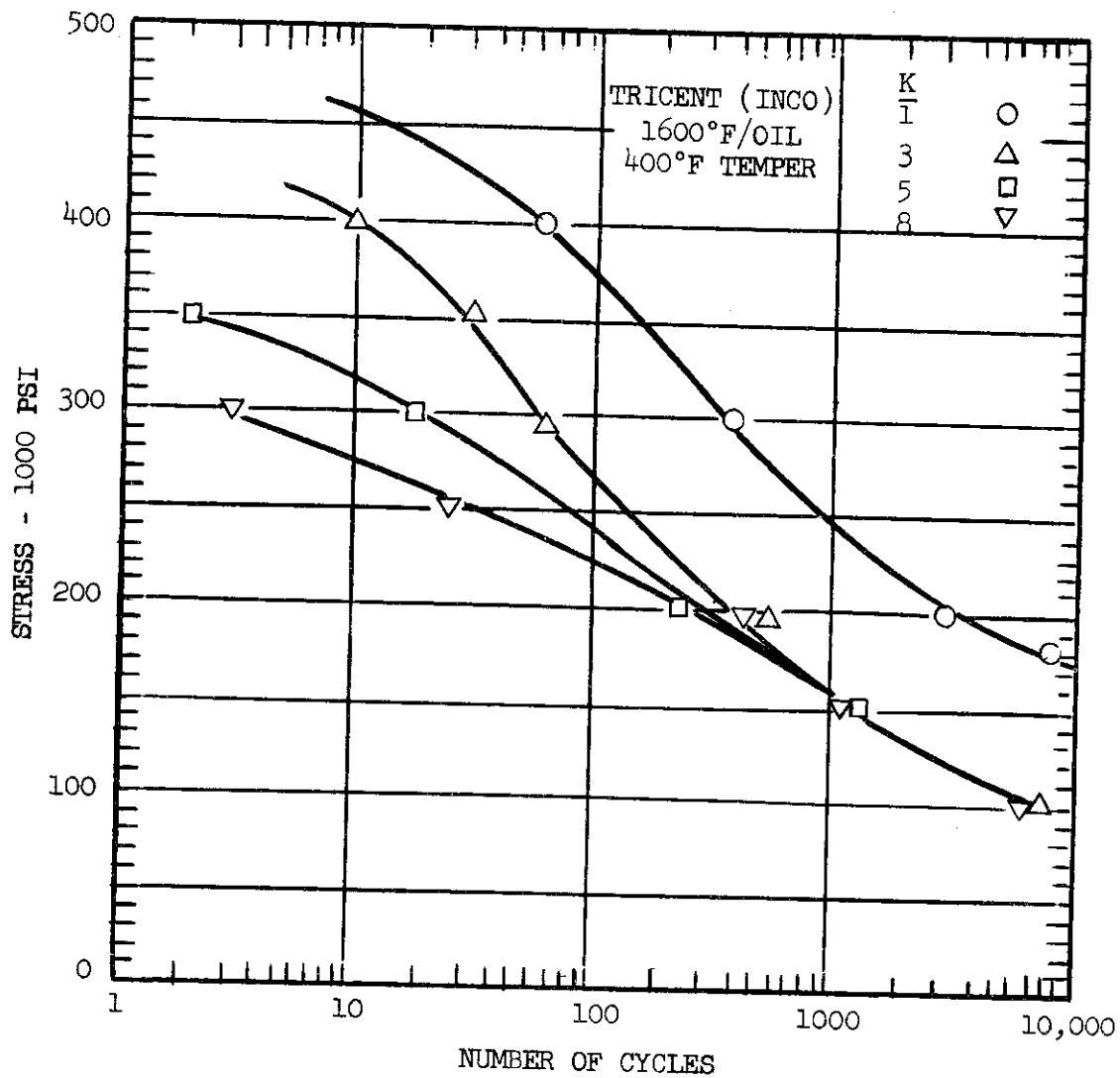BEAM FATIGUE SPECIMENS FROM TWO HEATS OF 4340 STEEL
TEMPERED AT 500°F.
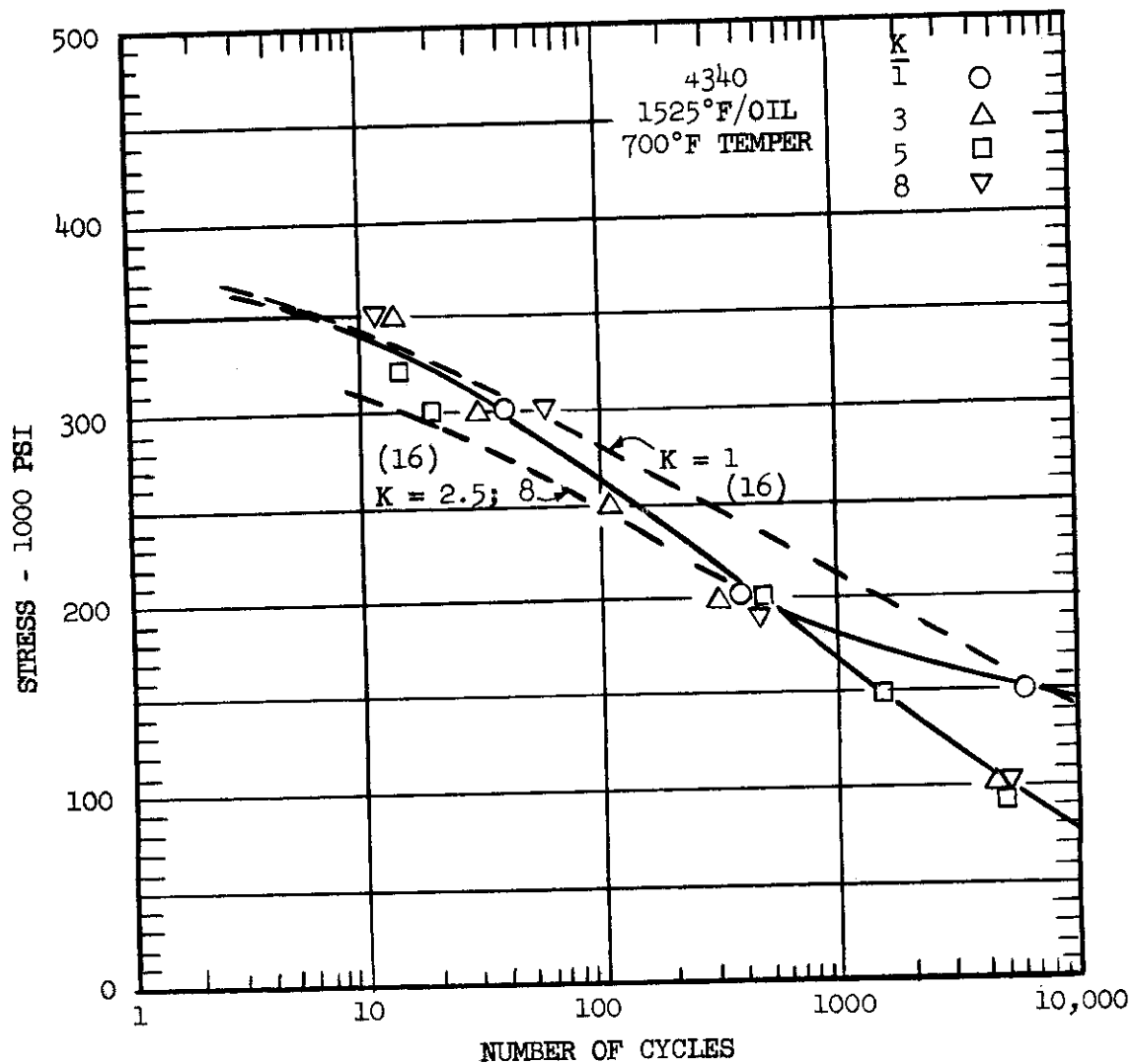
FIG. 50 S-N CURVES FOR EMBRITTLED SMOOTH AND NOTCHED ROTATING
BEAM FATIGUE SPECIMENS FROM TWO HEATS OF 4340 STEEL
TEMPERED AT 700°F.
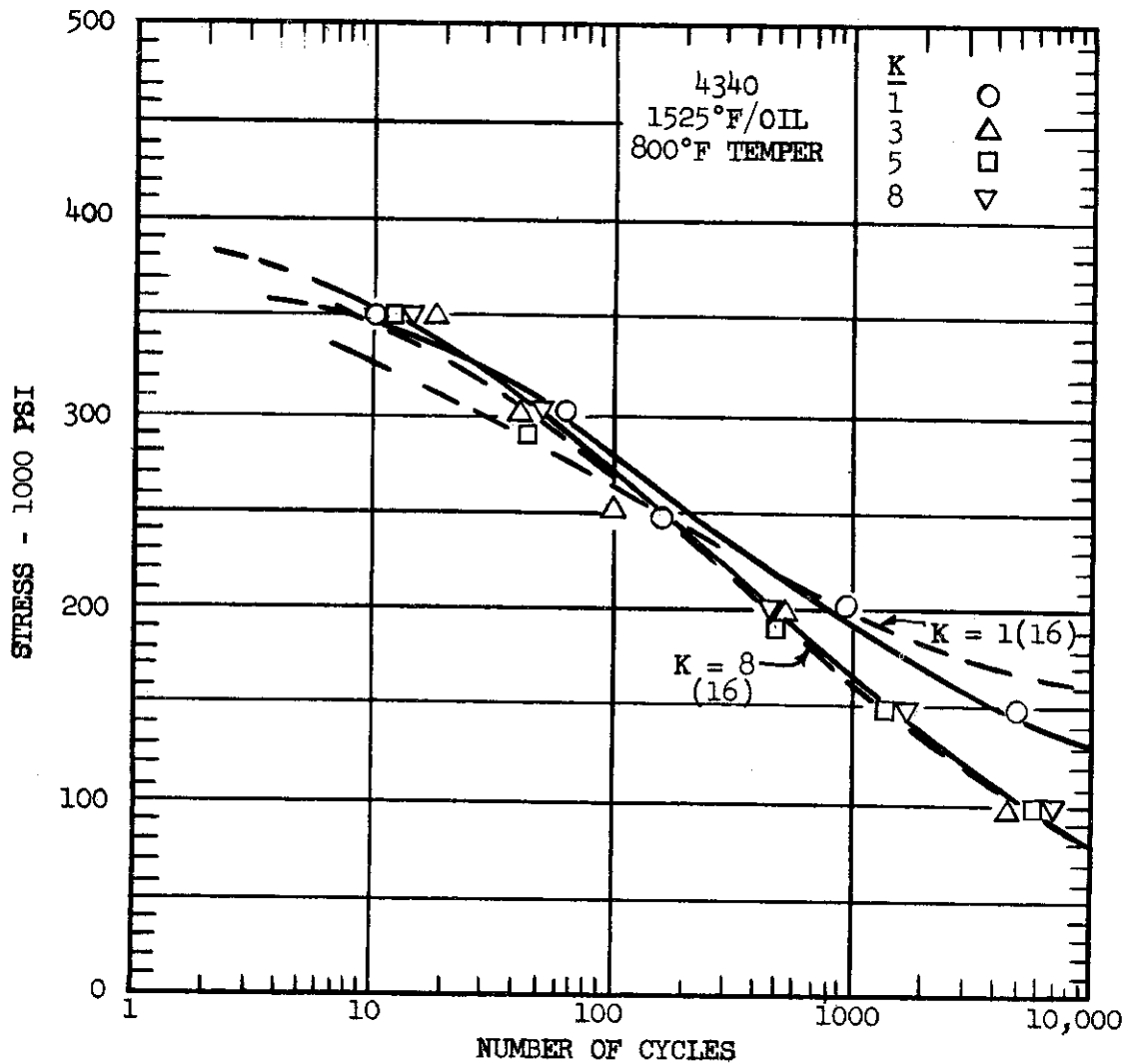
FIG. 51   S-N CURVES FOR EMBRITTLED SMOOTH AND NOTCHED ROTATING
BEAM FATIGUE SPECIMENS FROM TWO HEATS OF 4340 STEEL
TEMPERED AT 800°F.
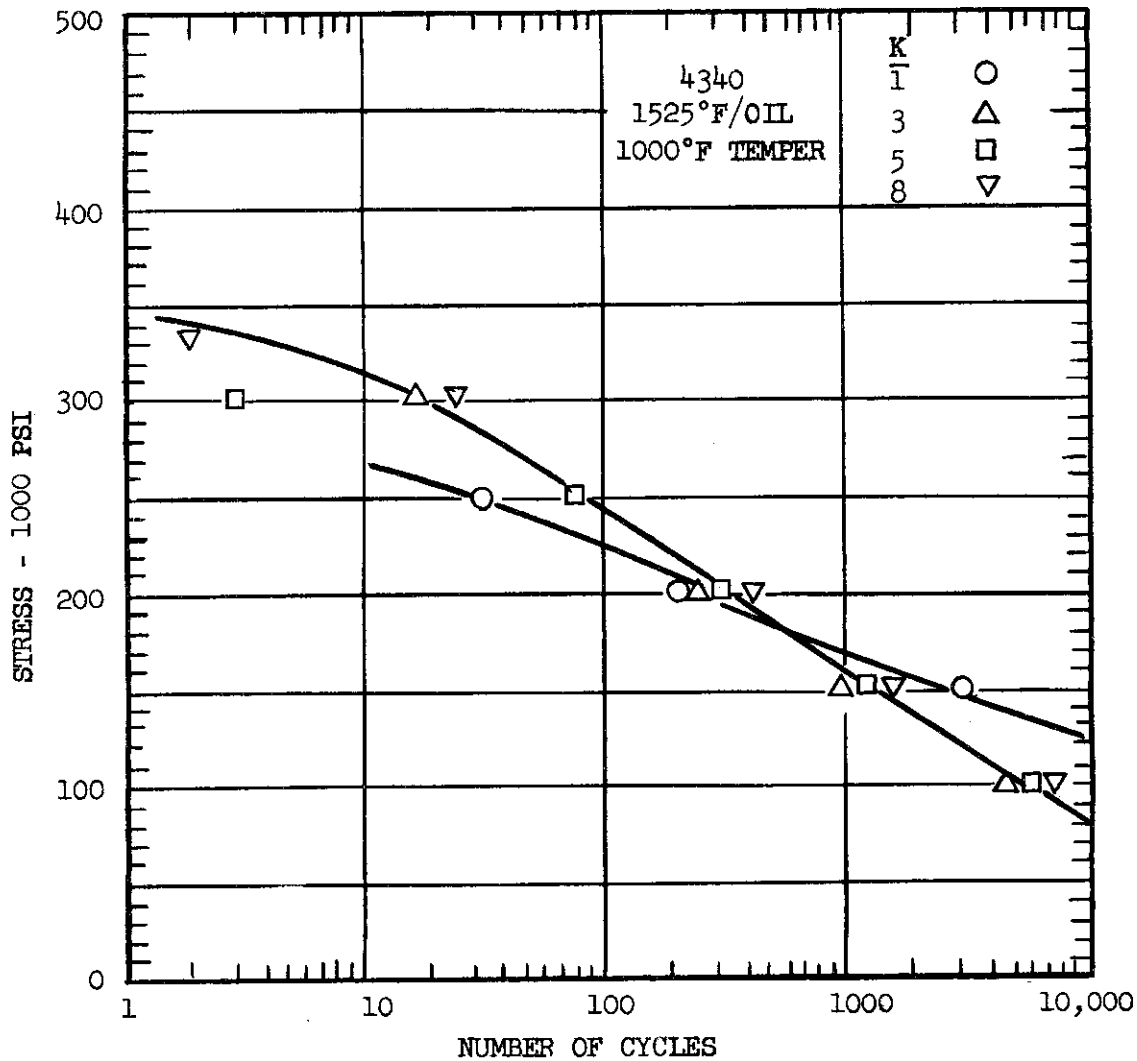
FIG. 52 S-N CURVES FOR EMBRITTLED SMOOTH AND NOTCHED ROTATING BEAM FATIGUE SPECIMENS FROM A 4340 STEEL.

FIG. 53 S-N CURVES FOR EMBRITTLED SMOOTH AND NOTCHED ROTATING BEAM FATIGUE SPECIMENS FROM TRICENT (INCO) STEEL.
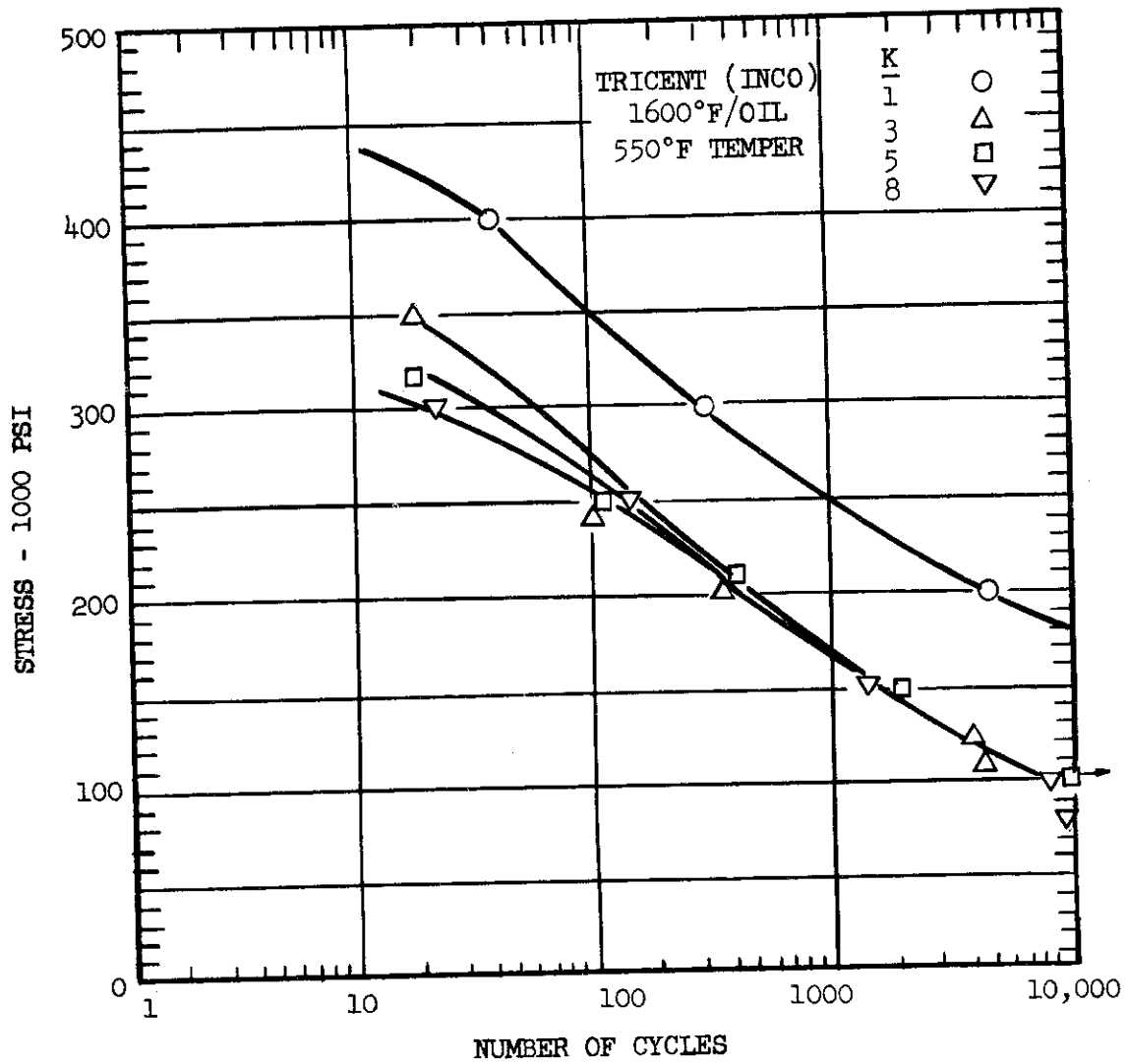
FIG. 54 S-N CURVES FOR EMBRITTLED SMOOTH AND NOTCHED ROTATING BEAM FATIGUE SPECIMENS FROM TRICENT (INCO) STEEL.
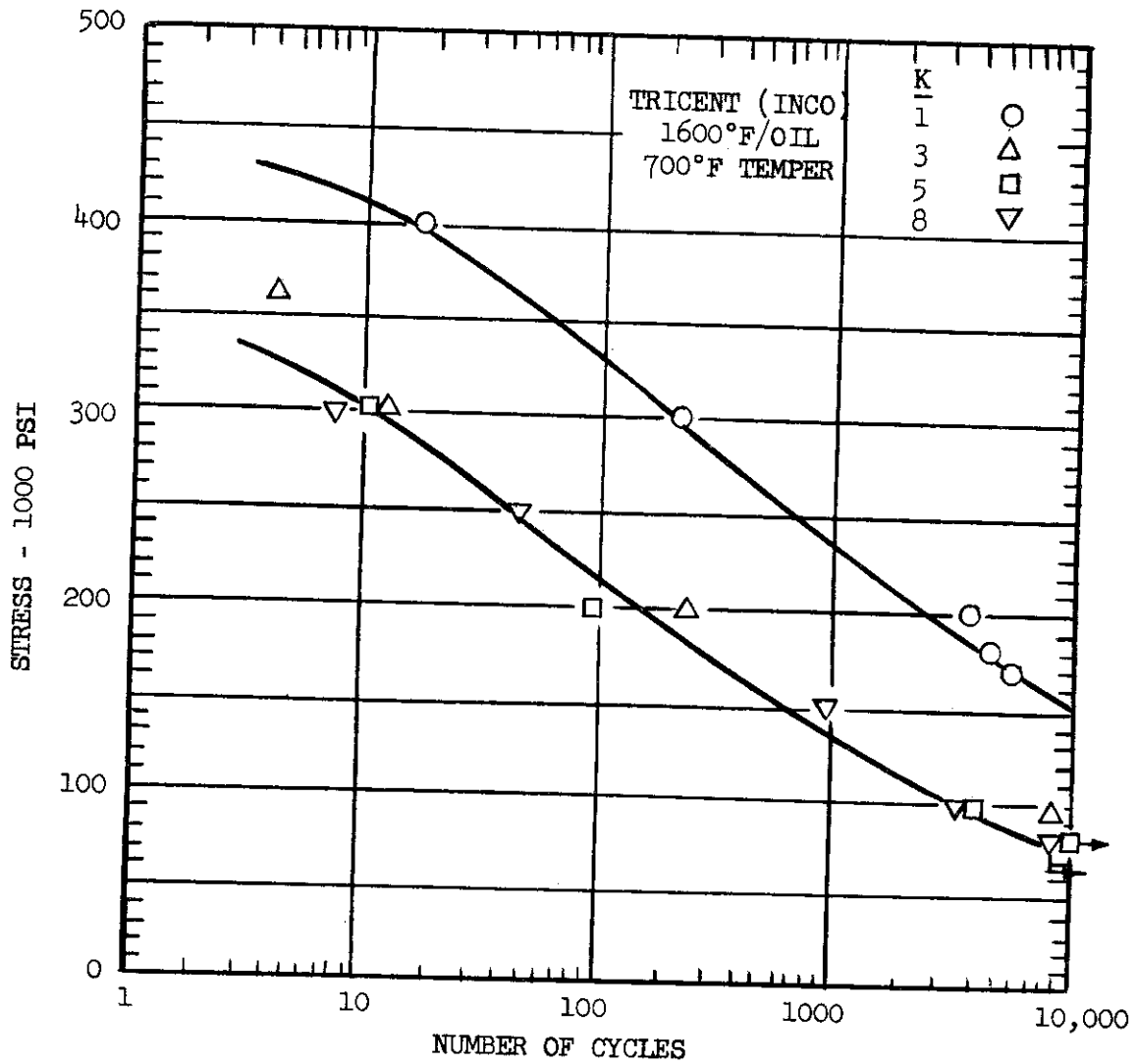
FIG. 55 S-N CURVES FOR EMBRITTLED SMOOTH AND NOTCHED ROTATING
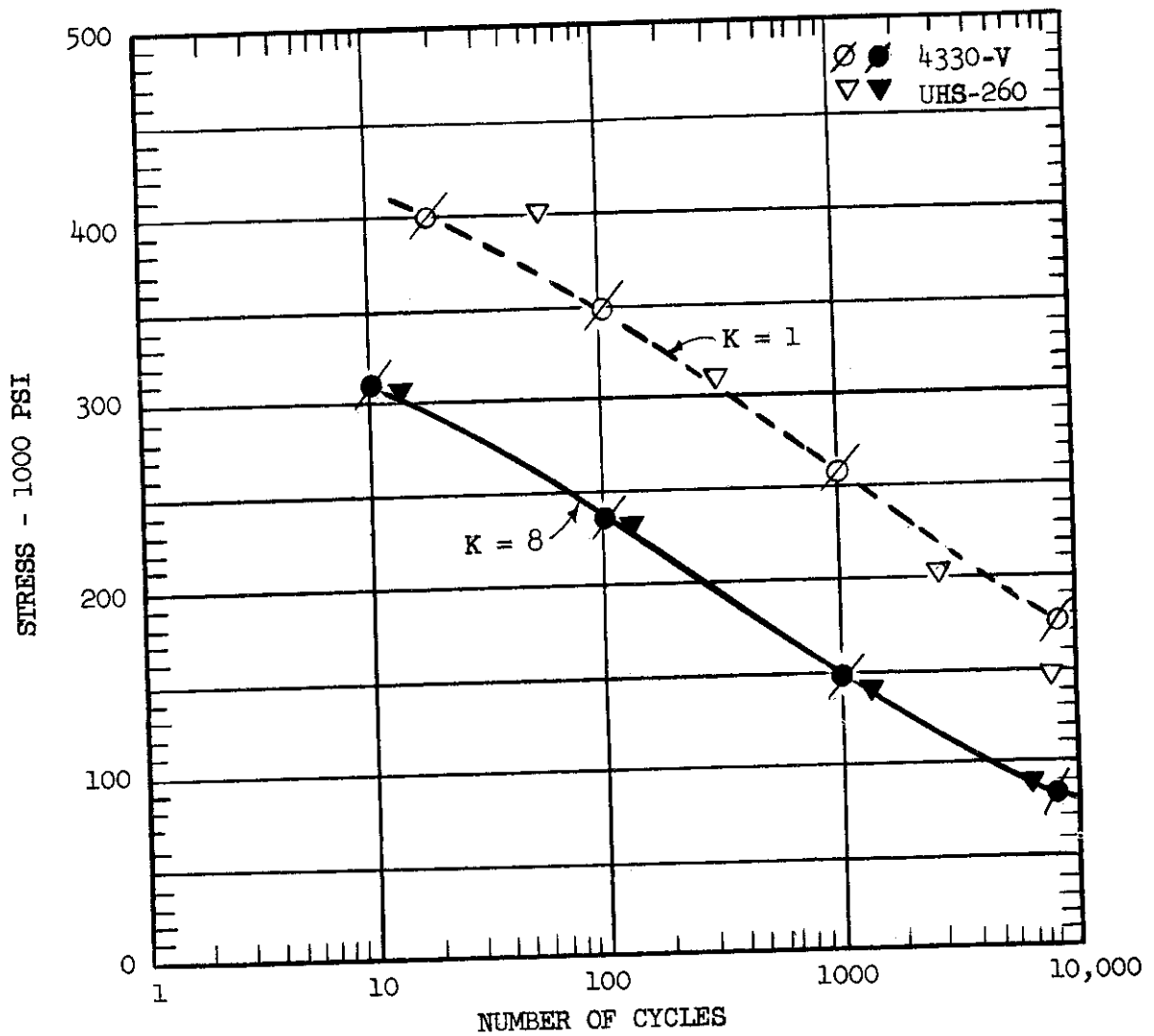BEAM FATIGUE SPECIMENS FROM TRICENT (INCO) STEEL.
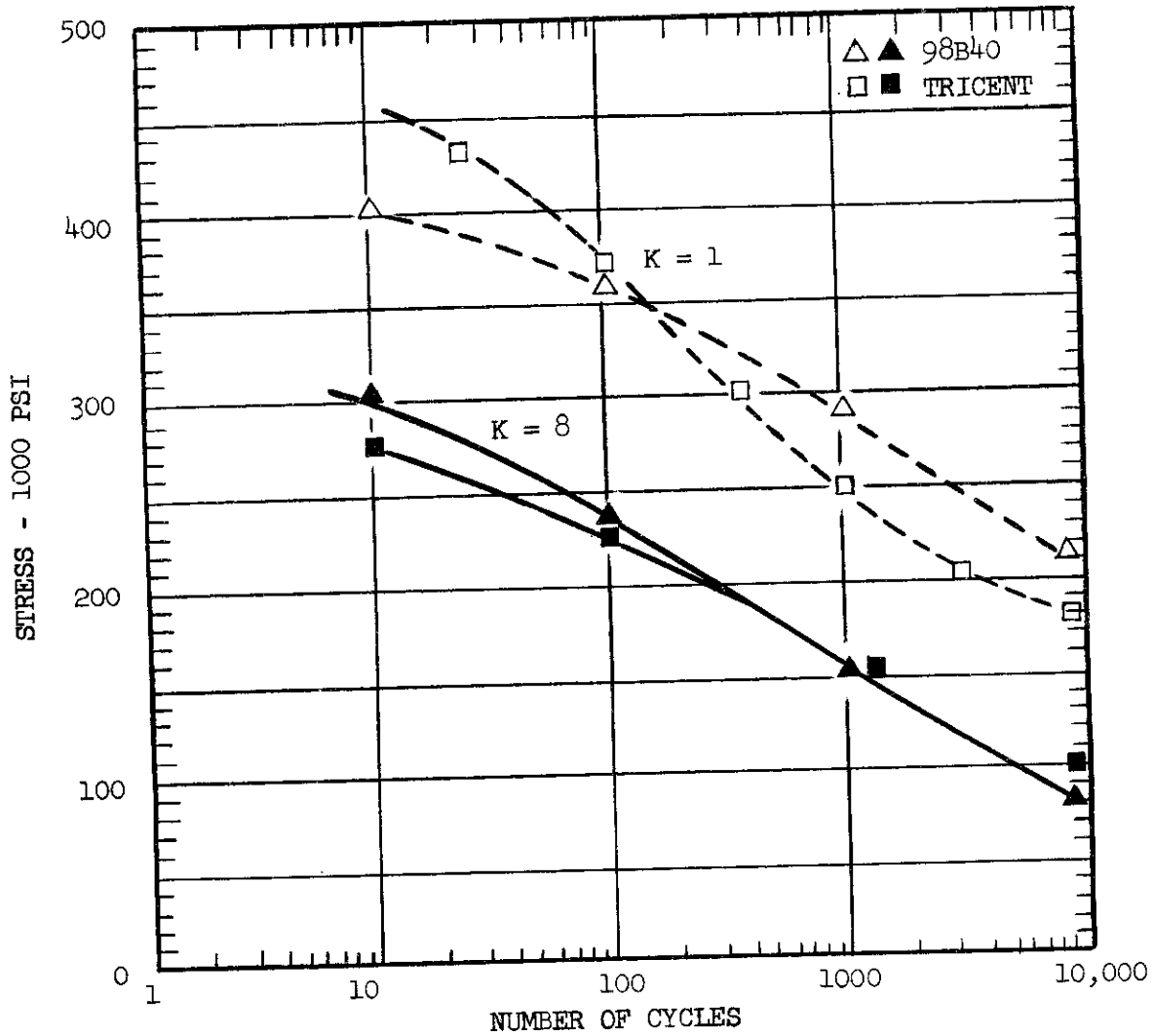
FIG. 56 S-N CURVES FOR EMBRITTLED SMOOTH AND NOTCHED $(K = 8)$
ROTATING BEAM FATIGUE SPECIMENS FOR STEELS TEMPERED
TO 290,000 PSI TENSILE STRENGTH.
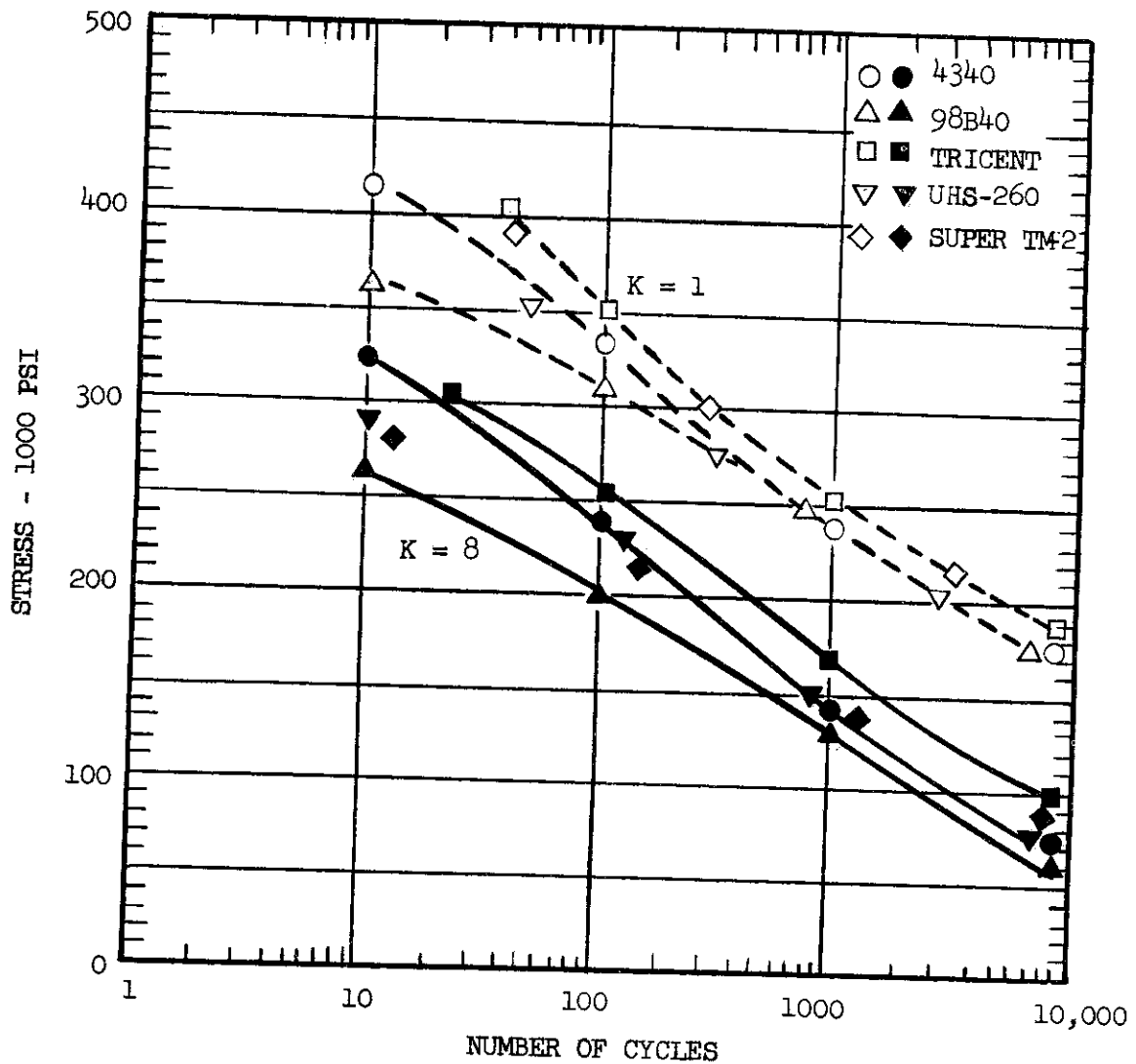
FIG. 57 S-N CURVES FOR EMBRITTLED SMOOTH AND NOTCHED (K = 8)
ROTATING BEAM FATIGUE SPECIMENS FOR STEELS TEMPERED
TO 270,000 PSI TENSILE STRENGTH.

FIG. 58   S-N CURVES FOR EMBRITTLED SMOOTH AND NOTCHED (K = 8)
ROTATING BEAM FATIGUE SPECIMENS FOR STEELS TEMPERED
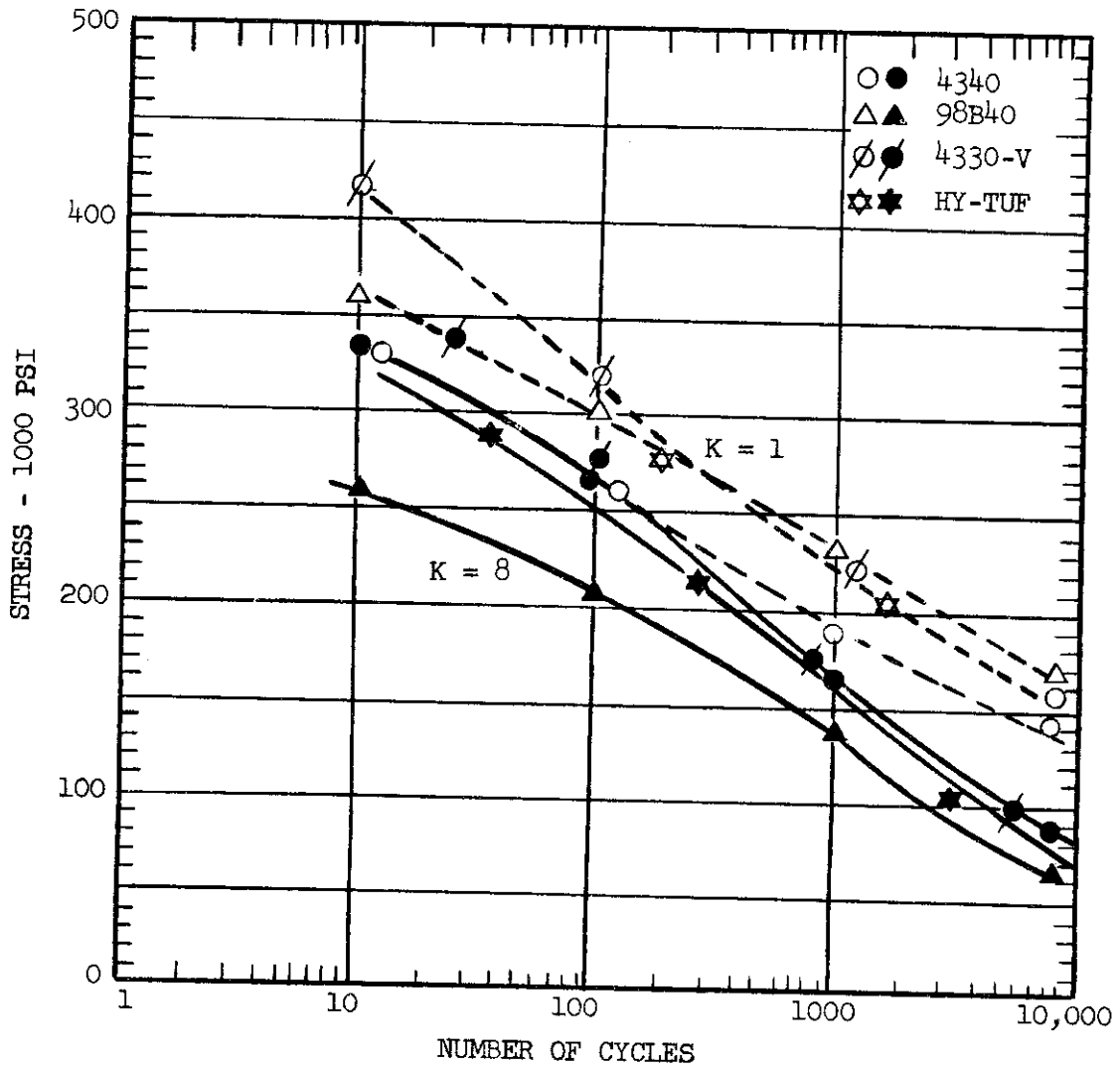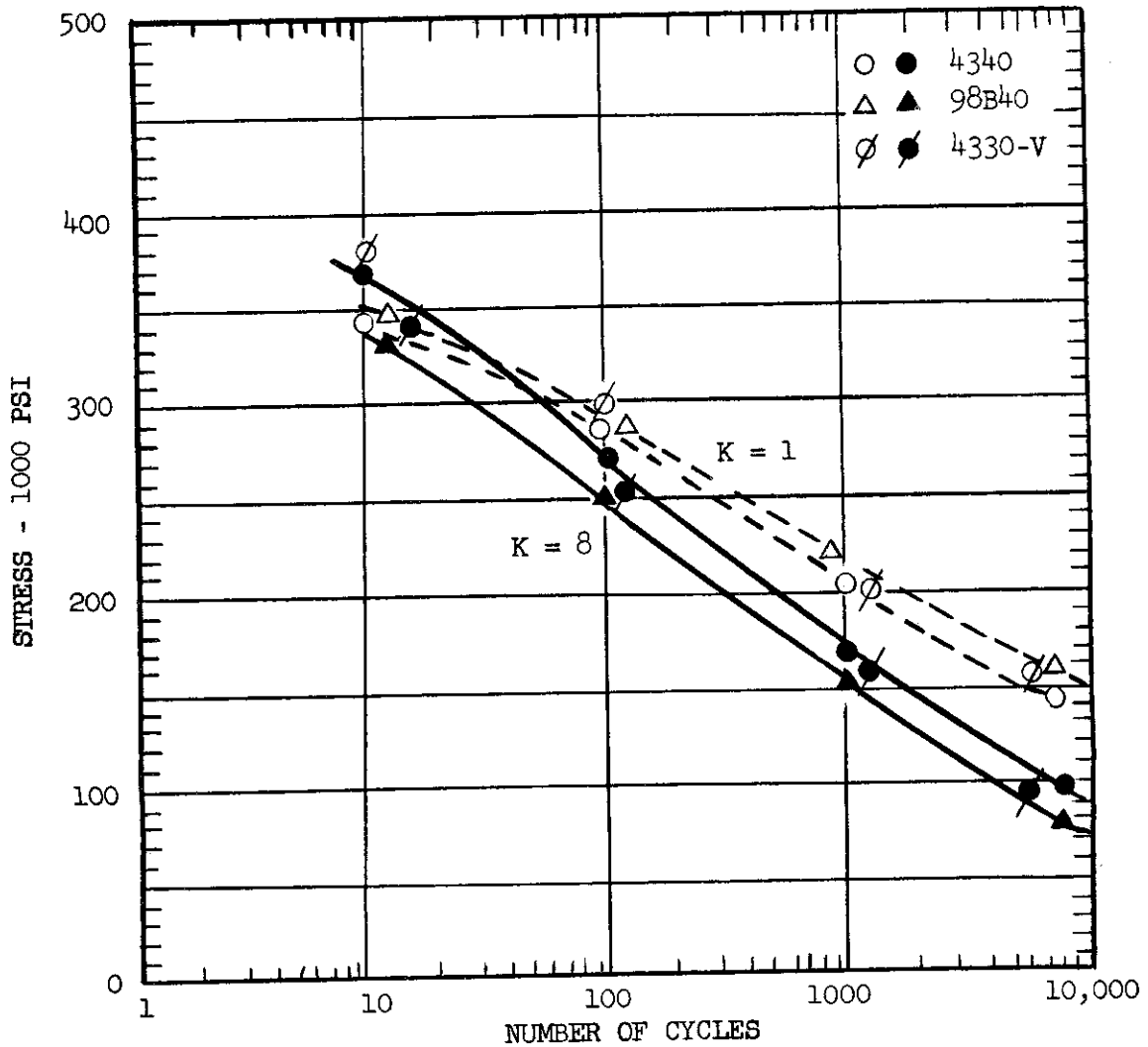TO 250,000 PSI TENSILE STRENGTH.

FIG. 59   S-N CURVES FOR EMBRITTLED SMOOTH AND NOTCHED (K = 8) ROTATING BEAM FATIGUE SPECIMENS FOR STEELS TEMPERED TO 230,000 PSI TENSILE STRENGTH.

FIG. 60 S-N CURVES FOR EMBRITTLED SMOOTH AND NOTCHED (K = 8)
ROTATING BEAM FATIGUE SPECIMENS FOR STEELS TEMPERED
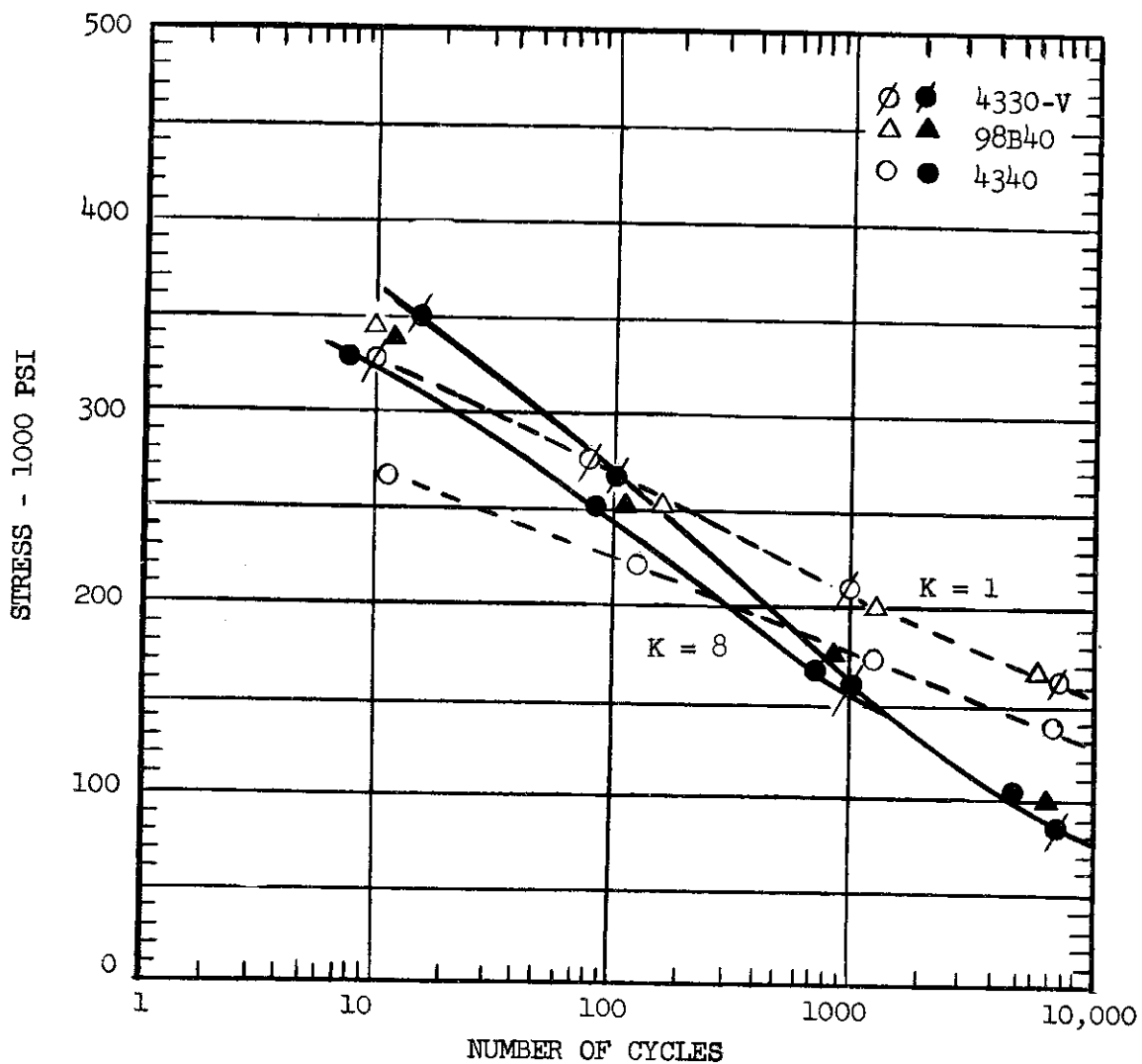TO 210,000 PSI TENSILE STRENGTH.

FIG. 61 S-N CURVES FOR EMBRITTLED SMOOTH AND NOTCHED (K = 8)
ROTATING BEAM FATIGUE SPECIMENS FOR STEELS TEMPERED
TO 180,000 PSI TENSILE STRENGTH.

~ 150 ~   ~ 2000 ~

575°F

700°F

800°F
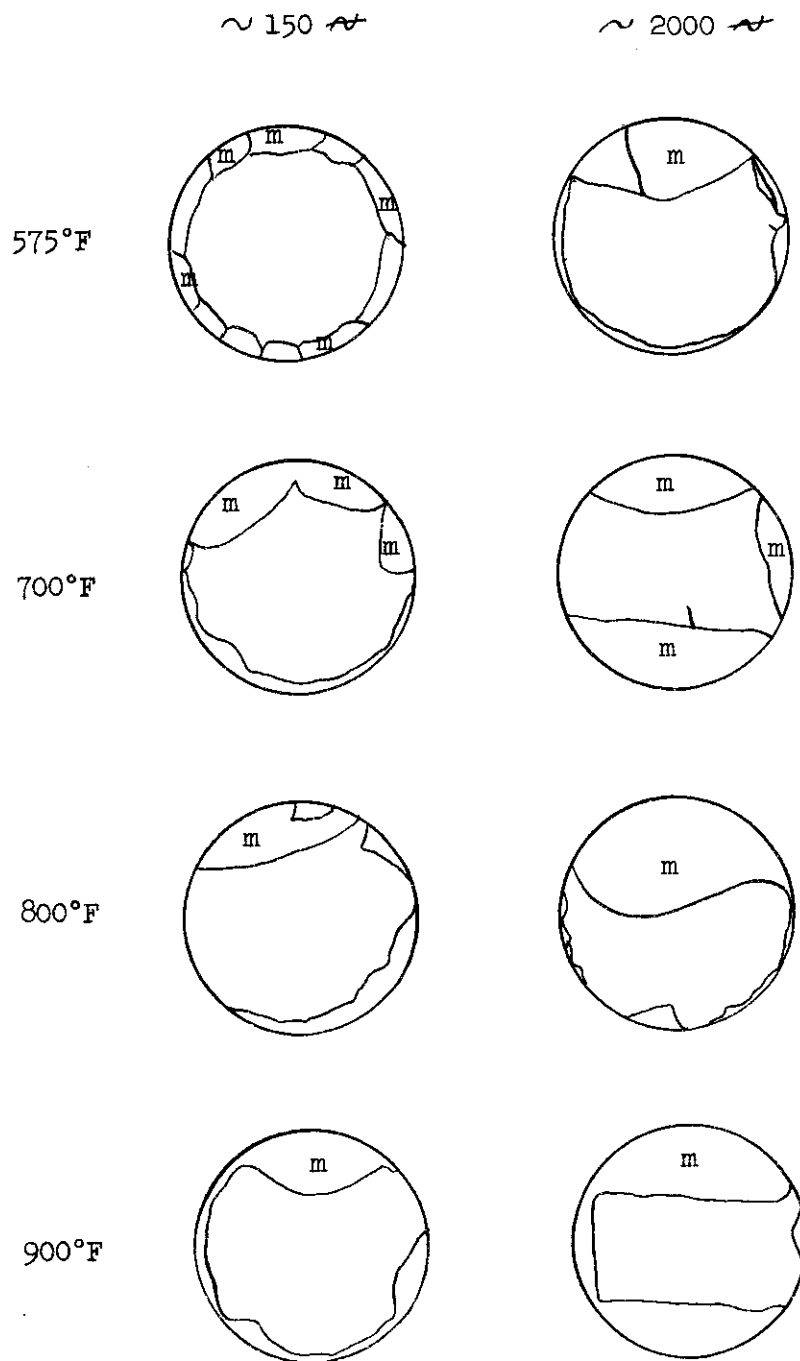
900°F

FIG. 62   SKETCHES OF FRACTURES FOR SMOOTH Cd-PLATED FATIGUE
          SPECIMENS OF 4340 STEEL FOR THE INDICATED TEMPERING
          TEMPERATURES AND CYCLES TO FAILURE.   (m INDICATES
          LOCATION OF MIRROR FRACTURE DEVELOPMENT.)
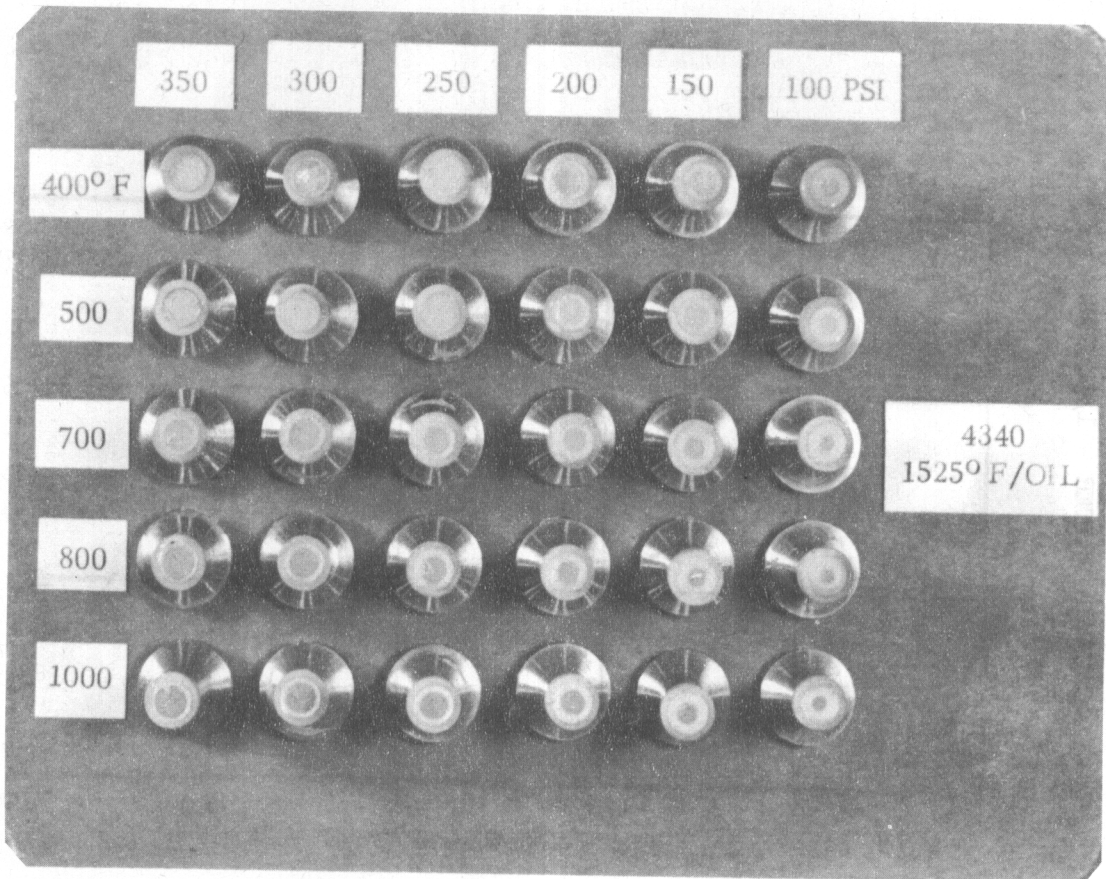
WADC TR 56-395 Pt 3   88

FIG. 63 FRACTURES FOR Cd-PLATED NOTCHED FATIGUE SPECIMENS
OF 4340 STEEL FOR THE INDICATED TEMPERING TEMPERATURES
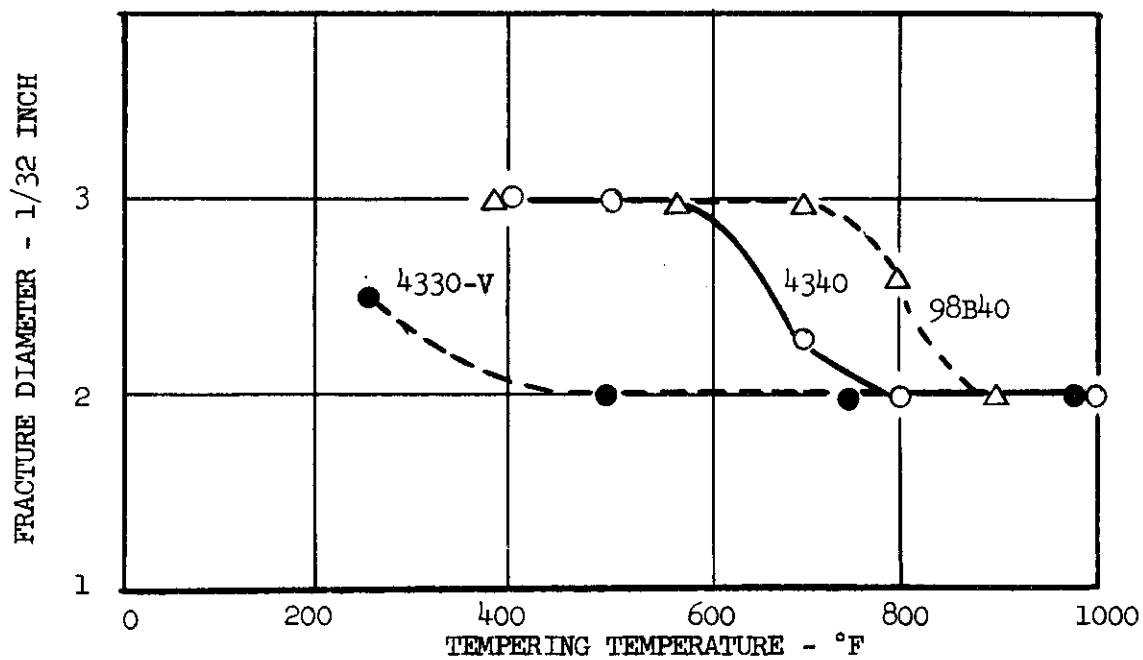AND INITIAL LOADING STRESSES.

FIG. 64   THE FATIGUE SPECIMEN FRACTURE DIAMETER VS. TEMPERING
TEMPERATURE FOR AN INITIAL STRESS OF 100,000 PSI FOR
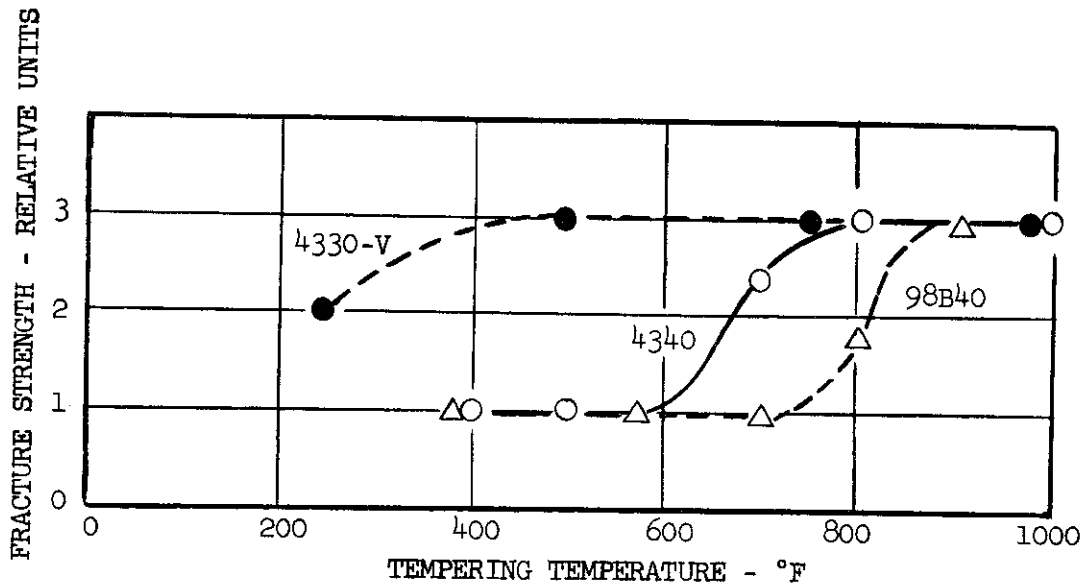THE INDICATED STEELS.

FIG. 65 THE FATIGUE SPECIMEN FRACTURE STRENGTH (ESTIMATED) VS.
TEMPERING TEMPERATURE FOR AN INITIAL STRESS OF 100,000
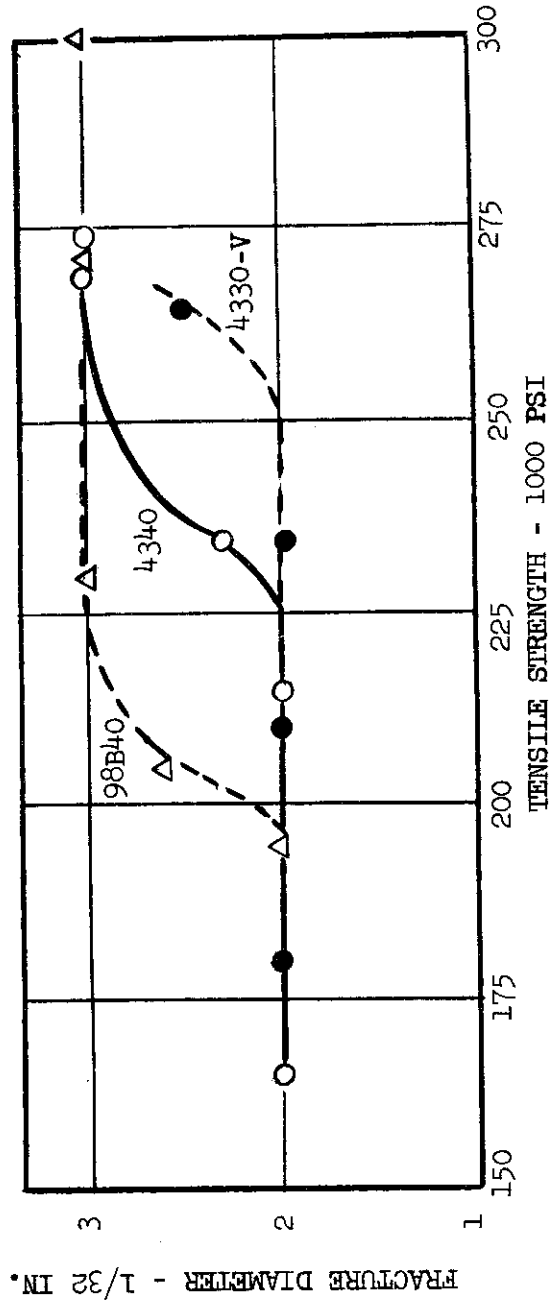PSI FOR THE INDICATED STEELS.

FIG. 66   THE FATIGUE SPECIMEN FRACTURE DIAMETER VS. TENSILE STRENGTH FOR
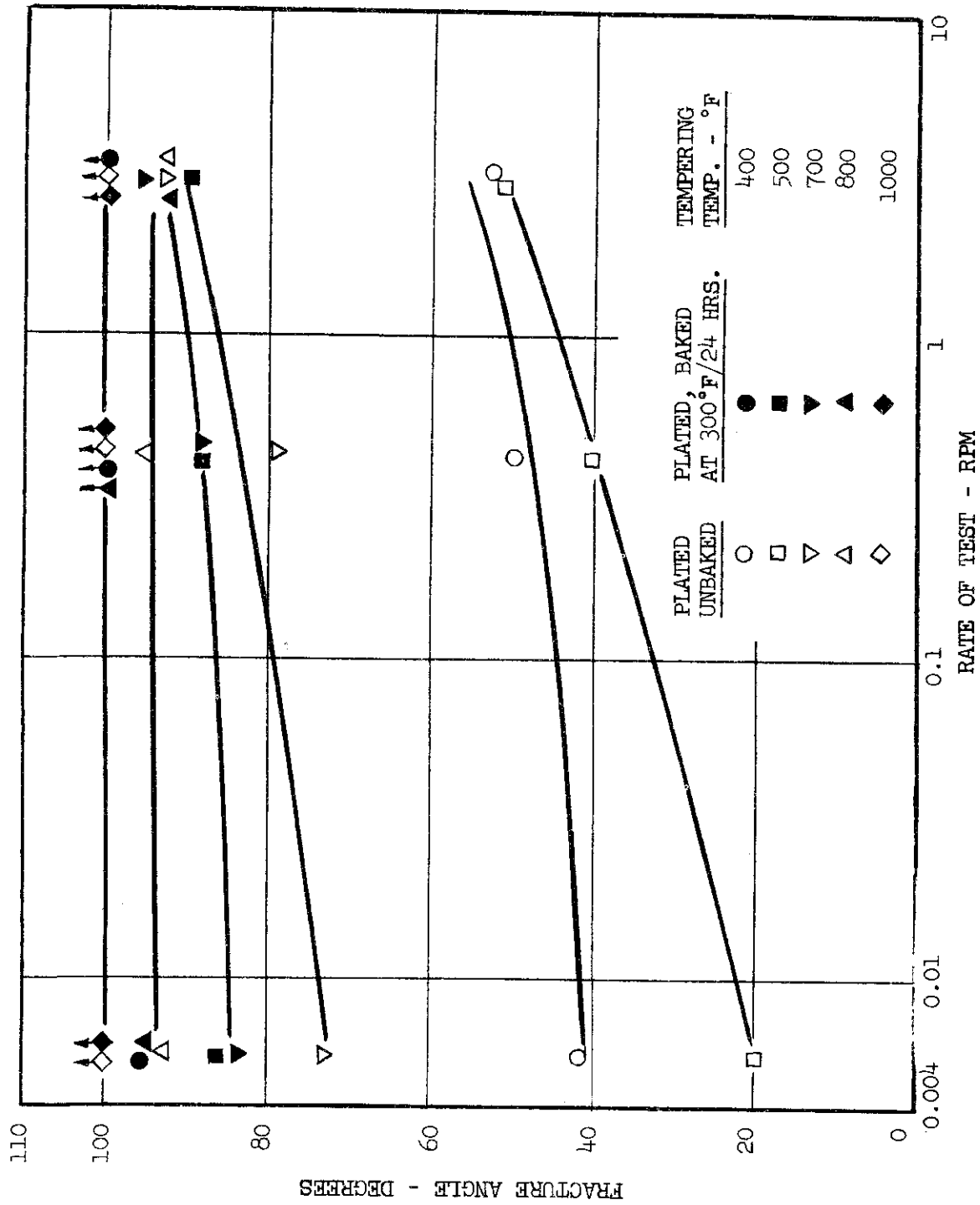AN INITIAL STRESS OF 100,000 PSI FOR THE INDICATED STEELS.

FIG. 67   THE BEND FRACTURE ANGLE VS. TESTING SPEED FOR Cd-PLATED 4340 STEEL WITH
TEMPERING TEMPERATURE AS PARAMETER FOR THE INDICATED TEST CONDITIONS.
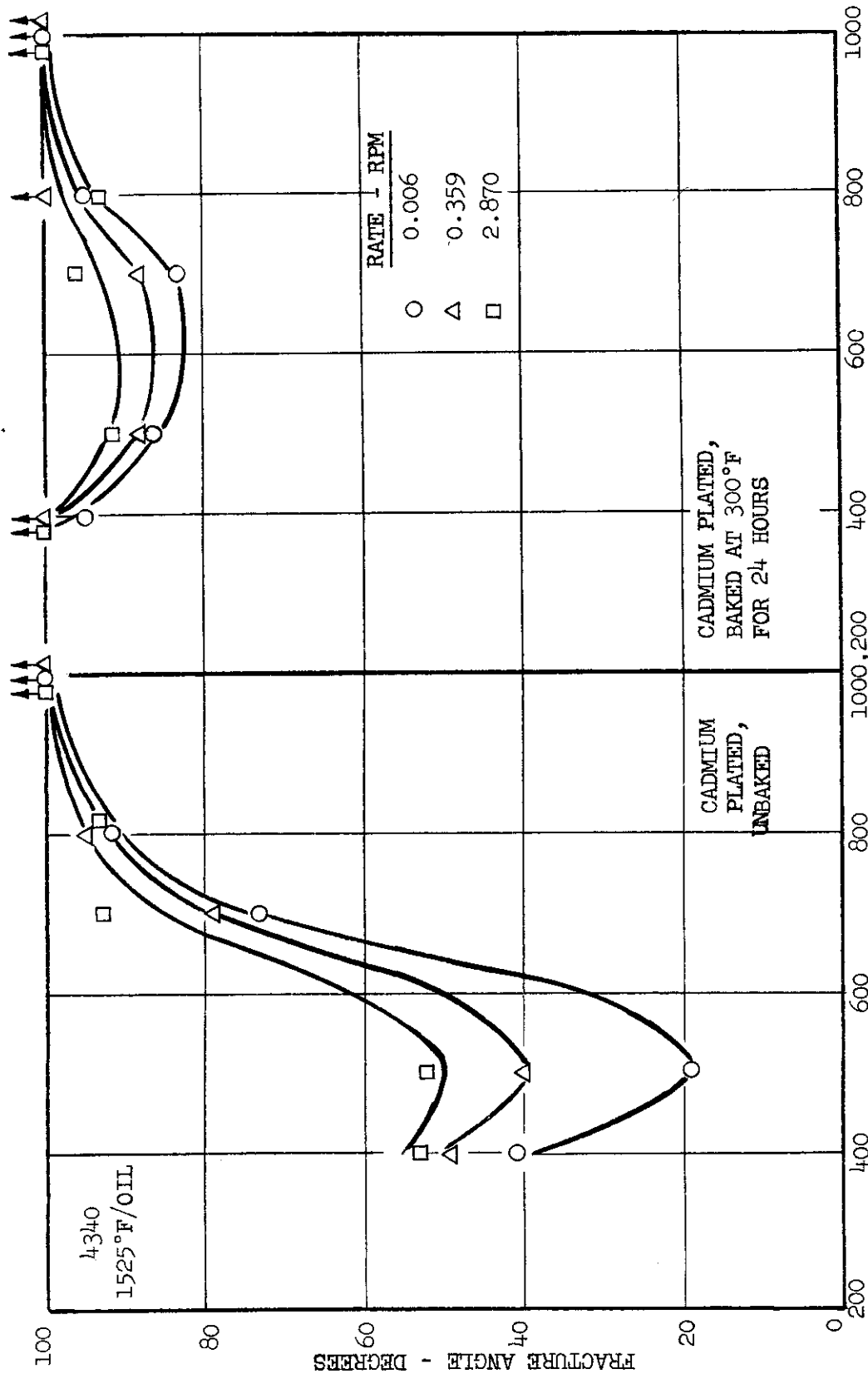
FIG. 68 THE BEND FRACTURE ANGLES VS. TEMPERING TEMPERATURE FOR Cd-PLATED 4340 STEEL WITH TESTING SPEED AS PARAMETER FOR THE INDICATED TEST CONDITIONS.
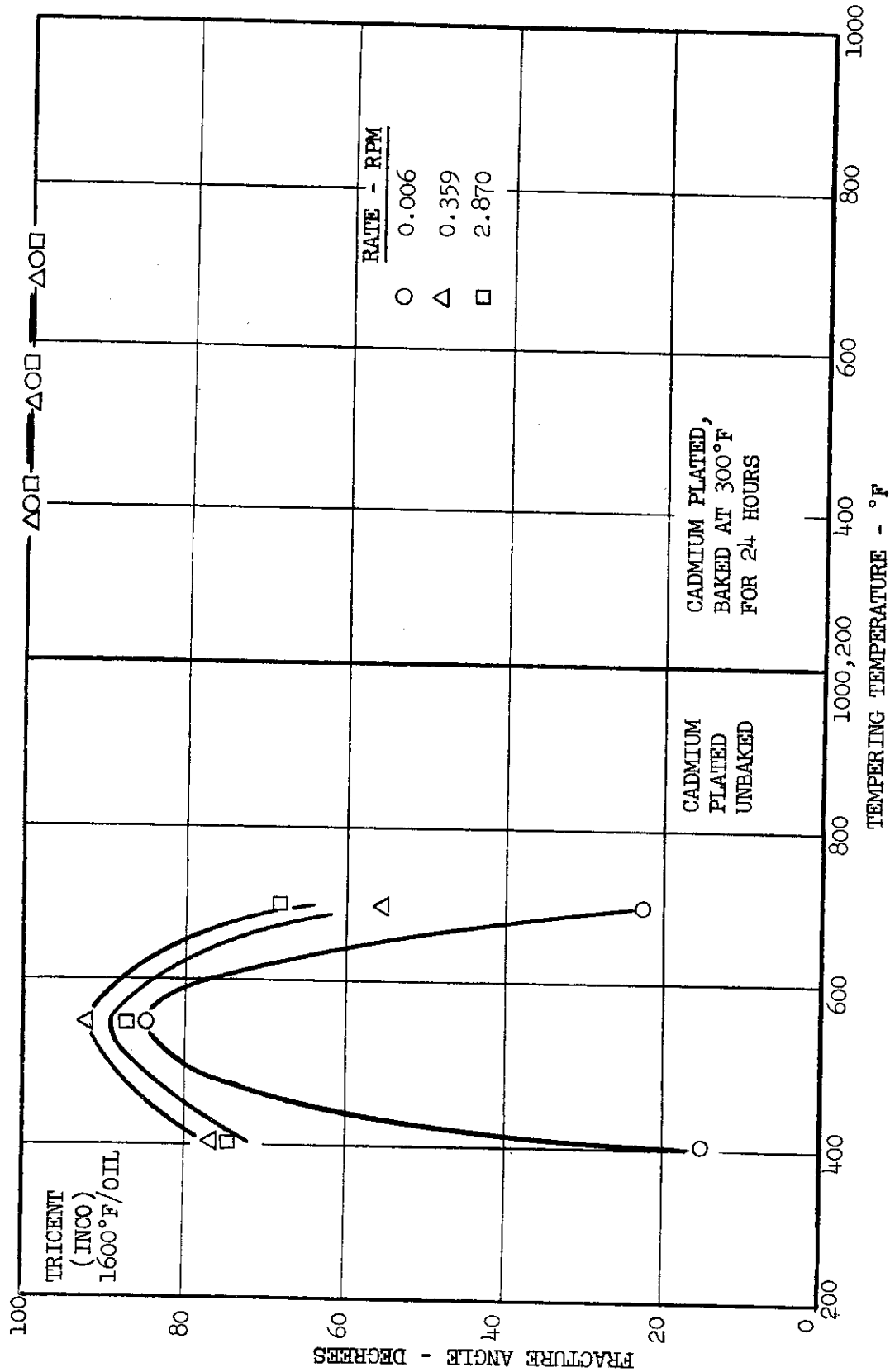
FIG. 69   THE BEND FRACTURE ANGLES VS. TEMPERING TEMPERATURE FOR Cd-PLATED TRICENT STEEL WITH TESTING SPEED AS PARAMETER FOR THE INDICATED TEST CONDITIONS.

FIG. 70   THE BEND FRACTURE ANGLE VS. TESTING SPEED FOR Cd-PLATED HY-TUF
AND CRUCIBLE UHS-260 STEELS WITH TEMPERING TEMPERATURE AS
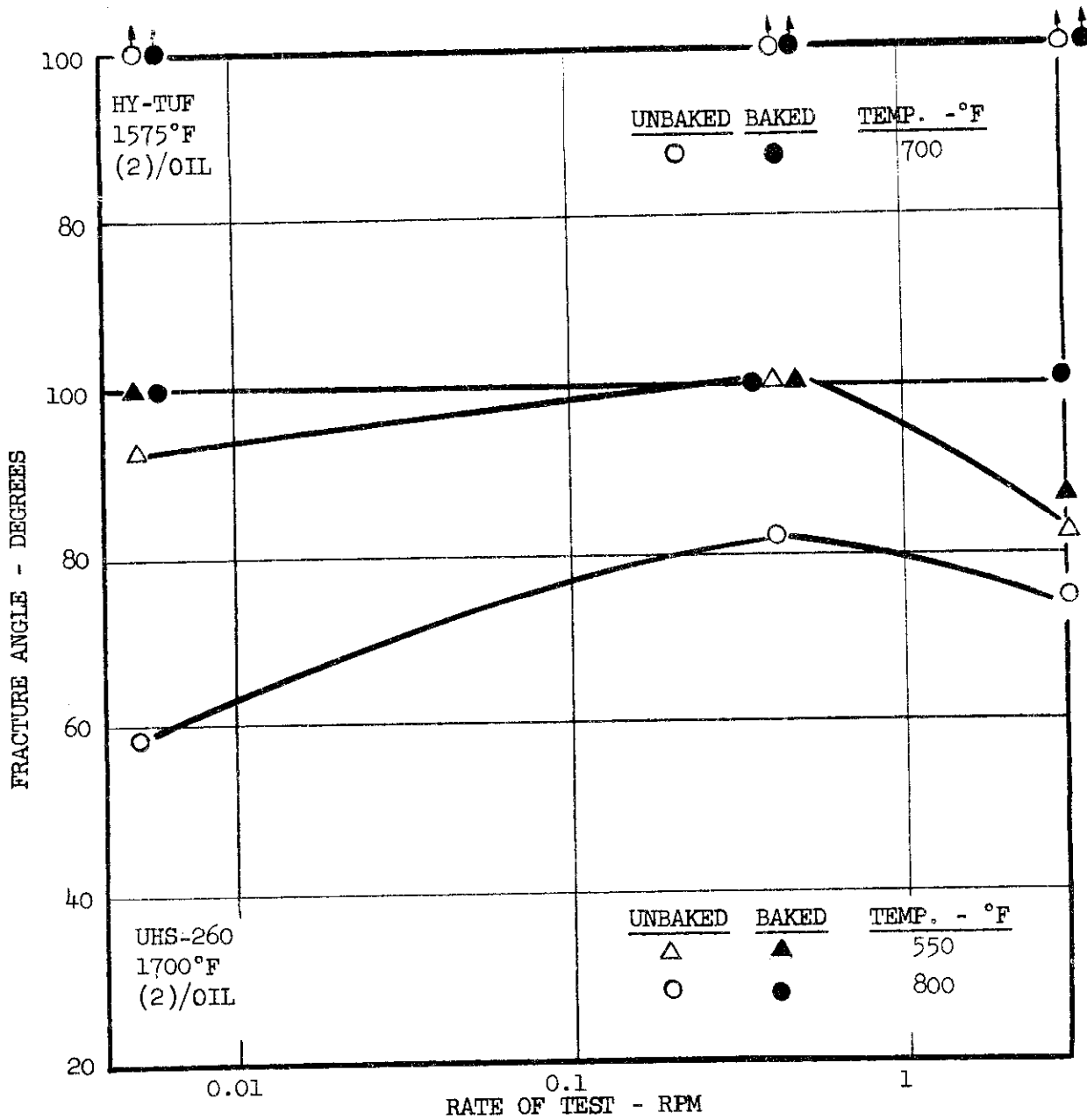PARAMETER FOR THE INDICATED TEST CONDITIONS.
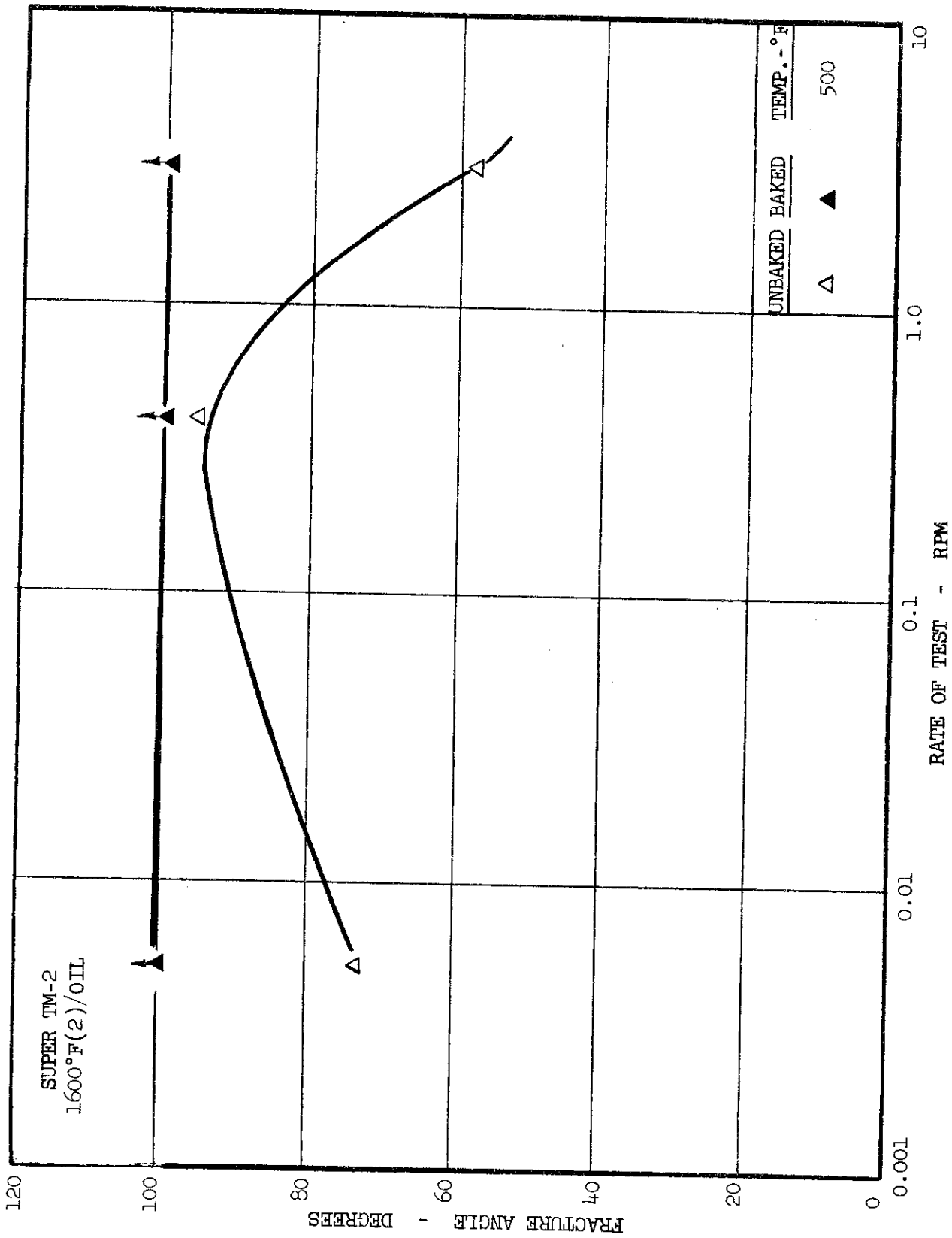
FIG. 71   THE BEND FRACTURE ANGLE VS. TESTING SPEED FOR Cd-PLATED SUPER TM-2 STEEL WITH TEMPERING TEMPERATURE AS PARAMETER FOR THE INDICATED TEST CONDITIONS.

FIG. 72   THE BEND FRACTURE ANGLE VS. TESTING SPEED FOR THE STEELS AT
A TENSILE STRENGTH = 290,000 PSI.

FIG. 73   THE BEND FRACTURE ANGLE VS. TESTING SPEED FOR THE STEELS AT A
TENSILE STRENGTH = 270,000 PSI.
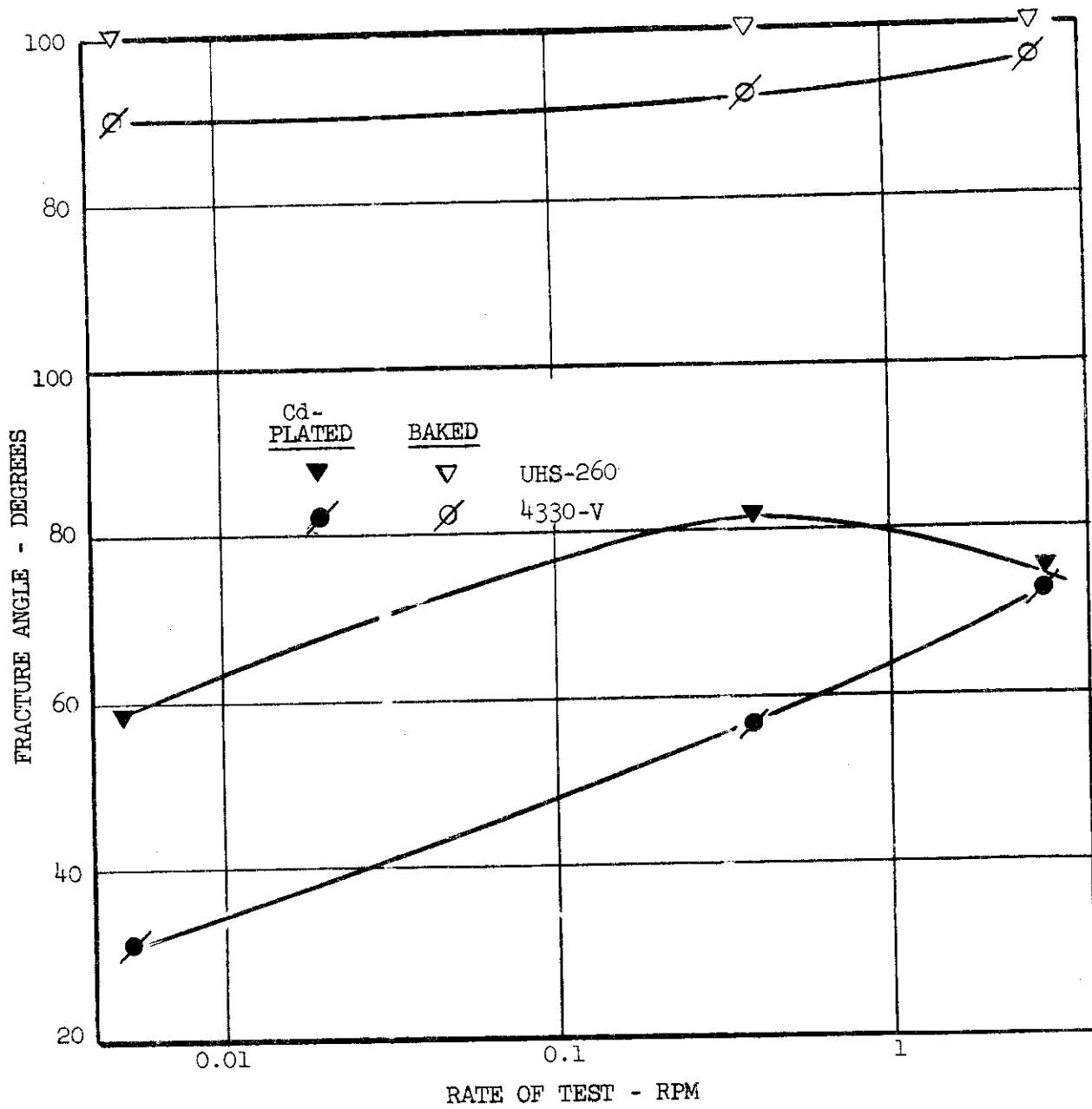
FIG. 74   THE BEND FRACTURE ANGLE VS. TESTING SPEED FOR THE STEELS AT A
TENSILE STRENGTH = 250,000 PSI.
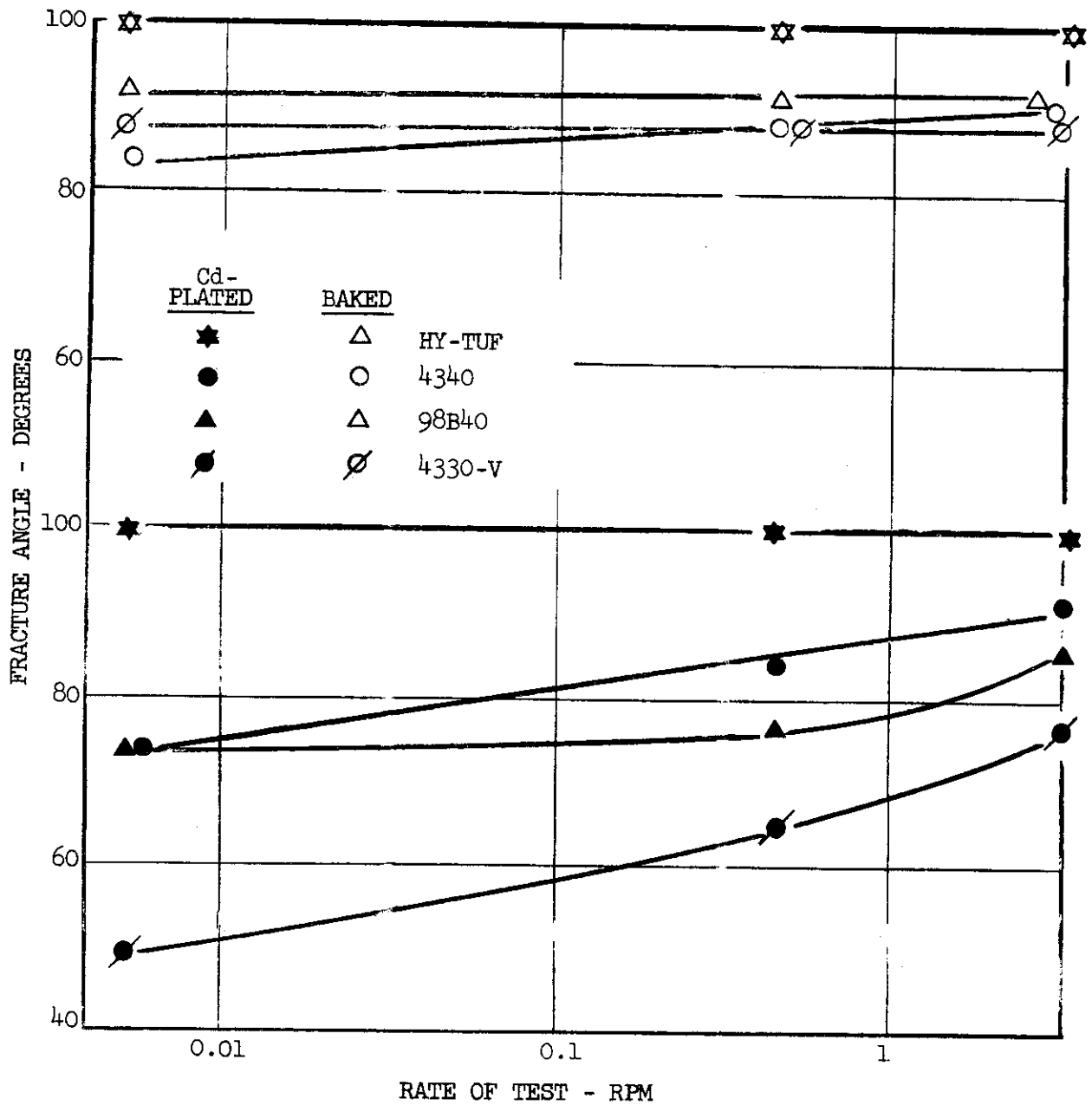
FIG. 75 THE BEND FRACTURE ANGLES VS. TESTING SPEED FOR THE STEELS AT
A TENSILE STRENGTH = 230,000 PSI.
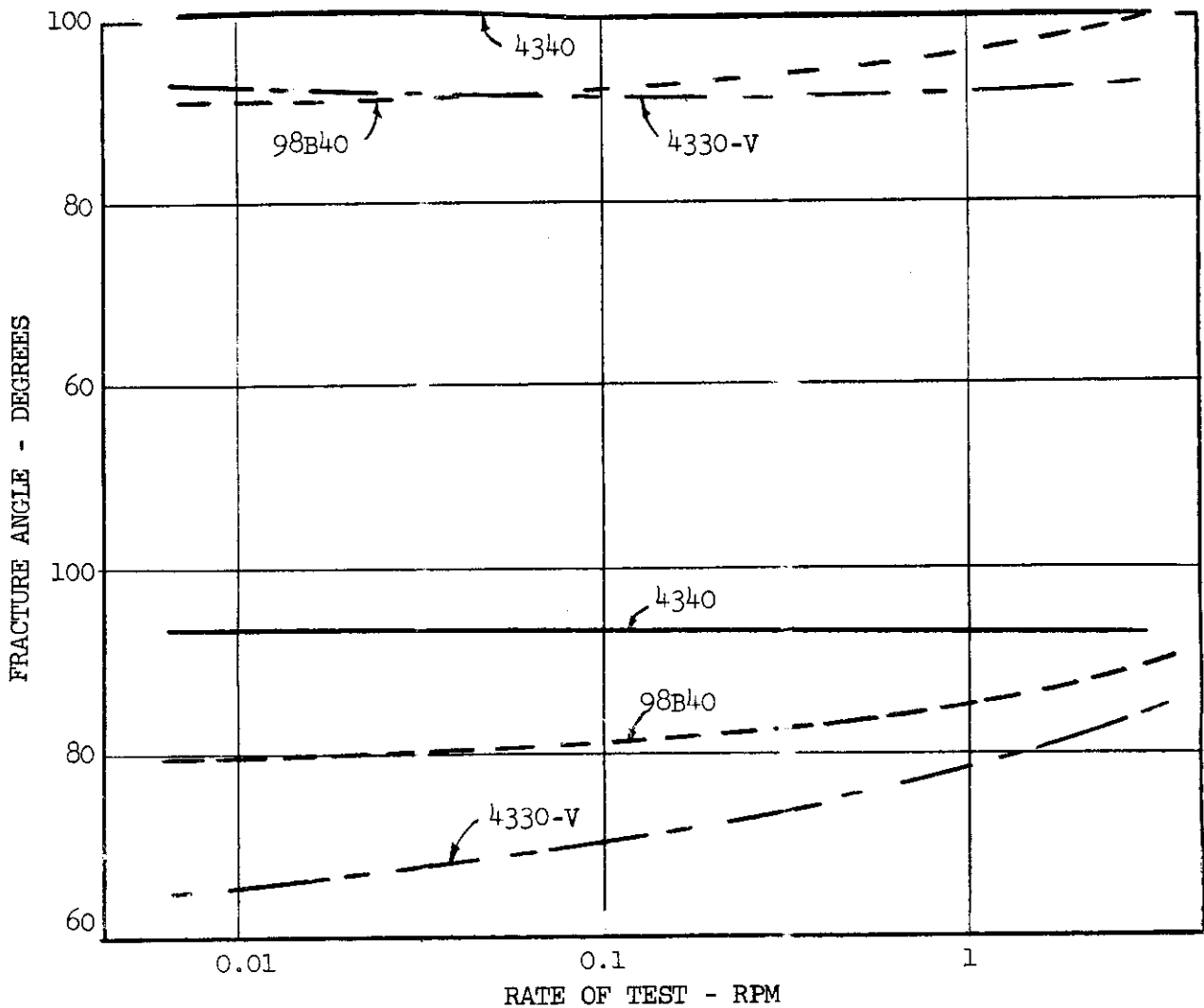
FIG. 76 THE BEND FRACTURE ANGLE VS. TESTING SPEED FOR THE STEELS AT
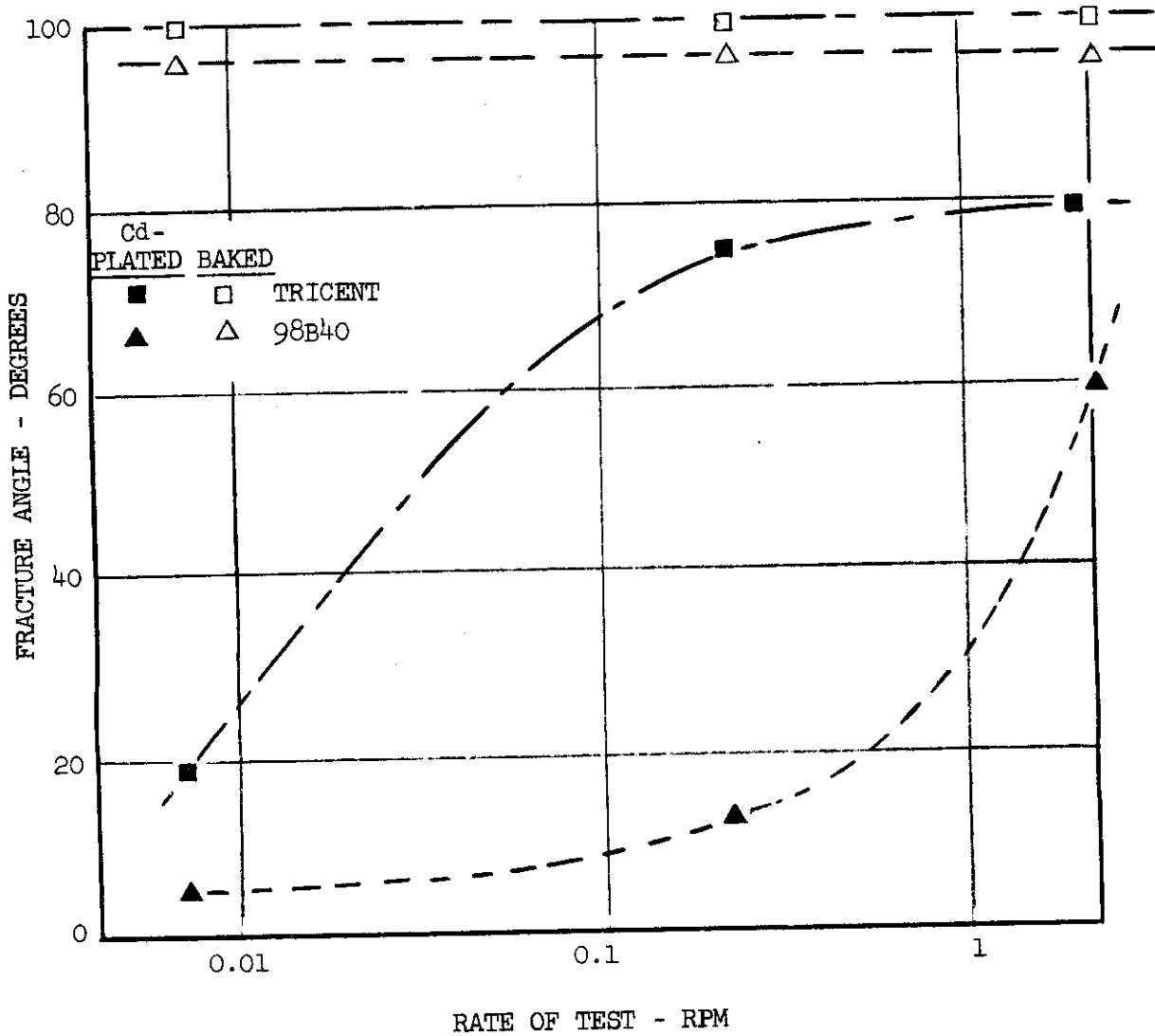A TENSILE STRENGTH = 210,000 PSI.

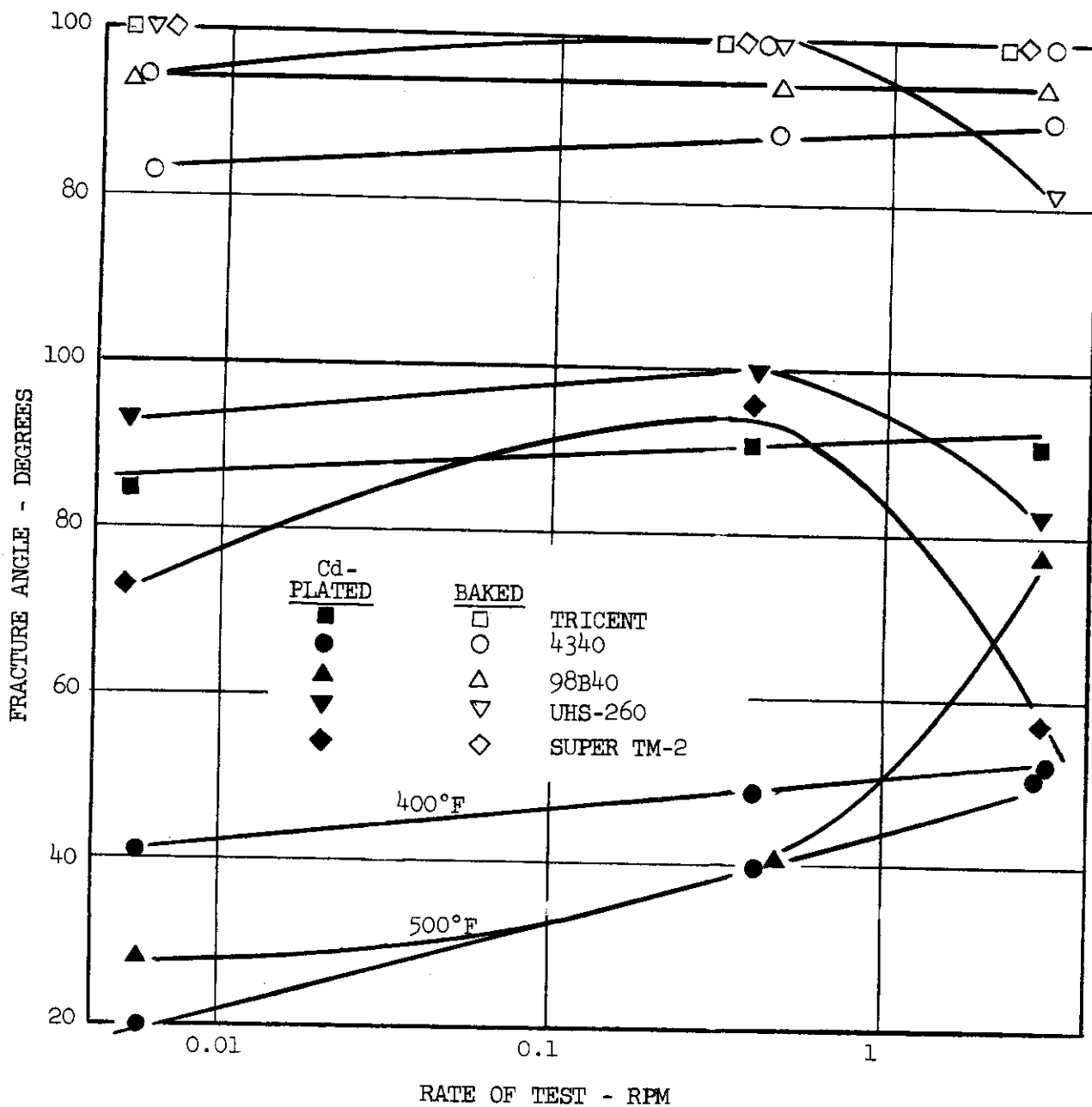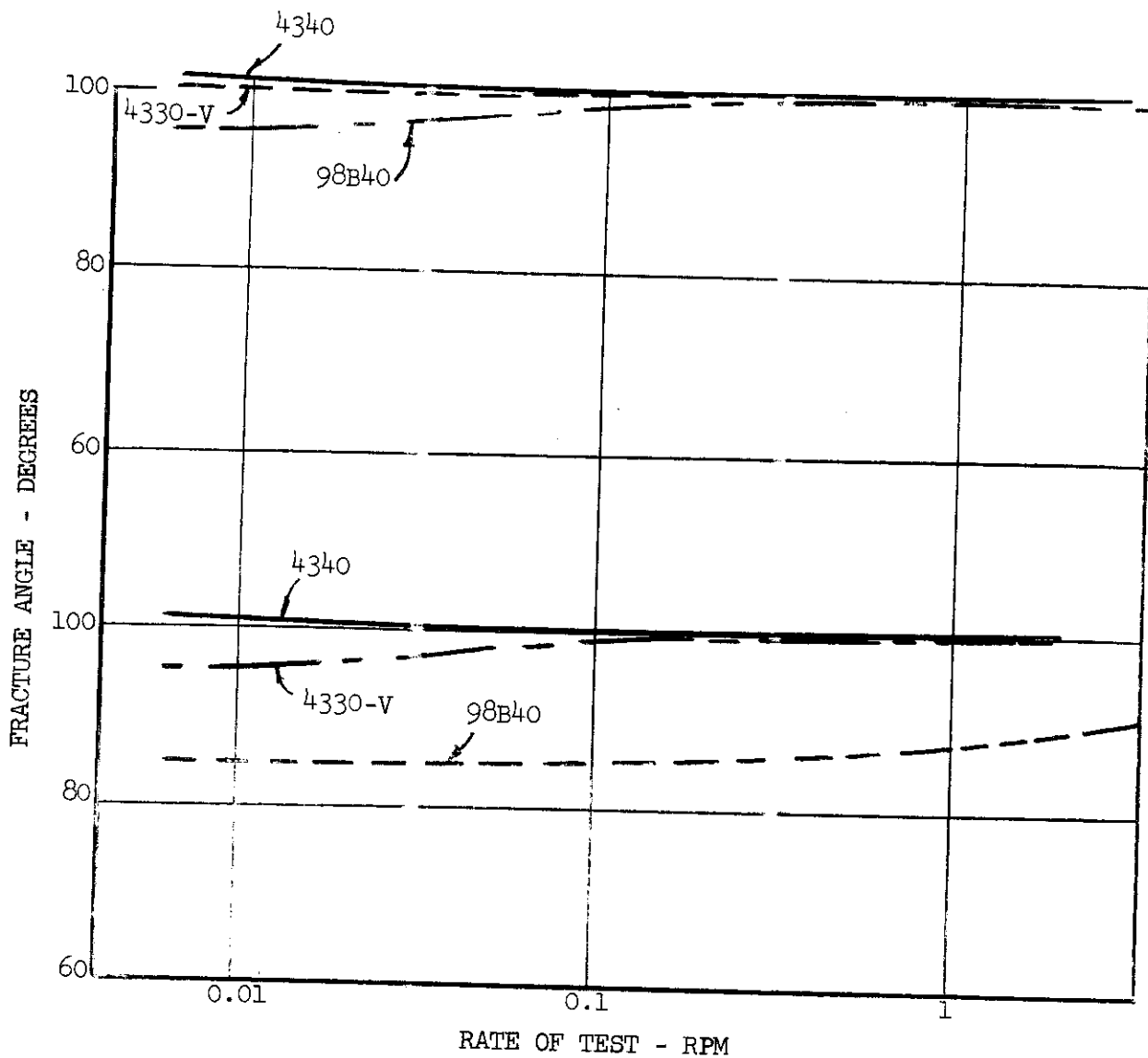FIG. 77 THE BEND FRACTURE ANGLE VS. TESTING SPEED FOR THE STEELS AT A TENSILE STRENGTH = 180,000 PSI.
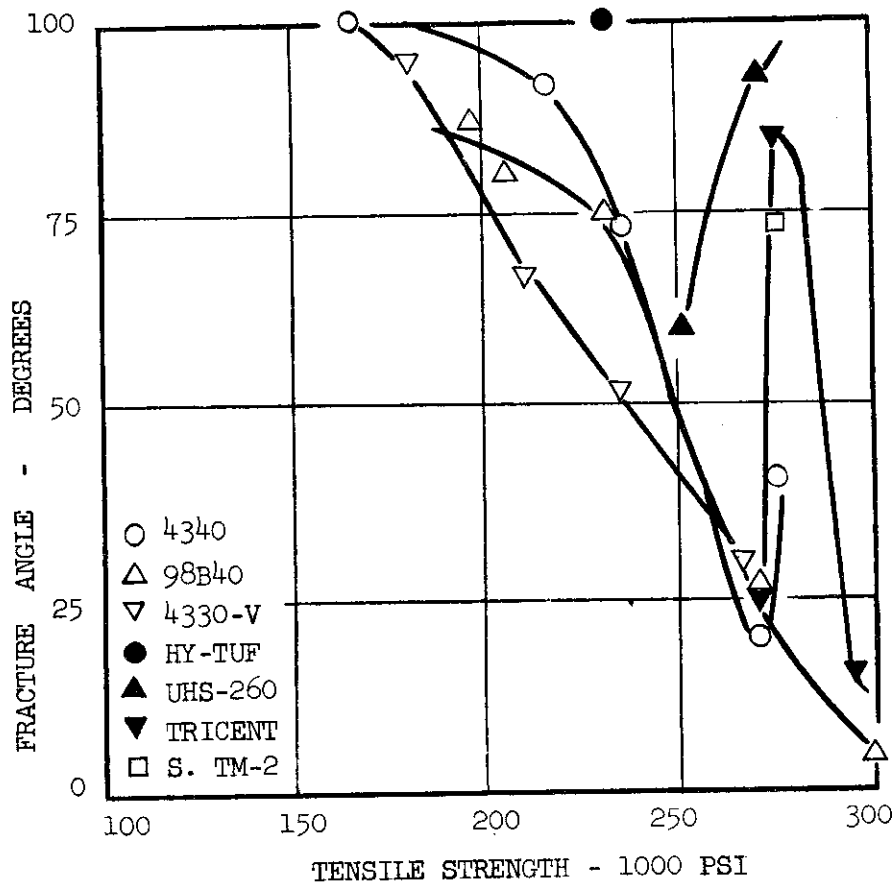
FIG. 78 THE BEND FRACTURE ANGLE VS. TENSILE STRENGTH FOR
THE STEELS STUDIED. (SLOW TESTING SPEED)
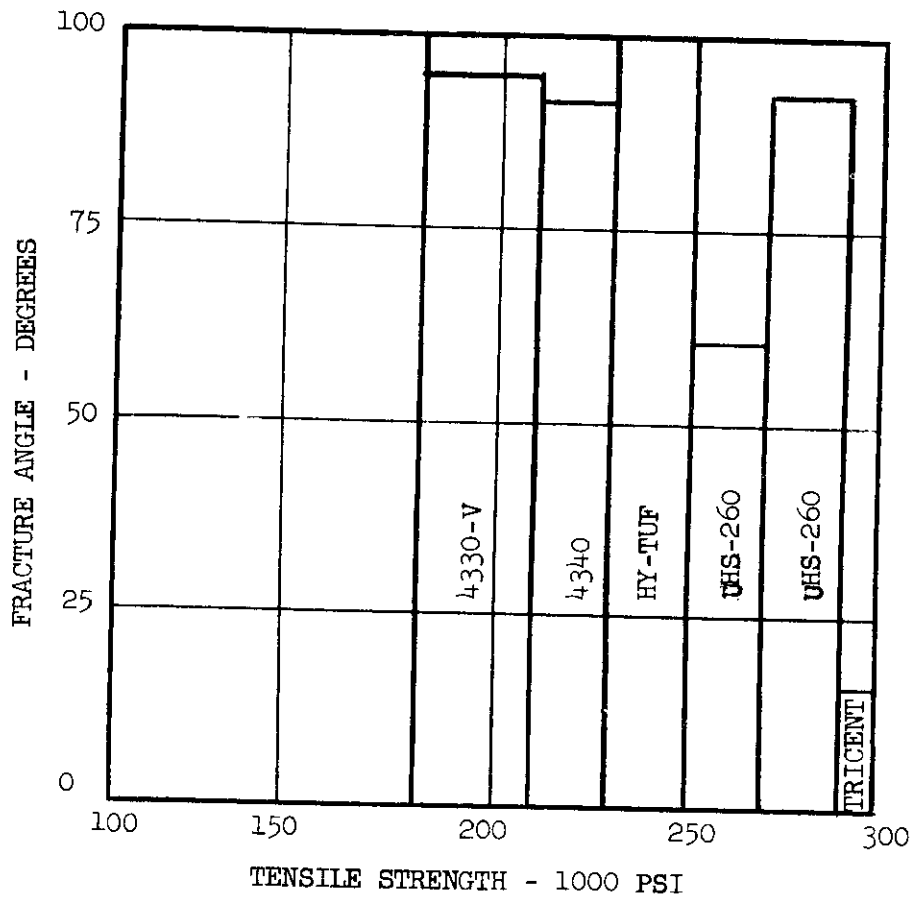
FIG. 79   THE MAXIMUM BEND FRACTURE ANGLES AND THE STEELS
WITH WHICH THEY WERE OBTAINED FOR THE INDICATED
TENSILE STRENGTH LEVELS.
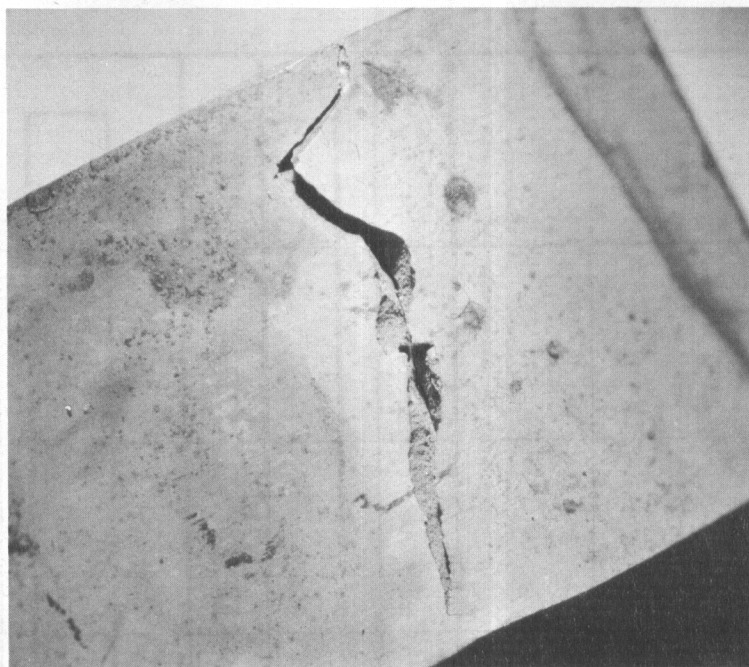
FIG. 80 SHEAR FRACTURE DEVELOPMENT IN
A Cd-PLATED BEND SPECIMEN
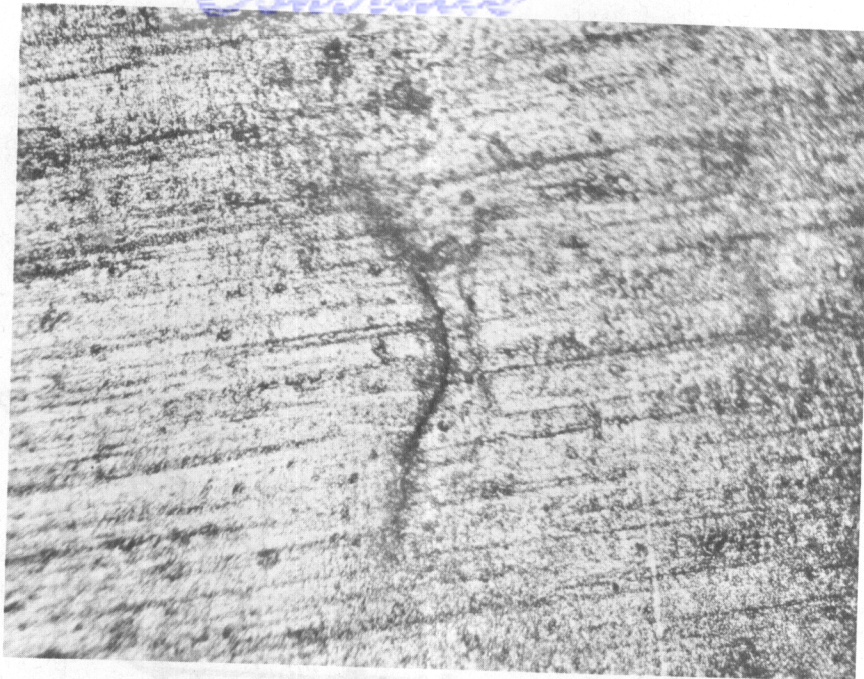
FIG. 81 CRACK DEVELOPMENT IN A Cd-PLATED BEND
SPECIMEN. TESTED AT HIGH SPEED

FIG. 82 CRACK DEVELOPMENT IN A Cd-PLATED BEND
SPECIMEN. TESTED AT SLOW SPEED
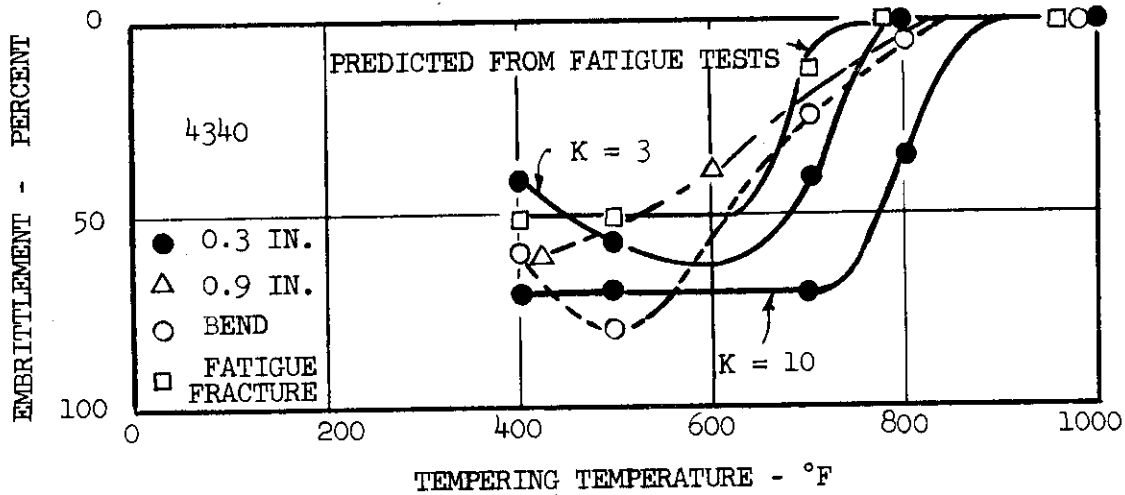
FIG. 83   THE EMBRITTLEMENT CHARACTERISTICS VS. TEMPERING TEMP-
ERATURE FOR A 4340 STEEL AS ESTABLISHED FROM THE
INDICATED TEST CONDITIONS.
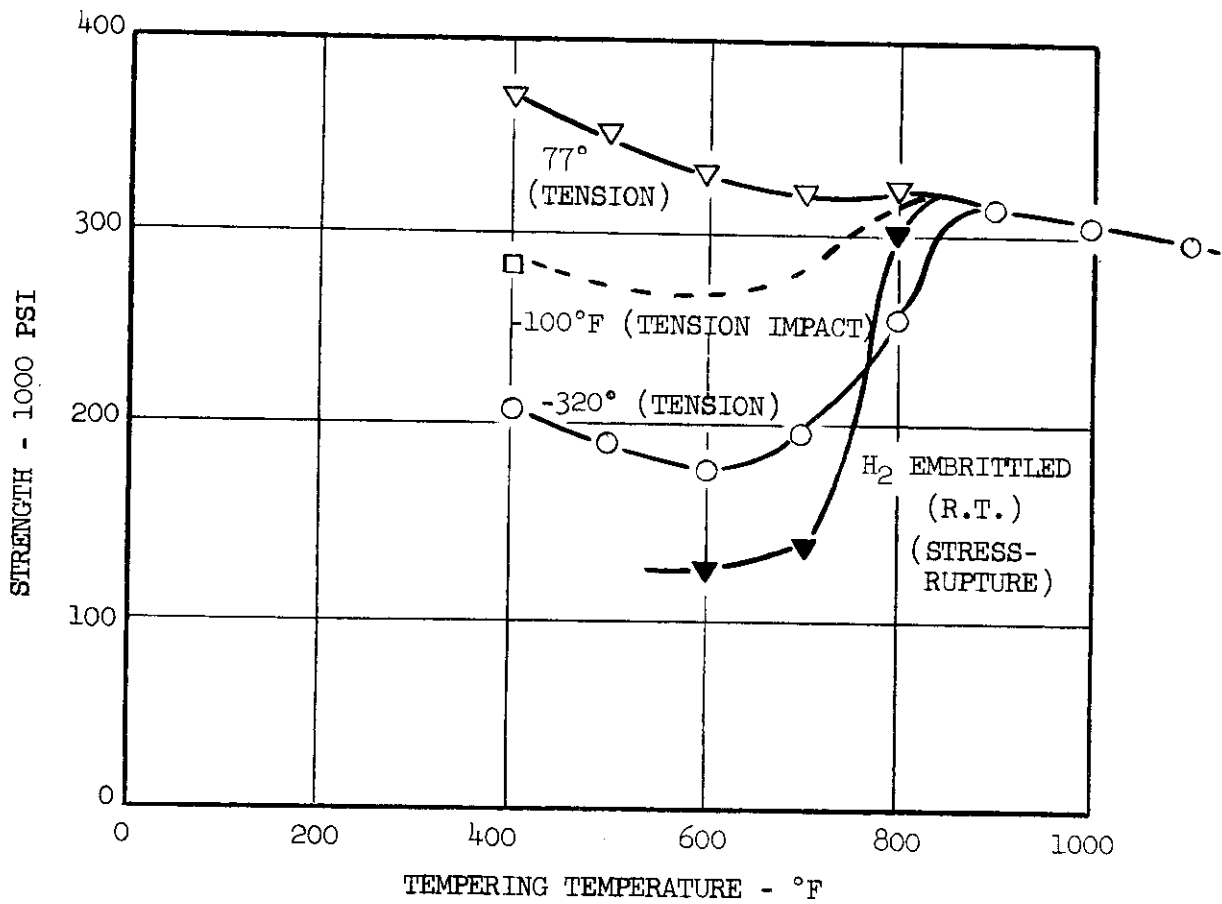
FIG. 84 THE INSTANTANEOUS NOTCH STRENGTH FOR SHARPLY NOTCHED 0.3 IN. DIA. SPECIMENS DETERMINED FOR THE INDICATED TEST CONDITIONS.
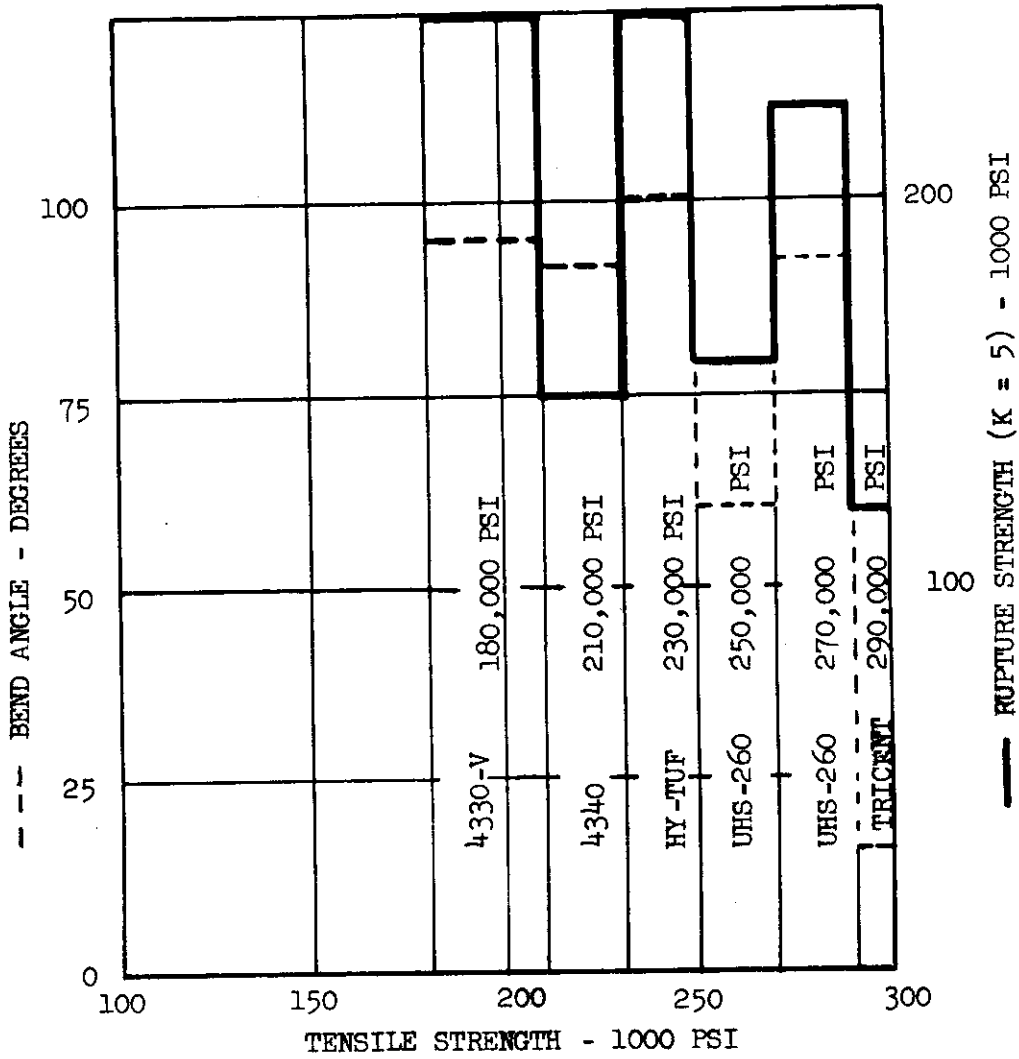
FIG. 85   COMPARISON OF BEND AND SUSTAINED-LOAD DATA.

TABLE IV

(a) PROGRAM OF HYDROGEN ANALYSES

R is the rate of loading, K is the stress concentration.

Alloy	Strength Level - Psi	Bend Test (Unbaked)			Bend Test (Baked)			Sustained-Load Test (Unbaked)			
		R_1	R_2	R_3	R_1	R_2	R_3	K=1	K=3	K=5	K=10
		L	L	L	L	L	L	L	L	L	L
4340	290,000	3			3			3	1	3	1
	270,000	1			1			1	1	1	1
	230,000	3			3			3	1	3	1
	210,000	1			1			1	1	1	1
	180,000	3			3			3	1	3	1
98B40	290,000	2			2			2		2	
	270,000										
	230,000	2			2			2		2	
	210,000										
	180,000	2			2			2		2	
V-Mod. 4330	270,000	3			3			3		3	
	230,000	3			3			3		3	
	210,000										
	180,000	3			3			3		3	
Hy-Tuf	230,000	2			2			2		2	
Crucible UHS-260	290,000	2			2			2		2	
	250,000	2			2			2		2	
Super TM-2	270,000	2			2			2		2	
Tricent (Inco)	310,000	1			1			1	1	1	1
	290,000	1			1			1	1	1	1
	270,000	1			1			1	1	1	1

TABLE IV (Cont'd)

HYDROGEN ANALYSES (BEND SPECIMENS) FOR 4340, 98B50 AND V-MOD. 4330 STEELS

		Hydrogen Content - ppm	
	Temp. Temp. °F	Unbaked	Baked
(b) 4340	400	4.7 2.5 1.7	3.5 7.9 7.3
	500	4.4	2.5
	700	5.2 2.9 2.3	2.8 10.2 10.1
	800	5.1	3.5
	1000	4.9 2.9 3.5	3.5 14.6 4.3
(c) 98B40	400	9.7 6.7	5.4 6.3
	700	12.7 14.3	5.1 6.5
	900	12.3 9.8	1.1 8.9
(d) V-Mod.	250	8.5 4.5 6.7	5.5 4.4 6.5
	500	7.3 5.8 1.9	12.4 6.8 2.1
	1000	3.6 9.9 7.0	1.3 1.6 1.4

TABLE IV (Cont'd)

HYDROGEN ANALYSES (STRESS-RUPTURE SPECIMENS) FOR 4340,
98B40 AND V-MOD. 4330 STEELS

Temp. Temp. °F	Stress Concentration			
	K = 1	K = 3	K = 5	K = 10
(e) 4340:				
400	2.3 1.4 3.2	2.1	1.7 1.6 0.7	1.1
500	1.8	1.5	1.8	1.6
700	2.5 1.7 0.9	1.5	1.0 0.9 0.8	0.8
800	1.1	1.0	1.3	1.4
1000	2.6 1.2	1.1	1.5 0.9	1.0
(f) 98B40:				
400	3.3 3.3		1.7 2.5	
700	2.7 5.1		2.0 2.8	
900	3.3 Lost		3.4 2.3	
(g) V-Mod. 4330:				
250	1.7 0.6 1.5		3.5 2.1 2.8	
500	3.3 2.5 3.0		3.2 2.1 3.3	
1000	3.4 2.0 1.4		2.4 2.6 3.9	

Hydrogen not detectable in a 4340 Stress-Rupture Specimen, K = 5, 500°F
Temper (No. 13A).

TABLE IV (Cont'd)

HYDROGEN ANALYSES (BEND SPECIMENS) FOR HY-TUF, CRUCIBLE
UHS-260 AND TRICENT STEELS

Temp. Temp. °F	Hydrogen Content - ppm	
	Unbaked	Baked

(h) Hy-Tuf:

700	3.8 4.6	4.8 7.7

(i) Crucible
UHS-260:

550	3.0 2.0	3.6 4.8
800	3.8 2.0	3.3 3.4

(j) Tricent:

400	4.1	3.0
550	0.8	3.4
700	1.5	2.1

TABLE IV (Cont'd)

HYDROGEN ANALYSES (STRESS-RUPTURE SPECIMENS) FOR HY-TUF,
CRUCIBLE UHS-260 AND TRICENT STEELS

Temp. Temp. °F	Stress Concentration			
	K = 1	K = 3	K = 5	K = 10

(k) Hy-Tuf:

Temp. °F	K = 1	K = 3	K = 5	K = 10
700	3.4 2.6		1.1 0.9	

(l) Crucible UHS-260:

Temp. °F	K = 1	K = 3	K = 5	K = 10
550	1.7 0.9		0.7 0.3	
800	1.1 3.9		1.4 0.8	

(m) Tricent:

Temp. °F	K = 1	K = 3	K = 5	K = 10
400	1.4	Lost	0.8	1.1
550	1.2	1.1	4.0	0.9
700	1.9	0.9	1.5	3.4

TABLE IV (Cont'd)

HYDROGEN ANALYSES (BEND AND STRESS-RUPTURE SPECIMENS)
FOR SUPER TM-2 STEEL

(n) Bend
    Specimens:

Temp. Temp. °F	Hydrogen Content - ppm	
	Unbaked	Baked
500	2.1	2.5
	5.3	2.4

(o) Stress-
    Rupture
    Specimens:

Temp. Temp. °F	Stress Concentration	
	K = 1	K = 5
200	3.2	1.4
	2.5	0.9